

ABSTRACT

WANG, FENG. Maternal Supplementation of Choline and Docosahexaenoic Acid (DHA) during Gestational Nutrition Restriction in a Swine Model Alters Hepatic miRNA and mRNA Expression Patterns in Full-Term Offspring. (Under the direction of Lin Xi).

Maternal undernutrition during pregnancy will not only cause short-term consequences, such as mortality, morbidity, disability but also impact intellectual ability, adult size, type 2 diabetes, cardiovascular disease, and immunodeficiency. However, the potential impairments of maternal undernutrition to metabolic pathways, especially involved the microRNA (miRNA) regulation, in offspring are not defined completely. In order to further clarify the potential impairments of maternal under nutrition on offspring metabolism, we explored the role of microRNA, as an epigenetic regulator, in hepatic metabolism during development of the fetus in this research via 3 studies.

In the first study, two groups of pregnant domestic pigs received nutritionally balanced gestation diets with or without 50% feed intake restriction from 0 to 35 gestation days and 70% from 35 to 114 gestation days. Full-term fetuses were collected via C-section on day 113/114 of gestation. Through miRNA and mRNA sequencing, 1189 mRNAs and 34 miRNAs were differentially expressed caused by maternal undernutrition. The correlation analyses showed that oxidative phosphorylation, death receptor signaling, neuroinflammation signaling pathway, and estrogen receptor signaling pathways were significantly modified by maternal undernutrition, and these changes were associated with miRNA regulation. Moreover, a stimulated oxidative phosphorylation pathway caused by maternal undernutrition was validated using RT-qPCR. These results provide the framework for further understanding maternal malnutrition's negative impacts on hepatic metabolic pathways via miRNA-mRNA interactions in full-term fetal pigs.

In the second study, we sequenced mRNA and miRNA on the same fetal liver samples,

that were obtained from pregnant pigs with restricted feed intake in a 2 (\pm choline) x 2 (\pm DHA) factorial design to investigate their individual and interaction effect on fetal liver during gestational nutrition restriction. By conducting 2 x 2 factorial analysis, and following ingenuity pathways analysis (IPA), we identified that cardiac hypertrophy signaling, IL-6 signaling, IL-3 signaling, Th1 pathway, and acute phase response signaling were inhibited by maternal supplementation of choline. Moreover, 5 inositol-related pathways and 5 immune-related pathways and another 7 pathways were inhibited by maternal supplementation of DHA, while PPAR signaling and RhoGDI signaling were stimulated. Furthermore, acute phase response signaling displayed a choline x DHA synergistic effect. In contrast, sirtuin signaling pathway, tRNA splicing, PPAR α /RXR α activation, and NAD signaling pathway, RNA polymerase I transcription pathway displayed a choline x DHA antagonistic effect. Through miRNA target prediction, we identified 20 miRNA-mRNA pairings and validated 10 of them using RT-qPCR.

In the third study, pig liver organoids were established and served as a model to investigate the proposed choline-miR-503-LIPG-HDL regulatory pathways. Liver organoids were transfected with various concentrations (1, 10, 100 nM) of miR-503 mimics and various concentrations (1, 10, 100 nM) of miR-503 mimics co-transfected with same concentration of miR-503 inhibitor. Results showed that the cytotoxicity (0.64%) and viability (95.50%) of the organoids remained unaffected across all the tested miR-503 mimic concentrations during the experiment. MiR-503 mimic at concentrations of 1, 10, and 100 nM significantly suppressed *LIPG* gene expression ($p < 0.05$), with a notable suppressed on LIPG protein production observed only at 10 nM ($p < 0.05$). No significant difference was observed between all miR-503 mimic co-transfected with miR-503 inhibitor groups and the control group ($p > 0.05$). The HDL content in liver organoids exhibited a notable increase upon transfection with the miR-503 mimic

at all concentrations ($p < 0.05$). However, co-transfection of miR-503 mimic with its inhibitor quenched the effect ($p > 0.05$).

Through these studies, we gained comprehensive insights into the impact of maternal undernutrition on hepatic mRNA and miRNA expression patterns, encompassing gene, pathway, and miRNA regulation in full-term offspring. Furthermore, we investigated the impact of maternal supplementation with choline and DHA during gestational nutrition restriction on altering hepatic miRNA and mRNA expression patterns in offspring. Additionally, a miRNA-regulated pathway identified through the analysis of sequencing data was validated using liver organoids established in this research.

© Copyright 2024 by Feng Wang

All Rights Reserved

Maternal Supplementation of Choline and Docosahexaenoic Acid (DHA) during Gestational Nutrition Restriction in a Swine Model Alters Hepatic miRNA and mRNA Expression Patterns in Full-Term Offspring

by
Feng Wang

A dissertation submitted to the Graduate Faculty of
North Carolina State University
in partial fulfillment of the
requirements for the degree of
Doctor of Philosophy

Animal Science

Raleigh, North Carolina
2024

APPROVED BY:

Dr. Lin Xi
Chair

Dr. Xiao-Qiu Wang

Dr. Jack Odle

Dr. Christian Maltecca

BIOGRAPHY

Feng Wang was born in Hinggan League, Inner Mongolia, China on September 23rd, 1992. He spent his childhood in a rural area, surrounded by family and friends, enjoying a peaceful and delightful life. He pursued a bachelor's degree in Veterinary Medicine at Inner Mongolia University for Nationalities, followed by a decision to continue his academic journey by earning a master's degree in Agricultural Extension at the same institution. In 2018, he started his pursuit of a Ph.D. in Animal Science at NC State under the guidance of Dr. Lin Xi. Following graduation, he aspires to remain in the academic field with a focus on animal science.

ACKNOWLEDGMENTS

I would like to acknowledge the guidance, support and outlook provided by Dr. Lin Xi throughout this journey. He allowed me to work on his project without knowing anything about me and gave me an opportunity that I had not otherwise had, and I hope I lived up to what he expected. Dr. Lin Xi taught me numerous techniques in the lab and how to analyze all the data gathered from the trails. He has also helped me extensively in crafting this thesis to best represent the works I accomplished. Moreover, he provides me guidance and opportunity for my further plan. For all his help and guidance, I am most appreciative. The journey was a long but an enjoyable one and Dr. Lin Xi was a major factor in the enjoyment of it.

I also want to give thanks to all my committee members, Drs. Jack Odle, Xiaoqiu Wang, and Christian Maltecca for their help on providing experimental facilities, guidance for my confusion, patience on communication, and all effort for serving on the graduate committee. I also want to thank Tim Boston, Daisy Cagle, Paige Meisner, Lin Yang, Jinan Zhao, Brandon Pike, and many other undergraduate student and visiting scholars who helped to make all my work possible.

Finally, I would like to acknowledge the many sacrifices my family has made for me to get to this point. Their unwavering support, both emotionally and financially, has been a cornerstone throughout my journey. I am truly grateful for the constant encouragement and unwavering support from my entire family, without their support I would not be where I am today.

TABLE OF CONTENTS

LIST OF TABLES	vii
LIST OF FIGURES	viii
Chapter I: Literature Review	1
I-1. Prevalence of Maternal Undernutrition	1
I-2. Consequences of Maternal Undernutrition in Their Offspring	1
I-3. Current Research toward Dysfunction of Fetal Liver Induced by Maternal Undernutrition	8
I-4. Modification of Lipoprotein Metabolism in the Liver Is Crucial for Serum Cholesterol Levels	12
I-5. The Development of Atherosclerotic Cardiovascular Disease is Related to High-Density Lipoprotein Metabolism in Liver	13
I-6. Maternal Undernutrition Alters Fetal Liver Gene Expression through Epigenetic Mechanisms	14
I-7. The Role of Maternal Choline in Fetal Liver Development	16
I-8. The Role of Maternal Docosahexaenoic acid in Fetal Liver Development	18
I-9. Significance of Pig Model in Addressing Maternal Undernutrition	20
I-10. Conclusions and Rationale	21
I-11. References	23
Chapter II: MicroRNA and mRNA Sequencing Analyses Reveal Key Hepatic Metabolic and Signaling Pathways Responsive to Maternal Undernutrition in Full-term Fetal Pigs ..	34
II-1. Abstract	34
II-2. Introduction	36
II-3. Materials and Methods	40
II-3.1. Experimental Design	40
II-3.2. mRNA and miRNA Sequencing	41
II-3.3. RNA-seq and miRNA Data Analysis	41
II-3.4. Gene Ontology Functional Analysis	42
II-3.5. Ingenuity Pathways Analysis and mi-mRNA Correlation Analysis	42
II-3.6. RNA Expression Level Analysis	43
II-3.7. Statistical Analysis	44
II-4. Results	44
II-4.1. Expression Profiling of mRNA	44
II-4.2. Full-nutrition Group vs. Restricted-nutrition Group mRNA Expression Profile	45

II-4.3. Differentially Expressed miRNAs Between Full-nutrition Group and Restricted-nutrition Group	46
II-4.4. Canonical Pathway Regulated by miRNAs.....	46
II-4.5. miRNA-mRNA Correlation in miRNA-regulated Pathways	47
II-4.6. RT-qPCR Validation of miRNAs and mRNAs in Oxidative Phosphorylation Pathway	47
II-5. Discussion	48
II-6. References	53
Chapter III Dietary Choline and Docosahexaenoic Acid (DHA) Supplementation to Pregnant Pigs Experiencing Gestational Nutrition Restrictions Impacts Hepatic miRNA and mRNA Expression in Full-term Fetal Pigs.....	96
III-1. Abstract	96
III-2. Introduction.....	98
III-3. Materials and Methods.....	102
III-3.1. Experimental Design.....	102
III-3.2. RNA Sequencing.....	102
III-3.3. Data Analysis for RNA-sequencing.....	103
III-3.4. 2 x 2 Factorial Analysis.....	104
III-3.5. Gene Ontology Enrichment Analysis and Ingenuity Pathways Analysis	105
III-3.6. miRNA Target Prediction Analysis	105
III-3.7. RT-qPCR Validation for miRNA-mRNA Pairings.....	106
III-3.8. Choline Content Measurement in Fetal Liver.....	106
III-3.8. Statistical Analysis	106
III-4. Results.....	106
III-4.1. The Statistical Summary of mRNA and miRNA in 2 x 2 Factorial Design	106
III-4.3. GO Enrichment Analysis and IPA Analysis for Genes Have the DHA Effect.....	108
III-4.4. GO Enrichment and IPA Analysis for Genes Having a Choline x DHA Interaction Effect	109
III-4.5. miRNA Target Prediction Analysis	110
III-4.6. RT-qPCR Validation for miRNA-mRNA Pairings.....	111
III-5. Discussion	112
III-6. References.....	119
Chapter IV: Modulation of MicroRNA-503 Alters Endothelial Lipase Expression and High-Density Lipoprotein Level in Porcine Liver Organoids	162

IV-1. Abstract.....	162
IV-2. Introduction.....	164
IV-3. Materials and Methods	172
IV-3.1. Liver Organoids Isolation and Culture.....	172
IV-3.2. Urea Assay (Functional Validation of Liver Organoids).....	175
IV-3.3. MiR-503 Mimic Transfection and Co-transfection with miR-503 Inhibitor	175
IV-3.4. MiR-503 Mimic Transfection Efficiency Assay - RT-qPCR	176
IV-3.5. Organoids Viability and Cytotoxicity Assay	177
IV-3.6. LIPG mRNA Expression Level Analysis – RT-qPCR	177
IV-3.7. LIPG Protein Expression Analysis – Western Blot	178
IV-3.8. HDL Measurement.....	179
IV-3.9. Choline Treatment.....	180
IV-3.10. Statistical Analysis.....	180
IV-4. Results.....	180
IV-4.1. Liver Organoid Urea Assay	181
IV-4.2. MiR-503 Transfection Efficiency Assay	181
IV-4.3. Cytotoxicity and Cell Viability Assay	181
IV-4.4. LIPG mRNA Expression Level Analysis – RT-qPCR	182
IV-4.5. LIPG Protein Expression Analysis – Western Blot	182
IV-4.6. HDL Measurement.....	182
IV-4.7. Choline Measurement in Liver Organoids.....	183
IV-4.8. LIPG and miR-503 Expression Level Analysis.....	183
IV-5. Discussion.....	183
IV-6. References	188
Chapter V: General Conclusions and Future Directions	206
V-1. General Conclusions	206
V-2. Future Directions.....	208

LIST OF TABLES

Table II-3.1-1 Composition of the gestation diet and supplement [@]	59
Table II-3.1-2 Timeline of experimental events and nutritional treatments.	60
Table II-3.6 The sequence of primers used for RT-qPCR.....	61
Table II-4.2 Canonical pathway analysis of genes differentially expressed between full-nutrition (F) group and restricted-nutrition (R) group.....	62
Table II-4.4 Canonical Pathways regulated by differentially expressed miRNAs.	64
Table II-4.5 Differentially expressed miRNAs and their targeted differentially expressed genes in canonical pathway.....	65
Table III-3.1-1 Composition of the gestation diet and supplement [@]	126
Table III-3.1-2 Timeline of experimental events and nutritional treatments.....	127
Table III-3.7 The sequence of primers used for RT-qPCR.....	128
Table III-4.1-1 Statistical result of mRNAs in 2 x 2 Factory Design.	130
Table III-4.1-2 Statistical result of miRNAs in 2 x 2 Factory Design.....	146
Table III-4.2 The effect of maternal supplemental choline on the metabolic pathways identified by IPA analysis.	148
Table III-4.3 The effect of maternal supplemental DHA on the metabolic pathways identified by IPA analysis.	149
Table III-4.4 The interaction effect of maternal supplemental choline and DHA on the metabolic pathways identified by IPA analysis.....	152
Table III-4.5 The list of miRNAs and their target mRNAs with same statistical category.....	153
Table III-4.6 RT-qPCR validation for miRNAs and their target mRNAs.....	154

LIST OF FIGURES

Figure II-4.2 mRNA profiles between full-nutrition (F) group and restricted-nutrition (R) group.	93
Figure II-4.3 miRNA profiles between full-nutrition (F) group and restricted-nutrition (R) group.	94
Figure II-4.6 Relative expression of miRNAs and genes and their correlational analysis in fetal liver in full-nutrition (F) group and restricted-nutrition (R) group.....	95
Figure III-4.2 Gene ontology (GO) biological process annotations for fetal hepatic mRNAs displaying a maternal supplemental choline effect, without Choline x DHA interaction.	155
Figure III-4.3 Gene ontology (GO) biological process annotations for fetal hepatic mRNAs displaying a maternal supplemental DHA effect, without Choline x DHA interaction.	156
Figure III-4.4 Gene ontology (GO) biological process annotations for fetal hepatic mRNAs displaying a maternal supplemental choline x DHA interaction effect.	157
Figure III-4.7-1 Schema showing potential binding sites of miR-503 with LIPG mRNA.....	158
Figure III-4.7-4 Schema showing our hypothesized pathway	161
Figure IV-4.2 Transfection efficiency of liver organoids after 48 h of transfection	196
Figure IV-4.3-1 Cytotoxicity assay of liver organoids after 48 h of transfection.....	197
Figure IV-4.3-2 Cell viability assay of liver organoids after 48 h of transfection.....	198
Figure IV-4.4 LIPG gene expression assay of liver organoids after 48 h of transfection	199
Figure IV-4.5 LIPG western blot assay of liver organoids after 48 h of transfection	200
Figure IV-4.6 HDL measurement in culture medium after 48 h of transfection	201
Figure IV-4.7. Measurement of choline content in liver organoids treated with varying concentrations of choline after 96 h.....	202
Figure IV-4.8-1 LIPG mRNA expression level assay in liver organoids treated with varying concentrations of choline after 96 h.....	203
Figure IV-4.8-2 MiRNA-503 expression level assay in liver organoids treated with varying concentrations of choline after 96 h.....	204
Figure IV-5-1 Examples of isolated and growing three-dimensional (3D) pig liver organoids.	205

Chapter I: Literature Review

I-1. Prevalence of Maternal Undernutrition

Undernutrition includes stunting (low height-for-age), wasting (low weight-for-height), and insufficiencies in crucial vitamins and minerals (collectively known as micronutrients) as a manifestation of malnutrition. Another form of malnutrition arises from obesity or the excessive consumption of specific nutrients. The term hunger, originally signifying the discomfort resulting from not consuming food, is also employed to characterize undernutrition, particularly concerning food insecurity. This situation arises when individuals lack both the physical and economic means to access adequate, safe, nutritious, and culturally acceptable food to fulfill their dietary requirements (UN Millennium Project, 2005). Undernutrition stands as a significant factor influencing maternal and child health (Caulfield, et al., 2004; Ezzati, et al., 2004).

Maternal undernutrition is a global health concern that significantly impacts child health outcomes. Therefore, *The Lancet*, a prestigious medical journal, published a series of papers focusing on maternal and child undernutrition to raise awareness, promote research, and advocate for comprehensive strategies aimed at combating this critical global health issue. Based on that series published in 2008 (Black, et al., 2008), maternal undernutrition, which uses body-mass index (BMI) of less than 18.5 kg/m² as an index, is widespread in various areas: 17 of 33 countries in Africa, and 10 of 19 counties in Asia, where more than 10% of women aged 15 – 49 have a BMI of less than 18.5 kg/m². The situation is even worse in sub-Saharan Africa, south-central and southeastern Asia, and Yemen where over 20% of women have a BMI below 18.5 kg/m². India, Bangladesh, and Eritrea have approximately 40% of women experiencing low BMI levels. Maternal low BMI has adverse effects on pregnancy outcomes.

I-2. Consequences of Maternal Undernutrition in Their Offspring

Intrauterine Growth Restriction and Low Birthweight

Maternal undernutrition (BMI < 18.5) is linked to intrauterine growth restriction (IUGR), where the fetus doesn't reach its growth potential (Ezzati, et al., 2004). This can result in low birth weight, small size for gestational age, and potential complications during birth. Low birthweight (LBW) refers to babies born at full term (37 weeks of gestation) but weighing less than 2.5 kg. This category typically indicates IUGR due to maternal undernutrition. In developing countries, this condition affects approximately 10.8% of live births annually (De Onis, et al., 1998). Although poor fetal growth is seldom a direct cause of death, it can indirectly contribute to neonatal mortality, particularly due to birth asphyxia and infections, accounting for about 60% of such deaths (Black, et al., 2008). A study conducted in Nepal, India, Pakistan, and Brazil indicated that the risk of neonatal death associated with IUGR and LBW (Black, et al., 2008). Babies born at term with weights between 1.5 – 2.0 kg had an 8.1-fold increased likelihood of mortality, while those weighing 2.0 – 2.5 kg were 2.8 times more likely to die from all causes during the neonatal phase compared to infants born weighing over 2.5 kg. In studies conducted in South Asia, regarding deaths attributed to birth asphyxia, the relative risks were 5.4 for infants weighing 1.5 – 2.0 kg and 2.3 for those weighing 2.0 – 2.5 kg at birth. For infectious causes, the relative risks were 4.2 for babies weighing 1.5 – 2.0 kg and 2.0 for those weighing 2.0 – 2.5 g.

However, mothers with LBW tend to have a heightened likelihood of delivering a baby with LBW. Ramakrishnan and collaborators (Ramakrishnan, et al., 1999) demonstrated that with every 100 g increase in maternal birthweight, her child's birthweight increased by 10 – 20g. However, these studies were predominantly conducted in high-income nations. Contrastingly, in Guatemala, each 100 g increase in maternal birthweight correlated with a 29 g rise in birthweight

for the child, while each 1 cm increase in mother's birth length led to a 0.2 cm increase in the child's birth length. In India, maternal birthweight remains a robust predictor of offspring birth weight, even after considering adjustments for the mother's adult size (Leary, et al., 2006).

Height and Body Composition

Height development is influenced by both genetic and environmental factors throughout the growth phase. Inadequate maternal nutrition and maternal short stature and reserves correlate with a higher likelihood of IUGR (Black, et al., 2008). Various studies conducted in low-income and middle-income countries indicate a positive relationship between adult height and birth measurements, including birthweight and length. For instance, an increase of 1 cm in birth length corresponds to a 0.7–1 cm increase in adult height (Sachdev, et al., 2005; Adair, 2006).

A mother's nutritional status during pregnancy can influence the size and composition of her offspring's body by potentially creating enduring deficiencies in fetal lean body mass (Yajnik, et al., 2003). This process might alter the sensitivity of the hypothalamic-pituitary-adrenal axis (Matthews, 2002), impacting appetite and physical activity (Vickers, et al., 2000; Vickers, et al., 2003). Studies conducted in low-income and middle-income nations indicated that inadequate fetal nutrition primarily leads to enduring deficiencies in lean body mass rather than fat mass. In New Delhi (India) (Sachdev, et al., 2005) and Guatemala (Li, et al., 2003), birthweight exhibited a positive correlation with adult lean mass in both men and women. However, this association with fat mass or the sum of skinfolds was observed solely in women. Birth length demonstrated positive connections with adult lean mass and the sum of skinfolds among Indian men and women, fat mass among Guatemalan men and women, fat-free mass in Guatemalan men, and the percentage of body fat in Guatemalan women.

Achieved Schooling and Educational Performance

Lately, there's been a growing interest in exploring the potential link between birthweight and later cognitive abilities. Early studies primarily compared individuals with LBW against those with normal birthweights (Strauss, 2000; Ounsted, et al., 1983). These studies revealed a higher occurrence of neurological issues and/or weaker cognitive skills throughout childhood among LBW individuals. Subsequent investigations examined whether this connection remains consistent across the entire spectrum of birthweights within the normal range (Richards, et al., 2002; Sorenson, et al., 1997). Adults who were born LBW exhibited notable distinctions in their academic accomplishments and career achievements when compared to adults who were born with normal birthweights (NBW) (Richards, et al., 2002).

Differences in birth weight, ranging from the lowest to the highest, showed a significant and positive correlation with cognitive abilities at the age of 8. Moreover, birth weight also demonstrated a connection with education, indicating that individuals with higher birth weights were more inclined to attain advanced qualifications (Richards M, 2001). The average score on the intelligence quotient (IQ) test (Boerge Prien test) rose from 39.9 for a birth weight of < 2500 g to 44.6 for a birth weight of 4200 g, even after accounting for factors like gestational age, birth length, maternal age, parity, and other relevant variables. However, beyond a birth weight of 4200 g, there was a slight decrease in the test score (Sorenson, et al., 1997). The average IQ showed a steady increase in tandem with birth weight across the birth weight spectrum in both genders, as per a linear regression analysis involving one randomly selected sibling per family ($n = 1683$). This analysis was adjusted for maternal age, race, education, socioeconomic status, and birth order (Matte, et al., 2001). As birth weight increased, there was a notable enhancement in all childhood cognitive assessments and educational accomplishments. Examination of math scores at age 7 and the highest qualifications attained by age 33 revealed strong associations that

remained consistent even after considering potential influencing factors. For every kilogram rise in birth weight, the math z-score rose by 0.17 for males and 0.21 for females (Jefferis, et al., 2002). The overall conclusion drawn from these studies is that the relationship does persist across various birthweight ranges considered normal (Landon, et al., 2006).

Cardiovascular Disease

The potential biological mechanisms linking undernutrition to cardiovascular disease, which is a multifactorial disease, and the risk factors include blood pressure, lipid abnormalities, and diabetes (Cole, et al., 2021). Lower birthweight is also associated with increased carotid intima-media thickness, reduced arterial compliance, and impaired endothelial function—considered precursors to cardiovascular disease (Fall, 2006). A systematic review concluded that lower infant weight heightens the risk of coronary heart disease in men (Fisher, et al., 2006). In low-income and middle-income countries, limited evidence exists, primarily from a single study in India, which revealed an inverse correlation between coronary heart disease prevalence and birthweight after adjusting for adult BMI (Stein, et al., 1996).

Blood pressure is one of cardiovascular disease risk factors, and it has been linked to long-term influence by maternal diet during pregnancy. Maternal calcium supplementation has shown a capacity to lower offspring blood pressure, demonstrated in an Argentina trial (Belizan, et al., 1997). Low maternal fat stores or inadequate pregnancy weight gain were associated with increased blood pressure in Jamaican children (Clark, et al., 1998) and Filipino adolescents (Adair, et al., 2001). Numerous reviews and meta-analyses have examined the correlation between birthweight and adult blood pressure (Law & Shiell, 1996; Hardy, et al., 2006). Most studies, covering a broad spectrum of birthweights, indicate an inverse relationship between birthweight and systolic blood pressure, as well as the prevalence of hypertension in later life.

There are also less pronounced and less consistent inverse associations observed with diastolic blood pressure. These effects tend to intensify with age (Lawlor, et al., 2002).

Another risk factor of cardiovascular disease is blood lipid. It has been suggested that lower birth size contributes to current higher blood lipid concentrations and later in life, but it is still controversial. Few studies examining newborn size and lipid concentrations revealed a combined estimate of -1.39 mg/L total cholesterol per kilogram of birthweight (Huxley, et al., 2004). A considerable volume of research has explored the relationship between general birth size and elements of the lipid profile during adulthood. These published findings indicate an association suggesting an increase of 2.0 to 10.0 mg/dL in total blood cholesterol for every 1-kg decrease in general birth weight (Bavdekar, et al., 1999; Ziegler, et al., 2000). In other words, offspring born with LBW are more likely to experience elevated blood lipid concentrations in their later years. Similarly, inverse correlations have been observed between general birth size and blood levels of low-density lipoprotein (LDL) cholesterol, apolipoprotein B, and triglycerides. Another study (Mi, et al., 2000) conducted among individuals in Beijing aged 45 with a history of LBW concluded that LBW correlated with elevated triglyceride levels and decreased high-density lipoprotein (HDL) cholesterol levels. However, in Guatemala, there wasn't a correlation between general birthweight and serum lipids at 24 years old. Among men, there were indications of inverse trends regarding total cholesterol and LDL cholesterol, with borderline significance. In Brazil, general birthweight was not associated with total cholesterol, its fractions, or triglycerides, in 18-year-old men (Victora, et al., 2008). Overall, the existing research in this field remains limited. To draw definitive conclusions, longitudinal studies with substantial power, comprehensive data, and ongoing prospective follow-ups are necessary.

Type 2 Diabetes

Type 2 diabetes arises from both insulin resistance and a decrease in insulin secretion. The ‘thrifty phenotype hypothesis’, presented by (Hales & Barker, 1992), suggests that undernourished fetuses and infants undergo alterations— such as reduced growth of lean tissue, decreased insulin sensitivity, increased cortisol axis activity, and impaired pancreatic development—resulting in diabetes later in life. Animal studies provide robust evidence that maternal dietary deprivation leads to diabetes and insulin resistance in offspring (Ozanne & Hales, 1999; Armitage, et al., 2004).

Research findings present conflicting evidence regarding the impact of maternal size and nutrition on insulin resistance and type 2 diabetes. In India, poor glucose tolerance was linked to higher maternal weight (Fall, et al., 1998), while in China, it correlated with lower maternal BMI (Mi, et al., 2000). However, across high-income countries, consistent associations exist between lower birthweight and later development of type 2 diabetes and insulin resistance (Boyko, 2000). This risk is particularly pronounced in individuals who later become obese. Adjusting for adult BMI consistently strengthens the link with LBW, suggesting the significance of weight gain in later life. High birthweight is linked to an elevated risk of diabetes, particularly associated with maternal diabetes during pregnancy (Harder, et al., 2007). In low-income and middle-income countries, studies adjusting for adult weight show higher glucose concentrations in individuals with lower birthweight (Levitt, et al., 2000), whereas studies without adjustments show no associations (Stein, et al., 2002). Regarding diabetes and impaired glucose tolerance, associations varied across studies in different regions, but overall, it displayed positive associations with lower birthweight while few studies showed no link (Choi, et al., 2000; Victora, et al., 2008).

Immunodeficiency

Studies conducted in the Gambia indicate that individuals born during periods of limited

food availability exhibit 10-fold higher risk of infection-related mortality, suggesting alterations in their immune systems (Prentice & Moore, 2005). These changes may have long-term programming effects. In Pakistani adults (Moore, et al., 2004) and Filipino adolescents (McDade, et al., 2001), those with a lower birthweight exhibited reduced antibody responses to specific vaccines compared to those born weighing 2.5 kg or more. Additionally, a study in Gambia demonstrated that young adults born during the annual period of food scarcity were considerably more susceptible to succumbing to infections than those born during the rest of the year (Moore, et al., 1999). However, this finding wasn't replicated in similar settings with seasonal variability and elevated adult mortality due to infectious diseases (Kynast-Wolf G, 2006), nor in the Dutch famine study of 1944 (Roseboom, et al., 2001). Further investigations are necessary to determine the clinical significance of these findings for adults.

I-3. Current Research toward Dysfunction of Fetal Liver Induced by Maternal

Undernutrition

Maternal Undernutrition Modified Fetal Liver Functional Index

One of the objectives of our study is to investigate the impact of maternal undernutrition on liver metabolism. Here, we present a summary of the current research in this area. A maternal undernutrition experiment (Gao, et al., 2014) was conducted in late pregnancy 90 days on ewes. It concluded that 74% feed restriction caused decreased fetal liver weight, and several functional indices of liver such as, antioxidant capacity, superoxide dismutase activity, cholinesterase, total protein, globulin, and alanine transaminase activity were decreased in fetal liver. While it led to increases in fetal hepatic collagen fibers and reticular fibers, glutathione peroxidase activity, malondialdehyde, nitric oxide, nitric oxide synthase activity, monoamine oxidase activity, albumin/globulin ratio, and aspartate transaminase activity. These findings suggest that

inadequate maternal nutrition is linked to compromised fetal liver growth, fibrosis, imbalance in antioxidants, and impaired function.

Maternal Undernutrition Modified Pathway in Fetal Liver may Contribute to IUGR

A research team from the University of Western Ontario in Canada conducted a series of experiment focusing on maternal undernutrition and IUGR. Pregnant baboons were subjected to a 70% calorie restriction starting at gestational day 30. At gestational day 120 (with term set at 185 days), fetal liver tissue samples were collected. This investigation revealed a series of events, including the inhibition of mTOR, activation of amino acid response (AAR) and casein kinase (CK)2, heightened expression and phosphorylation of insulin-like growth factor (*IGF*) binding protein (*IGFBP*)-1 in the fetal liver, and an increase in the concentration and phosphorylation of *IGFBP-1* in cord plasma (Kakadia, et al., 2020). Importantly, their previous studies using primary baboon fetal hepatocytes and HepG2 cells demonstrated a mechanistic connection between mTOR inhibition, AAR activation, and the heightened expression and phosphorylation of *IGFBP-1* (Abu-Shehab, et al., 2014; Damerill, et al., 2016; Malkani, et al., 2015). This mechanism notably results in a substantial reduction in the bioavailability and bioactivity of *IGF-1* (Abu-Shehab, et al., 2013). Thus, it indicates that maternal undernutrition triggers the hyperphosphorylation of *IGFBP-1* in the fetal liver by inhibiting mTOR and activating both AAR and CK2. These molecular events subsequently lead to IUGR.

Maternal Undernutrition Modified Carbohydrate Metabolism in Fetal Liver

The impact of maternal undernutrition on the carbohydrate metabolism of offspring has been explored in multiple studies. Pregnant ewes were restricted to 50% food intake starting from day 28 to day 78 which later recovered to 100% throughout gestation and lactation. Adult ewe offspring undergoing maternal undernutrition exhibited higher and faster food consumption,

increased weight gain, and enhanced gain efficiency. They also displayed a reduced insulin sensitivity, elevated insulin secretion, and higher hepatic lipid and glycogen levels compared to offspring from control ewes (George, et al., 2012). Similarly, Jones *et al.* observed heightened expression of genes associated with gluconeogenesis/glycolysis, transcription factor regulation, and cytokine responses in the livers of IUGR fetal ewes. Additionally, there was a decrease in the expression of genes associated with cholesterol synthesis, amino acid degradation, and detoxification pathways (Jones, et al., 2019). Another study indicated that low-protein diets in rats induced hypomethylation in glucocorticoid receptor (*NR3C1*, formerly known as GR) in the offspring's liver (Lillycrop, et al., 2005). This shift in the epigenetic control of hepatic *NR3C1* expression could contribute to impaired carbohydrate metabolism.

Maternal Undernutrition Modified Lipid Metabolism in Fetal Liver

Several case studies were analyzed to understand the impact of maternal nutrition on lipid metabolism in fetal liver. Firstly, pregnant ewes were restricted to 30% intake for a period of 15 days starting from 115 day of gestation (Xue, et al., 2019). The transcriptome results from fetal hepatic samples revealed that maternal undernutrition induced changes in the overall transcriptome profile and metabolic pathways within the fetal liver. Specifically, in the livers of undernourished ewes' fetuses, there was an increase in fatty acid oxidation and ketogenesis, potentially linked to the activation of the peroxisome proliferator-activated receptor α (*PPAR α*) signaling pathway due to the upregulation of *PPAR α* . Conversely, processes related to cholesterol, steroid, and fatty acid synthesis were inhibited. Additionally, as indicated by RNA-seq analysis, maternal undernutrition led to a heightened triglyceride synthesis, reduced triglyceride degradation, and suppression of phospholipid synthesis and degradation within the fetal liver.

Secondly, a proteomic analysis was conducted on fetal rats exhibiting growth restriction due to maternal diet restriction by 50% from the 15th day onward, with birth weights falling below 2 standard deviations from the mean birth weight of the control group's offspring (Sarli, et al., 2021). Results from fetal liver proteomic analysis and IPA analysis revealed changed pathways, including induction of the super pathway of cholesterol biosynthesis, inhibition of thyroid hormone metabolism, fatty acid beta oxidation, and apelin liver signaling pathway.

Additionally, fetal livers with IUGR were obtained for microarray analysis from pregnant rats exposed to a 50% feed restriction. Results show that, within the PPAR signaling pathway, the fatty acid binding protein (*FABP*) family exhibited elevated *FABP4* and suppressed *FABP1*, *FABP2*, and *FABP7*. Similarly, the Acyl-CoA synthetase long-chain (*ACSL*) family showed upregulated *ACSL4* and downregulated *ACSL1*. Furthermore, in the adipocytokine signaling pathway, there was noticeable differential expression, with neuropeptide Y (*NPY*), solute carrier family (*SLC2a1*), NF-kappa-B inhibitor family (*NFKBIA*), protein kinase AMP-activated catalytic subunit alpha 2 (*PRKAA2*), and *PPARG* coactivator 1 alpha (*PPARGC1A*) being upregulated, and retinoid X receptor gamma (*RXRG*) being downregulated. These findings suggest that the PPAR signaling pathway could be a pivotal factor in the development of metabolic syndrome induced by IUGR (Shen, et al., 2022). Another similar study indicated that low-protein diets in rats induced hypomethylation in *PPARα* in the offspring's liver (Lillicrop, et al., 2005). This change in the epigenetic regulation of hepatic *PPARα* expression may play a role in disrupting fat metabolism. Lipoprotein metabolism is also disrupted in the fetal liver due to maternal undernutrition. During pregnancy, inadequate maternal nutrition (50% food-restricted) resulted in elevated hepatic triglycerides in 3-week-old male offspring of rats (Zhu, et al., 2016 May). Increased hepatic expression levels of liver X receptor-α (*LXRα*) and increased binding to

the potential *LXR* response elements within the lipoprotein lipase (*LPL*) promoter regions also were observed. Moreover, there was noticeable augmentation in histone H3 lysine 9 (*H3K9*) and *H3K14* acetylation around the *LPL* promoter. The author concluded that maternal undernutrition during pregnancy may lead to an increase in hepatic triglycerides, via alterations in the transcriptional and epigenetic regulation of the *LPL* gene.

I-4. Modification of Lipoprotein Metabolism in the Liver Is Crucial for Serum Cholesterol Levels

The liver plays a crucial role in controlling serum cholesterol levels. It manages cholesterol through five primary pathways, and any modifications to these pathways can lead to the accumulation of cholesterol in the liver (Zinkhan, et al., 2016). The initial pathway involves the liver's regulation of cholesterol by uptaking low-density lipoprotein (LDL) from the blood using the LDL receptor (LDLR). The second pathway is the export of high-density lipoprotein (HDL) to the blood facilitated by ATP binding cassette transporter g1 (ABCG1) and ATP binding cassette subfamily A member 1 (ABCA1). The third pathway includes the export of very low-density lipoprotein (VLDL) to the blood through fatty acid synthase (FASN), acetyl-coA carboxylase (ACC), and microsomal transferase protein (MTP). The fourth pathway encompasses cholesterol metabolism into bile acids via key proteins liver X receptor α (*LXR α*) and cytochrome P450 family 7 subfamily A member 1 (*CYP7A1*). Lastly, the fifth pathway involves the de novo synthesis of cholesterol via sterol-responsive element-binding protein 2 (*SREBP2*) and 3-hydroxy-3-methylglutaryl-CoA reductase (*HMGCR*). These interconnected pathways collaboratively regulate both serum and hepatic cholesterol levels.

Evidence from an illustrative case study demonstrated this phenomenon. A low-protein diet during pregnancy programmed atherosclerosis development in ApoE3-Leiden mice, known

for a heightened susceptibility to atherosclerosis with a cholesterol-rich diet. Fetal exposure to protein restriction led to increased dyslipidemia in mice on an atherogenic diet, with low-protein-exposed ApoE3 mice having significantly higher total plasma cholesterol and triglycerides compared to those on a control diet in utero. The DNA array analysis indicated that low-density lipoprotein receptor (*LDLR*) and retinoid X receptor (*RXR*) were downregulated, suggesting the potential role of disordered lipoprotein metabolism in fetal programming of atherosclerosis (Yates, et al., 2009).

I-5. The Development of Atherosclerotic Cardiovascular Disease is Related to High-Density Lipoprotein Metabolism in Liver

Cardiovascular disease (CVD) stands as the primary cause of global mortality. Statistics from 2019 revealed approximately 17.9 million deaths attributed to CVDs, accounting for 32% of all worldwide fatalities (World Health Organization, 2021). Among these, 85% were linked to heart attacks and strokes triggered by cholesterol plaque accumulation within blood vessel walls, causing arterial blockage and impeding blood flow and this progression known as atherosclerosis (AS) (Levinson & Wagner, 2015). The development of AS involves a sequence of pathological events, encompassing disruptions in lipid metabolism, inflammation, oxidative stress, and the creation of foam cells, in which dyslipidemia is considered to be one of most important factors (Zhang, et al., 2022).

The disruption in cholesterol metabolism is widely recognized as the basis for the onset and progression of AS. Cholesterol balance is primarily controlled through intestinal cholesterol absorption, hepatic synthesis of cholesterol, and its excretion (Yin, et al., 2019). Notably, the liver plays a predominant role in managing cholesterol metabolism through de novo synthesis and reverse cholesterol transport (RCT) pathway (Kiamehr, et al., 2017). Firstly, liver is a

primary site for endogenous cholesterol production within the body. Aberrant synthesis and uptake of hepatic cholesterol often elevate plasma cholesterol levels, leading to the accumulation of cholesterol outside the liver and the formation of atherosclerotic plaques at sites of vascular injury (Yu, et al., 2019). Secondly, RCT refers to the mechanism through which cholesterol exits cells within peripheral tissues (including foam cells within atherosclerotic plaques), enters the bloodstream, and ultimately gets eliminated through feces (Ouimet, et al., 2019). The equilibrium between transporting lipoproteins from the liver to peripheral tissues and the process of RCT maintains the proper levels of cholesterol in circulation. In contrast, disrupted RCT results in heightened lipid buildup within the aortic wall, and then triggers the conversion of macrophages into foam cells, serving as significant risk factors for atherosclerosis (Zhang, et al., 2022).

Together, maternal undernutrition led to a multitude of functional and metabolic changes in the fetal liver. Present investigations primarily concentrate on the mRNA level, with less emphasis on exploring the role of microRNA (miRNA) and its regulatory impact on metabolism. To address this gap in understanding, our study aimed to investigate the involvement of miRNA, an essential epigenetic regulatory machinery, in the fetal liver concerning maternal undernutrition. In this context, we initially address the concept of epigenetics and its potential to influence fetal development in response to maternal undernutrition.

I-6. Maternal Undernutrition Alters Fetal Liver Gene Expression through Epigenetic Mechanisms

Epigenetics encompasses alterations in gene expression that arise not from DNA sequence changes but from modifications to the DNA structure itself. These modifications typically result from factors like nutrients, physical condition, and environmental elements, such

as dietary patterns, physical activity, exposure to harmful substances, and genetic influences (Feinberg, 2018). Epigenetics plays a significant role in fetal development, influencing how genes are expressed and regulated during critical stages of growth in the uterus. Over recent years, the increasing evidence indicates that genome-wide epigenetic status is established starting from early life, while different cell types have different epigenetic patterns carried through later life (Zeisel, 2017). Thus, epigenetic patterns in early life have an impact on organ's function and metabolism in later life. According to the latest definition, epigenetic controls encompass DNA methylation, modifications to histones, and the regulation by noncoding RNA, such as miRNA.

The Role of miRNA in mRNA Regulation and Fetal Development

MiRNAs represent an essential epigenetic regulatory mechanism. They are short, noncoding endogenous RNAs of 20–27 nucleotides in length, which are processed from DNA sequences into primary miRNA, precursor miRNAs and mature miRNAs (O'Brien, et al., 2018). The biological function of miRNAs is post-transcriptional regulation of gene expression (Ameres & Zamore, 2013). Typically, miRNAs engage with the 3 prime untranslated region (3'UTR) of target mRNAs, leading to translational repression and degradation (Ambros, 2004). It has been estimated that up to 60% of protein-coding genes are under modulation of miRNA in the human genome (Friedman, et al., 2009). Thus, miRNAs possess the capacity to regulate a variety of messenger RNA targets, enabling them to influence numerous developmental processes. However, only a limited number of miRNAs have been extensively documented in terms of their functions to date.

In recent years miRNA Target-Prediction Strategies have been applied to study the biological function of miRNA. The miRNA sequence is complementary to the 3'-untranslated region (3'-UTR) sequence of possible mRNA's targets. Seed sequence of a miRNA, which is

defined as the first 2 – 7 nucleotides in its 5'-region, is considered critical for mRNA targeting. Most of the available target prediction algorithms require Watson-Crick pairing (adenosine pairs with uracil and guanine pairs with cytosine) with the targeted sites (Akhtar, et al., 2019). Since numerous algorithms and software are evolving to predict targets of miRNAs, more miRNA-mRNA interactions and mechanisms will be revealed in the future. In our study, maternal undernutrition related miRNA and mRNA regulation in liver will be explored.

The Role of DNA Methylation in miRNA and mRNA Regulation

DNA methylation is another integral epigenetic regulation mechanism which generally refers to the addition of methyl groups to the DNA molecule. It happens primarily on the 5-carbon of the cytosine residues of Cytidine-Guanine dinucleotides (CpG, p indicates a phosphate group between the two nucleotides) and it was proposed as a “silencing” epigenetic mark (Jones, 2012). Around 70–80% of CpG sites in the mammalian genome are estimated to undergo methylation (Jörg, 2010). DNA methylation affects gene transcription through the methylation of DNA itself because it may physically interfere with the recruitment and binding of transcriptional proteins to the gene (Mun-Kit Choy, 2010). Additionally, methylated DNA may be bound by other proteins and then alter chromatin structure that also impacts gene transcription (Veronika, et al., 2019). DNA methylation can not only repress mRNA transcription but also hinder the expression of miRNA by suppressing the transcription of genes responsible for coding miRNA. It is approximately 10% of miRNA expression is under the control of DNA methylation (Macfarlane & Murphy, 2010). The methylation level in fetal liver is closely related to the availability of maternal one-carbon resources (Lima, et al., 2017), with a particular emphasis on choline in our study.

I-7. The Role of Maternal Choline in Fetal Liver Development

One of the objectives of our study was to explore the influence of choline on liver metabolic impairment induced by maternal undernutrition. Choline, a crucial dietary element, is essential for the normal functioning of every cell. It, along with its metabolites, plays a key role in maintaining the structural integrity and signaling functions of cell membranes. Choline, upon entering the brain, might initially enter a storage reserve and then convert to acetylcholine by choline acetyltransferase (Blusztajn & Wurtman, 1983). Acetylcholine is a crucial neurotransmitter—a chemical messenger that transmits signals across nerve synapses. Without adequate choline, the production of acetylcholine would be limited, impacting nerve signaling and various functions dependent on this neurotransmitter (Zeisel & Blusztajn, 1994).

Choline also has a major role involved in DNA methylation, especially during fetal development (Niculescu, et al., 2006). With the assistance of riboflavin (B-2), pyridoxine (B-6), folate (B-9), and cobalamin (B-12), choline contributes methyl groups for the synthesis of S-adenosylmethionine (SAM), a vital methyl donor pivotal for the process of DNA methylation (Kok, et al., 2015). SAM provides a methyl group to DNA molecules, adding methyl groups to cytosine residues (Kovacheva, et al., 2007). DNA methylation alters accessibility to cellular machinery responsible for gene transcription into proteins, impacting various diseases.

Additionally, choline serves as a fundamental precursor in synthesizing membrane phospholipids – phosphatidylcholine. As a major component of mammalian cell membranes, phosphatidylcholine plays indispensable roles in cell membrane structure, cell signaling, fat transport, and other physiological processes (Ridgway, 2013). Furthermore, it can combine with docosahexaenoic acid (DHA) to form phosphatidylcholine- DHA, although its specific benefits are not extensively studied (Patrick, 2019).

While vitamins B2, B6, B9 and B12 are well-known involved in animal one-carbon

metabolism, choline appears to have a distinct role in epigenetic regulation. Acting as a biological bridge connecting one-carbon and lipid metabolism, choline can be converted to betaine, providing three methyl units for the remethylation of homocysteine to methionine, whereas betaine cannot be converted back to choline (Zeisel, 2017). Folic acid and other vitamins involved in one-carbon metabolism are abundant in leafy green vegetables, beans, peas, beets, and various plant-based foods, while choline is primarily sourced from soy, egg yolks, and other meat or soy-based products (Thus, in our experiment, isolated soy protein was used instead of soybean meal in order to minimize the choline content of the basal diet) (Zeisel & Blusztajn, 1994). This discrepancy in food sources raises concerns about the risk of inadequate choline intake, particularly in impoverished populations in developing countries. However, it remains unclear whether the effects of choline deficiency on DNA methylation are primarily due to its impact on one-carbon metabolism, DHA metabolism, or a combination of both. Consequently, our project incorporated an examination of another essential nutrient, DHA.

I-8. The Role of Maternal Docosahexaenoic acid in Fetal Liver Development

In addition to choline, our study also aims to investigate the impact of DHA on liver metabolism impairment induced by maternal undernutrition. Furthermore, we examined their potential interaction effects. DHA, one of omega-3 long-chain polyunsaturated fatty acids (LC-PUFA), offering a diverse range of health advantages (Su, et al., 2008). DHA becomes part of various bodily components, including cell membranes (Lazzarin, et al., 2009), contributing to anti-inflammatory functions and impacting cell membrane fluidity (Smith, et al., 2011). The presence of DHA is crucial for fetal development and supports healthy aging (Dunstan, et al., 2007). DHA is distributed in different tissues of the body (Lacombe, et al., 2018), with a notable concentration in the brain and retina. Its presence in these areas is crucial for normal neurological

and visual function. The liver also plays a role in the storage and release of DHA, helping to maintain adequate levels throughout the body.

Recently, there's a growing recognition of the significance of fatty acids in this context (Ramakrishnan, et al., 2010). DHA holds a greater significance in ensuring proper cell membrane functionality and plays a crucial role in fetal brain and retina development (Ramakrishnan, et al., 2010). In the third trimester of pregnancy, substantial quantities of DHA accumulate in fetal tissues. Among these, the retina and brain show the highest infiltration, potentially contributing to regular eyesight and optimal brain function (Dunstan, et al., 2008). A study revealed that infants whose mothers received DHA supplementation during pregnancy exhibited notably improved problem-solving abilities at 9 months old (Judge, et al., 2007). Another study evaluated children 2.5 years after mothers took DHA+ EPA (Eicosapentaenoic acid, another LC-PUFA) supplements from the 20th week of pregnancy until delivery. Children from the supplemented group showed notably improved eye and hand coordination scores compared to the placebo group (Furuhjelm, et al., 2009).

Additionally, DHA is presumed to benefit cardiovascular health. First, DHA can lower triglyceride levels in the bloodstream, contributing to a healthier lipid profile. After fish oil supplementation, a decrease in plasma triglycerides and an increase in platelet phospholipid arachidonic acid and plasma HDL were noted (Lovegrove, et al., 2004). Simultaneously, there were elevations in plasma HDL, platelet phospholipid EPA, and DHA levels. These effects stemmed from a reduced hepatic very-low-density lipoprotein (VLDL) synthesis, decreased hepatic enzyme activity in triglyceride synthesis, and enhanced hepatic phospholipid synthesis (Jump, 2011). Second, it possesses anti-inflammatory effects, which may help mitigate chronic inflammation associated with cardiovascular disease (CVD). DHA has been observed to

diminish inflammatory markers like interleukin-1 beta (IL-1 β), tumor necrosis factor alpha (TNF- α), and IL-6. The potential of using DHA in treating inflammation-linked diseases has been illustrated (Honda, et al., 2015). Third, DHA supports the proper functioning of endothelial cells lining blood vessels, promoting better vasodilation and blood flow regulation (Yamagata, 2017). Moreover, supplementation of DHA in clinical study has been shown to prevent coronary heart disease, stroke, and total mortality after stroke and alleviate arteriosclerosis and hypertension in humans (Mori, 2014).

Thus, considering the limitations mentioned and current practices, advocating for choline and DHA supplementation in pregnancy becomes crucial in addressing adverse outcomes of offspring caused by maternal undernutrition.

I-9. Significance of Pig Model in Addressing Maternal Undernutrition

Pigs are valuable models for studying the effects of maternal nutrition on offspring due to several advantages. 1. Prevalence LBW or IUGR: the prevalence of LBW littermates in pigs, usually numbering between one to two per litter, simplifies the exploration of naturally occurring IUGR in humans. 2. Dual Benefits: This dual benefit, contributing to both agriculture and medicine, coined the term "agrimedical research," demonstrating a judicious and effective utilization of federal research funding. Discoveries from pig-based research not only stand to enhance pork production efficiency but also enable profound insights into the mechanistic aspects of nutrient functionality (Odle, et al., 2014). 3. Similarities to Humans: Pigs share physiological similarities with humans, especially in their digestive system, metabolism, organ development, and immune responses. This similarity facilitates studies that involve assessing the impact of maternal nutrition on organ development and function in offspring (Odle, et al., 2014). 4. Gestation Period: The gestation period of pigs is closer to humans compared to mice or other

commonly used animal models. This similarity allows researchers to study the impact of maternal nutrition on fetal development over a period more akin to human pregnancies. 5. Reproductive Features: Litter sizes commonly surpass 10 piglets, enabling the application of statistical blocking designs in nutrition studies to accommodate genetic diversity. 6. Feasibility of Dietary Manipulation: Pigs can be easily fed controlled diets, making it feasible to study specific nutritional interventions and their effects on offspring development.

I-10. Conclusions and Rationale

Severe maternal undernutrition leads to significant rises in mortality rates and the overall burden of disease on offspring. We focus on the beneficial effect of maternal supplementation of choline and DHA on alleviating adverse outcomes caused by maternal undernutrition. Our research used swine as a model other than rats or mice because swine experience the most severe IUGR, and newborn pig mortality contributes to substantial economic loss in the US.

Firstly, we used high-throughput sequencing on fetal liver tissue from dams with regular feeding (control) and those experiencing maternal undernutrition to acquire miRNA and mRNA expression profiles from the same liver sample in the offspring. This method enabled the identification of new mRNAs and miRNAs showing differential expression triggered by maternal undernutrition. Moreover, undernutrition related metabolic pathway will be revealed, which provides evidence to evaluate the long-term consequence. We may also find out multiple miRNA–mRNA regulatory connections that influence several crucial pathways triggered by maternal undernutrition.

Secondly, we conducted a factorial analysis, in which the influences of the 2 factors \pm choline and \pm DHA and their interactions on hepatic metabolism in offspring from dams with limited feed intake were evaluated via mRNA and miRNA sequencing. We gained a big picture

of how choline, DHA and their interaction impact the mRNA and miRNA profile and fetal programming via epigenetic regulation. More importantly, we identified several miRNA-mRNA regulatory pathways in their offspring associated with maternal supplemental choline, DHA and their interaction effect. That would reveal the key role of choline and DHA in fetal programming through miRNA regulation and their beneficial effect on offspring in supplemented diet during pregnancy.

Thirdly, we proposed a regulatory pathway from the result of miRNA-mRNA sequencing analysis. It starts with choline regulating miR-503 expression in the liver by influencing DNA methylation. Reduced methylation in the miR-503 gene's promoter region increases miR-503 production. This released miR-503 diminishes *LIPG* mRNA stability and inhibits *LIPG* translation, lowering LIPG protein production. This reduction elevates HDL-C levels by limiting HDL-C breakdown and excretion, aiding in cholesterol removal, preventing plaque formation, and reducing the risk of stroke, heart attack, and other ASCVDs. We tested the pathway using pig liver organoids and tried to examine the regulatory role of miR-503 enrichments on LIPG gene expression and HDL concentration. This provides another road for further investigation in understanding HDL regulation, with potential benefits for ASCVD. Additionally, it underscores the importance of choline intake during pregnancy for the health of offspring.

I-11. References

- Abu-Shehab, M. et al., 2014. Liver mTOR controls IGF-I bioavailability by regulation of protein kinase CK2 and IGFBP-1 phosphorylation in fetal growth restriction. *Endocrinology*, Volume 155, p. 1327–1339.
- Abu-Shehab, M. et al., 2013. Phosphorylation of IGFBP-1 at discrete sites elicits variable effects on IGF-I receptor autophosphorylation. *Endocrinology*, Volume 154, p. 1130–1143.
- Adair, L., 2006. Size at birth and growth trajectories to young adulthood. *Am J Hum Biol*, Volume 19, p. 327–37.
- Adair, L., Kuzawa, C. & Borja, J., 2001. Maternal energy stores and diet composition during pregnancy program adolescent blood pressure.. *Circulation*, p. 104:1034–1039.
- Akhtar, M. et al., 2019. A Practical Guide to miRNA Target Prediction. *Methods in molecular biology (Clifton, N.J.)*, Volume 1970, p. 1–13.
- Ambros, V., 2004. The functions of animal microRNAs. *Nature*, Volume 431, pp. 350–355.
- Ameres, S. L. & Zamore, P. D., 2013. Diversifying microRNA sequence and function. *Nature reviews. Molecular cell biology*, 14(8), p. 475–488.
- Armitage, J. et al., 2004. Developmental programming of the metabolic syndrome by maternal nutritional imbalance: how strong is the evidence from experimental models in mammals?. *J Physiol*, p. 561:355–377.
- Bavdekar, A. et al., 1999. Insulin resistance syndrome in 8-year-old Indian children: small at birth, big at 8 years, or both?. *Diabetes*, pp. 48:2422–2429.
- Belizan, J., Villar, J. & Bergel, E., 1997. Long-term effect of calcium supplementation during pregnancy on the blood pressure of offspring: follow up of a randomised controlled trial.. *BMJ*, p. 315:281–285.

Black, R. et al., 2008. Maternal and child undernutrition: global and regional exposures and health consequences. *The Lancet Journal*, pp. 19;371(9608):243-60.

Blusztajn, J. & Wurtman, R., 1983. Choline and cholinergic neurons. *Science*, p. 221:614–20.

Boyko, E., 2000. Proportion of type 2 diabetes cases resulting from impaired fetal growth.. *Diabetes Care*, p. 23:1260–1264.

Caulfield, L., de Onis, M., Blossner, M. & Black, R., 2004. Undernutrition as an underlying cause of child deaths associated with diarrhea, pneumonia, malaria, and measles.. *Am J Clin Nutr*, p. 80: 193–98.

Choi, C., Kim, C. & Lee, W., 2000. Association between birth weight and insulin sensitivity in healthy young men in Korea: role of visceral adiposity.. *Diabetes Res Clin Pract*, p. 49:53–59.

Clark, P. et al., 1998. Weight gain in pregnancy, triceps skinfold thickness, and blood pressure in offspring.. *Obstet Gynecol*, p. 91:103–107.

Cole, J. et al., 2021. *Atherosclerotic cardiovascular disease in hyperalphalipoproteinemia due to LIPG variants.*, 15(1):142-150.e2.: J Clin Lipidol.

Damerill, I. et al., 2016. Hypoxia increases IGFBP-1 phosphorylation mediated by mTOR inhibition. *Mol Endocrinol*, Volume 30, p. 201–216.

De Onis, M., Blössner, M. & Villar, J., 1998. Levels and patterns of intrauterine growth retardation in developing countries. *European Journal of Clinical Nutrition*, Volume 52 Suppl 1, pp. S5-15.

Dunstan, J. et al., 2007. The effects of fish oil supplementation in pregnancy on breast milk fatty acid composition over the course of lactation: a randomized controlled trial. *Pediatr Res*, p. 62:689–94.

Dunstan, J., Simmer, K., Dixon, G. & Prescott, S., 2008. Cognitive assessment of children at age

2(1/2) years after maternal fish oil supplementation in pregnancy: a randomised controlled trial. *Arch Dis Child Fetal Neonatal Ed*, p. 93:F45–50.

Ezzati, M., Lopez, A. D., Rodgers, A. & Murray, C. J., 2004. *Comparative Quantification of Health Risks: Global and Regional Burden of Disease Attributable to Selected Major Risk Factors*. Geneva: World Health Organization.

Fall, C., 2006. *Developmental origins of cardiovascular disease, type 2 diabetes and obesity in humans. Early life origins of health and disease..* New York:: Springer Science.

Fall, C., Stein, C. & Kumaran, K., 1998. Size at birth, maternal weight, and type 2 diabetes in South India.. *Diabet Med*, p. 15:220–227.

Feinberg, A. P., 2018. The Key Role of Epigenetics in Human Disease Prevention and Mitigation.. *The New England journal of medicine*, pp. 378(14), 1323–1334.

Fisher, D., Baird, J. & Payne, L., 2006. *Are infant size and growth related to burden of disease in adulthood? A systematic review of literature..* Int J Epidemiol.: 35:1196–1210.

Friedman, R., Farh, K., Burge, C. & Bartel, D., 2009. Most mammalian mRNAs are conserved targets of microRNAs. *Genome research*, pp. 19(1), 92–105.

Furuhjelm, C. et al., 2009. Fish oil supplementation in pregnancy and lactation may decrease the risk of infant allergy. *Acta Paediatr*, p. 98:1461–7.

Gao, F. et al., 2014. Effects of maternal undernutrition during late pregnancy on the development and function of ovine fetal liver.. *Anim Reprod Sci.*, pp. 147(3-4):99-105.

González-Becerra, K. et al., 2019. Fatty acids, epigenetic mechanisms and chronic diseases: a systematic review. *Lipids in health and disease*, 18(1), p. 178.

Hales, C. & Barker, D., 1992. Type 2 (non-insulin-dependent) diabetes mellitus: the thrifty phenotype hypothesis.. *Diabetologia*, pp. 35, 595–601.

Harder, T. et al., 2007. Birth weight and subsequent risk of type 2 diabetes: a meta-analysis.. *Am J Epidemiol*, p. 165:849–857.

Hardy, R., Sovio, U. & King, V., 2006. Birthweight and blood pressure in five European birth cohort studies: an investigation of confounding factors.. *Eur J Public Health*, p. 16:21–30.

Honda, K. et al., 2015. Docosahexaenoic acid differentially affects TNF α and IL-6 expression in LPS-stimulated RAW 264.7 murine macrophages. *Prostaglandins Leukot Essent Fatty Acids*, p. 97:27–34.

Huxley, R. et al., 2004. Birth Weight and Subsequent Cholesterol Levels: Exploration of the “Fetal Origins” Hypothesis. *JAMA*, p. 292(22):2755–2764.

Jefferis, B., Power, C. & Hertzman, C., 2002. Birthweight, childhood socioeconomic environment, and cognitive development in the 1958 British birth cohort study. *BMJ*, pp. 325, 305–11.

Jones, A. et al., 2019. Differential effects of intrauterine growth restriction and a hypersinsulinemic-isoglycemic clamp on metabolic pathways and insulin action in the fetal liver. *Am J Physiol Regul Integr Comp Physiol*, 316(5), pp. R427-R440.

Jones, P. A., 2012. Functions of DNA methylation: islands, start sites, gene bodies and beyond. *Nature reviews. Genetics*, pp. 13(7), 484–492..

Jörg, T., 2010. DNA methylation: an introduction to the biology and the disease-associated changes of a promising biomarker. *Molecular biotechnology*, pp. 44(1), 71–81.

Judge, M., Harel, O. & Lammi-Keefe, C., 2007. Maternal consumption of a docosahexaenoic acid-containing functional food during pregnancy: benefit for infant performance on problem-solving but not on recognition memory tasks at age 9 mo. *Am J Clin Nutr*, p. 85:1572–7.

Jump, D., 2011. Fatty acid regulation of hepatic lipid metabolism. *Curr Opin Clin Nutr Metab*

Care, p. 14:115–120.

Kakadia, J. et al., 2020. Hyperphosphorylation of fetal liver IGFBP-1 precedes slowing of fetal growth in nutrient-restricted baboons and may be a mechanism underlying IUGR. *Am J Physiol Endocrinol Metab*, 319(3), pp. E614-E628.

Kiamehr, M. et al., 2017. Lipidomic profiling of patient-specific iPSC-derived hepatocyte-like cells.. *Dis Model Mech*, pp. 10(9):1141-1153.

Kok, D. et al., 2015. The effects of long-term daily folic acid and vitamin B12 supplementation on genome-wide DNA methylation in elderly subjects. *Clinical epigenetics*, pp. 7, 121.

Kovacheva, V. et al., 2007. Gestational choline deficiency causes global and Igf2 gene DNA hypermethylation by up-regulation of Dnmt1 expression. *The Journal of biological chemistry*, pp. 282(43), 31777–31788.

Kynast-Wolf G, H. G. M. O. K. B. B. H., 2006. Season of death and birth predict patterns of mortality in Burkina Faso.. *Int J Epidemiol.* , p. 352:427–435.

Landon, J., Davison, M. & Breier, B., 2006. The developmental environment: influences on subsequent cognitive function and behaviour. In: Gluckman P, Hanson M, eds. In: *Developmental Origins of Health and Disease*. Cambridge: Cambridge University Press, pp. 370-378.

Law, C. & Shiell, A., 1996. Is blood pressure inversely related to birth weight? The strength of evidence from a systematic review of the literature.. *J Hypertens*, p. 14:935–941.

Lawlor, D., Ebrahim, S. & Davey, S. G., 2002. Is there a sex difference in the association between birth weight and systolic blood pressure in later life? Findings from a meta-regression analysis.. *Am J Epidemiol*, p. 156:1100–1104.

Lazzarin, N. et al., 2009. Low-dose aspirin and omega-3 fatty acids improve uterine artery blood

flow velocity in women with recurrent miscarriage due to impaired uterine perfusion. *Fertil Steril*, p. 92:296–300.

Leary, S., Fall, C. & Osmond, C., 2006. Geographical variation in relationships between parental body size and offspring phenotype at birth. *Acta Obstet Gynecol Scand*, p. 85:1066–1079.

Levinson, S. & Wagner, S., 2015. Implications of reverse cholesterol transport: recent studies. *Clin Chim Acta*, Volume 439, pp. 154-61.

Levitt, N. et al., 2000. Impaired glucose tolerance and elevated blood pressure in low birth weight, nonobese, young south african adults: early programming of cortisol axis.. *J Clin Endocrinol Metab*, p. 85:4611–4618.

Li, H. et al., 2003. Associations between prenatal and postnatal growth and adult body size and composition.. *Am J Clin Nutr*, p. 77:1498–1505.

Lillycrop, K. et al., 2005. Dietary protein restriction of pregnant rats induces and folic acid supplementation prevents epigenetic modification of hepatic gene expression in the offspring.. *J Nutr*, p. 135:1382–1386.

Lima, H. et al., 2017. Supplementation of Maternal Diets with Docosahexaenoic Acid and Methylating Vitamins Impacts Growth and Development of Fetuses from Malnourished Gilts.. *Current developments in nutrition*, pp. 2(3), nzx006..

Lovegrove, J. et al., 2004. Moderate fish-oil supplementation reverses low-platelet, long-chain n-3 polyunsaturated fatty acid status and reduces plasma triacylglycerol concentrations in British indo-Asians. *Am J Clin Nutr*, p. 79:974–982.

Macfarlane, L. & Murphy, P., 2010. MicroRNA: Biogenesis, Function and Role in Cancer. *Current genomics*, 11(7), p. 537–561.

Malkani, N., Jansson, T. & Gupta, M., 2015. IGFBP-1 hyperphosphorylation in response to

leucine deprivation is mediated by the AAR pathway. *Mol Cell Endocrinol* , Volume 412, p. 182–195.

Matte, T., Bresnahan, M., Begge, M. & Susser, E., 2001. Influence of variation in birthweight within normal range and within sibships on IQ at age 7 years: cohort study. *BMJ*, pp. 323, 310–14.

Matthews, S., 2002. Early programming of the hypothalamo-pituitary-adrenal axis. *Trends Endocrinol Metab*, p. 13:373–380.

McDade, T., Beck, M., Kuzawa, C. & Adair, L., 2001. Prenatal undernutrition, postnatal environments, and antibody response to vaccination in adolescence.. *Am J Clin Nutr.*, p. 74:543–548.

Mi, J. et al., 2000. Effects of infant birthweight and maternal body mass index in pregnancy on components of the insulin resistance syndrome in China.. *Ann Intern Med*, p. 132:253–260.

Moore, S. et al., 1999. Prenatal or early postnatal events predict infectious deaths in young adulthood in rural Africa. *Int J Epidemiol.*, Volume 28, p. 1088–1095.

Moore, S. et al., 2004. Birth weight predicts response to vaccination in adults born in an urban slum in Lahore, Pakistan.. *Am J Clin Nutr.*, Issue 80, p. 453–459.

Mori, T., 2014. Dietary n-3 PUFA and CVD: a review of the evidence. *Proc Nutr Soc*, Volume 73, p. 57–64.

Mun-Kit Choy, M. M. H.-G. G. M. R. B. T. A. D. R. S. Y. F., 2010. Genome-wide conserved consensus transcription factor binding motifs are hyper-methylated. *BMC genomics*, pp. 11, 519.

Niculescu, M. D., Craciunescu, C. N. & Zeisel, S. H., 2006. Dietary choline deficiency alters global and gene-specific DNA methylation in the developing hippocampus of mouse fetal brains. *FASEB journal : official publication of the Federation of American Societies for Experimental*

Biology, pp. 20(1), 43–49.

O'Brien, J., Hayder, H., Zayed, Y. & Peng, C., 2018. Overview of microRNA biogenesis, mechanisms of actions, and circulation. *Front Endocrinol*, Volume 9 , p. 402.

Odle, J. et al., 2014. The suckling piglet as an agrimedical model for the study of pediatric nutrition and metabolism.. *Annu Rev Anim Biosci.*, pp. 2:419-44.

Ouimet, M., Barrett, T. & Fisher, E., 2019. HDL and Reverse Cholesterol Transport: Basic Mechanisms and their Roles in Vascular Health and Disease. *Circ Res*, p. 124(10): 1505–1518.

Ounsted, M., Moar, V. & Scott, A., 1983. Small-for-dates babies at the age of four years: health, handicap, and developmental status.. *Early Hum. Dev.*, pp. 8, 243–58.

Ozanne, S. & Hales, C., 1999. The long-term consequences of intra-uterine protein malnutrition for glucose metabolism. *Proc Nutr Soc*, p. 58:615–619.

Prentice, A. & Moore, S., 2005. Early programming of adult diseases in resource poor countries. *Arch Dis Child*, Volume 90, p. 429–32.

Ramakrishnan, U., Martorell, R., Schroeder, D. & Flores, R., 1999. Role of intergenerational effects on linear growth. *J Nutr*, p. 129(suppl):544S–549S.

Ramakrishnan, U. et al., 2010. Effects of docosahexaenoic acid supplementation during pregnancy on gestational age and size at birth: randomized, double-blind, placebo-controlled trial in Mexico. *Food Nutr Bull*, p. 31:S108–16.

Richards, M., Hardy, R., Kuh, D. & Wadsworth, M., 2002. Birthweight, postnatal growth and cognitive function in a national UK birth cohort.. *Int. J. Epidemiol*, pp. 31, 342–8.

Roseboom, T. et al., 2001. Adult survival after prenatal exposure to the Dutch famine 1944-45. *Paediatr Perinat Epidemiol*, Volume 15, p. 220–25.

Sachdev, H., Fall, C. & Osmond, C., 2005. Anthropometric indicators of body composition in

young adults: relation to size at birth and serial measurements of body mass index in childhood in the New Delhi birth cohort.. *Am J Clin Nutr.*, p. 82:456–466.

Sarli, P. et al., 2021. Liver Proteome Profile of Growth Restricted and Appropriately Grown Newborn Wistar Rats Associated With Maternal Undernutrition. *Front Endocrinol (Lausanne)*, Volume 12, p. 684220.

Shen, Z., Zhu, W. & Du, L., 2022. Analysis of Gene Expression Profiles in the Liver of Rats With Intrauterine Growth Retardation. *Front Pediatr*, Volume 10, p. 801544.

Smith, G. et al., 2011. Dietary omega-3 fatty acid supplementation increases the rate of muscle protein synthesis in older adults: a randomized controlled trial. *Am J Clin Nutr*, p. 93:402–12.

Sorenson, H. et al., 1997. Birthweight and cognitive function in young adult life: historical cohort study.. *BMJ*, pp. 315, 401–3.

Stein, A. et al., 2002. Cardiovascular disease risk factors are related to adult adiposity but not birth weight in young guatemalan adults.. *J Nutr*, p. 132:2208–2214.

Stein, C. et al., 1996. *Fetal growth and coronary heart disease in south India*.. *Lancet*: 348:1269–1273.

Strauss, R., 2000. Adult functional outcome of those born small for gestation age: twenty-six-year follow-up of the 1970 British birth cohort. *JAMA*, pp. 283, 625–32.

Su, K. et al., 2008. Omega-3 fatty acids for major depressive disorder during pregnancy: results from a randomized, double-blind, placebo-controlled trial. *J Clin Psychiatry*, p. 69:644–51.

UN Millennium Project, 2005. *Halving Hunger: It Can Be Done*. London: Routledge.

Veronika, V. et al., 2019. DNA methylation and chromatin modifiers in colorectal cancer. *Molecular aspects of medicine*, pp. 69, 73–92.

Vickers, M. et al., 2000. Fetal origins of hyperphagia, obesity, and hypertension and postnatal

amplification by hypercaloric nutrition. *Am J Physiol Endocrinol Metab*, p. 279:E83–E87.

Vickers, M., Breier, B., McCarthy, D. & Gluckman, P., 2003. Sedentary behavior during postnatal life is determined by the prenatal environment and exacerbated by postnatal hypercaloric nutrition.. *Am J Physiol Regul Integr Comp Physiol.*, p. 285:R271–R273.

Victora, C. et al., 2008. Maternal and child undernutrition: consequences for adult health and human capital. *Lancet*, pp. 26;371(9609):340-57.

World Health Organization, 2021. World Health Organization Fact sheet. *Cardiovascular diseases (CVDs)*.

Xue, Y. et al., 2019. Maternal undernutrition induces fetal hepatic lipid metabolism disorder and affects the development of fetal liver in a sheep model.. *FASEB J*, pp. 33(9):9990-10004.

Yajnik, C., Fall, C. & Coyaji, K., 2003. Neonatal anthropometry: the thin-fat Indian baby. The Pune Maternal Nutrition Study. *Int J Obes Relat Metab Disord*, p. 27:173–180.

Yamagata, K., 2017. Docosahexaenoic acid regulates vascular endothelial cell function and prevents cardiovascular disease. *Lipids in health and disease*, pp. 16(1), 118.

Yates, Z., Tarling, E., Langley-Evans, S. & Salter, A., 2009. Maternal undernutrition programmes atherosclerosis in the ApoE*3-Leiden mouse. *The British journal of nutrition*, 101(8), p. 1185–1194.

Yin, J. et al., 2019. The fucoidan from the brown seaweed *Ascophyllum nodosum* ameliorates atherosclerosis in apolipoprotein E-deficient mice.. *Food Funct*, pp. 10(8):5124-5139.

Yu, X., DW, Z. & Zheng XL, T. C., 2019. Cholesterol transport system: An integrated cholesterol transport model involved in atherosclerosis. *Prog. Lipid Res*, pp. 73, 65-91..

Zeisel, S., 2017. Choline, Other Methyl-Donors and Epigenetics. *Nutrients*, 9(5), p. 445.

Zeisel, S. & Blusztajn, J., 1994. Choline and human nutrition. *Annu. Rev. Nutr*, p. 14:269–96.

Zhang, S., Hong, F., Ma, C. & Yang, S., 2022. Hepatic Lipid Metabolism Disorder and Atherosclerosis.. *Endocr Metab Immune Disord Drug Targets*, pp. 22(6):590-600.

Zhu, W. et al., 2016 May. Maternal undernutrition leads to elevated hepatic triglycerides in male rat offspring due to increased expression of lipoprotein lipase. *Mol Med Rep*, pp. 13(5):4487-93.

Ziegler, B. et al., 2000. Inverse association between birth weight, birth length and serum total cholesterol in adulthood.. *Scand Cardiovasc J*, pp. 34:584-588.

Zinkhan, E. et al., 2016. Intrauterine growth restriction combined with a maternal high-fat diet increases hepatic cholesterol and low-density lipoprotein receptor activity in rats. *Physiol Rep*, 4(13), p. e12862.

Chapter II: MicroRNA and mRNA Sequencing Analyses Reveal Key Hepatic Metabolic and Signaling Pathways Responsive to Maternal Undernutrition in Full-term Fetal Pigs

II-1. Abstract

Maternal undernutrition is highly prevalent in developing countries, leading to severe fetus/infant mortality, intrauterine growth restriction, stunting, and severe wasting. However, the potential impairments of maternal undernutrition to metabolic pathways in offspring are not defined completely. In this study, two groups of pregnant domestic pigs received nutritionally balanced gestation diets with or without 50% feed intake restriction from 0 to 35 gestation days and 70% from 35 to 114 gestation days. Full-term fetuses were collected via C-section on day 113/114 of gestation. MicroRNA (miRNA) and mRNA deep sequencing were performed using the Illumina GAIIx system on fetal liver samples. The mRNA-miRNA correlation and associated signaling pathways were analyzed via CLC Genomics Workbench and Ingenuity Pathway Analysis Software. A total of 1189 and 34 differentially expressed mRNA and miRNAs were identified between full-nutrition (F) and restricted-nutrition (R) groups. The correlation analyses indicated that metabolic and signaling pathways such as oxidative phosphorylation, death receptor signaling, neuroinflammation signaling pathway, and estrogen receptor signaling pathways were significantly modified, and the abundances of key genes modified in these pathways were associated with the miRNA changes induced by the maternal undernutrition. For example, the stimulated ($p < 0.05$) oxidative phosphorylation pathway in R group was validated using RT-qPCR, and the correlational analysis indicated that miRNA (miR)-221, 103, 107, 184, and 4497 correlate with their target genes NADH:ubiquinone oxidoreductase subunit A1 (*NDUFA1*), subunit A11 (*NDUFA11*), subunit B10 (*NDUFB10*) and core subunit S7 (*NDUFS7*) in this pathway. These results provide the framework for further understanding

maternal undernutrition's negative impacts on hepatic metabolic pathways via miRNA-mRNA interactions in full-term fetal pigs.

II-2. Introduction

Undernutrition during pregnancy remains a critical global public health problem that causes neonatal mortality and overall disease burden within impoverished populations in developing countries. Even though prevalence has decreased in recent decades, nearly 10% of women are undernourished (assessed by height and body mass index below 18.5 kg/m^2), especially in South Asia with the highest prevalence of undernutrition estimated at 24.0% in 2014 (NCD Risk Factor Collaboration, 2016). Maintaining good nutritional status during pregnancy is important for a healthy pregnancy outcome (Kramer, 1987; Kramer & Victora, 2001). Otherwise, maternal undernutrition can lead to increased mortality, morbidity, and disability in offspring (Black, et al., 2008; Victora, et al., 2008). Furthermore, it can result in intrauterine growth restriction (IUGR) and low birth weight (LBW), exerting lasting effects on the offspring's later life (Black, et al., 2008).

Strauss (2000) has shown increased prevalence of neurological issues and weaker cognitive skills in childhood among LBW individuals, and adults born with LBW demonstrated significant differences in their academic achievements and career advancements compared to those born with normal birth weights (Richards, et al., 2002). Moreover, maternal undernutrition heightens the risk of various diseases in later life, including cardiovascular disease (Fisher, et al., 2006), type 2 diabetes (Harder, et al., 2007), and immunodeficiency (Moore, et al., 2004). Meanwhile a variety of metabolic pathways and biological functions were also interrupted, such as cardiac and vascular function (Zelko, et al., 2019), liver function (Xue, et al., 2019), lipoprotein metabolism (Zhu, et al., 2016), energy metabolism (George, et al., 2012), hypothalamic–pituitary–adrenal function (Vieau, et al., 2007), testicular function (Pedrana, et al., 2020), and growth of tibiae (Kimura, et al., 2018).

Aiming to clarify the connections between LBW and the onset of metabolic diseases (aiming type 2 diabetes) in adulthood, the 'thrifty phenotype' hypothesis was proposed by Hales & Barker (1992). From an evolutionary standpoint, this hypothesis appears plausible. In situations of inadequate in utero nutrition, the fetus adapts by conserving nutrients and maximizing nutrient uptake to ensure survival, while this condition affects fetal programming by inducing epigenetic changes. This adaptation results in a more conservative metabolism, known as the 'thrifty phenotype'. When these infants encounter a similarly poor postnatal diet, this programmed phenotype might confer an advantage, as they are biologically prepared to cope with such conditions. Challenges arise when the postnatal diet surpasses the expected range of these adaptive responses. This discrepancy could potentially lead to the development of metabolic syndrome (Gallou-Kabani & Junien, 2000). Therefore, understanding epigenetic modifications during fetal programming is crucial in investigating the development of future diseases.

MicroRNA is one of integral parts of epigenetic regulatory machinery. MiRNA, ranging from 20 to 27 nucleotides, is noncoding endogenous RNA derived from stem-loop regions within longer RNA transcripts. They function biologically as post-transcriptional regulators of gene expression (Ameres & Zamore, 2013). As of current estimates, approximately 60% of protein-coding genes in the human genome are believed to be subject to modulation by miRNAs (Friedman, et al., 2009). Hence, they play a role in nearly all recognized physiological processes, including cell growth, differentiation, apoptosis, organismal metabolism, and development (Catalanotto, et al., 2016).

Recently, several studies have indicated that maternal undernutrition disrupts the miRNA profile in offspring, potentially linking it to later metabolic disorders. For example, a research team (Zhu, et al., 2021) investigated miRNA profiles in rat liver samples from offspring whose mothers

were either fed a 50% feed-restricted diet or standard feed during pregnancy. The results revealed a downregulation of miRNA 181a (miR-181a), known for its involvement in lipid metabolism, in the livers of offspring from the feed-restricted group compared to control group at 1 day of age. Additionally, manipulating miR-181a levels showed that its overexpression reduced lipid droplets after a 48-hour treatment with oleic acid in BRL-3A cells. This overexpression suppressed the expression of sirtuin 1 (*SIRT1*), forkhead box protein O1 (*FOXO1*), krueppel-like factor 6 (*KLF6*), and peroxisome proliferator-activated receptor gamma (*PPAR γ*), while decreased miR-181a expression had the opposite effect. Furthermore, in adult offspring from the feed-restricted group, they observed increased triglyceride content, decreased miR-181a expression, and increased expression levels of *SIRT1*, *FOXO1*, *KLF6*, and *PPAR γ* in liver tissues.

Another study assessed miRNA and mRNA expression in rat aortic specimens from offspring at 1-day and 12-month ages, born to dams subjected to 50% feed restriction from gestation day 10 to term (Khorram, et al., 2010). Maternal undernutrition notably decreased miRNAs 29c, 183, and 422b in the 1-day group and miRNAs 200a, 129, 215, and 200b in the 12-month group, while increasing miR-189 in the 1-day group and miR-337 in the 12-month group. The targeted genes of these altered miRNAs were involved in structural aspects such as collagen, elastin, and enzymes regulating extracellular matrix remodeling, as well as angiogenic factors. Undernutrition during pregnancy predominantly influenced mRNA expression related to cell cycle/mitosis in the 1-day group and anatomic structure and apoptosis in the 12-month group. These findings collectively suggest that maternal undernutrition modulating gene expression in offspring might involve miRNA-related mechanisms.

Together, the primary function of miRNAs in life is to regulate gene expression in a specific, sequence-dependent manner. Thus, identifying which mRNA is bound by specific

miRNAs is crucial for unraveling the function of miRNAs. Recent advancements in RNA sequencing (RNA-seq) and miRNA target-prediction strategies have made this exploration feasible. RNA-seq is a powerful molecular technique used to analyze and quantify RNA molecules within a biological sample. It provides a comprehensive view of the transcriptome—the complete set of RNA transcripts present in a cell or tissue at a specific time. To perform RNA-seq, it has several steps, including RNA extraction, library preparation, sequencing, and data analysis (McCombie, et al., 2019). In this project, RNA-seq enables the quantification of gene expression levels across the entire genome, allowing us to identify which genes are active and their expression levels in conditions of maternal undernutrition. Moreover, by comparing gene expressions between different samples [full-nutrition (F) vs. restricted-nutrition (R)] to identify genes that are upregulated or downregulated under specific conditions. Therefore, it helps in understanding molecular mechanisms underlying developmental processes, responses to stimuli, cellular signaling pathways, and disease progression (Ozsolak & Milos, 2011).

Likewise RNA seq, miRNA seq is used to analyze and quantify the presence and expression levels of miRNAs in biological samples (Crocker, et al., 2022). Technically, the miRNAs need to be separated from the rest of the RNA present in the cell. Because of the smaller size, miRNA can be filtrated out from other RNA species using commercial kits (e.g., mirVana miRNA isolation kit) (Guo, et al., 2014), and next steps like RNA sequencing. By combining miRNA and mRNA expression data, a big picture of how miRNA is involved in mRNA regulation will be revealed (Ritchie, et al., 2013).

In this project, our focus was on the liver because it is a major parenchymatous organ for nutrient absorption, metabolism, and energy homeostasis. During pregnancy, undernourishment affects not only the development of fetal liver but also its physiological function (Widdowson,

1971; Xue, et al., 2019). Research on fetal liver metabolism induced by maternal undernutrition revealed multiple metabolic disorders including but not limited to impaired lipid metabolism, amino acids metabolism, mitochondrial function, antioxidant capacity, and altered nutrient metabolism (Kloesz, et al., 2001; Zhu, et al., 2021).

Overall, we applied high-throughput sequencing on fetal liver tissue from normal feeding (control) dams and maternal undernutrition dams to obtain miRNA and mRNA expression profiles from the same piglets. Using this approach, we identified novel differentially expressed mRNAs, miRNAs and numerous miRNA–mRNA regulatory correlations, which further controls several key pathways induced by maternal undernutrition.

II-3. Materials and Methods

II-3.1. Experimental Design

Fetal liver samples were obtained from the experiment as described previously (Lima, et al., 2017). Briefly, pregnant pigs (Landrace x Yorkshire x Duroc) with first parity were individually housed at the Swine Educational Unit in North Carolina State University. Pigs were divided into the full-nutrition (F) group and the restricted-nutrition (R) group, both receiving a nutrient-balanced gestation diet that met the National Research Council (NRC, 2012) requirements for gestating pigs. The diet included a basal vitamin premix and a supplemented mixture of methylating vitamins (MVs), choline (1250 mg/kg feed, vitamins donated by DSM, Heerlen, Netherlands), and DHA (2420 mg/kg feed; life's DHA S35-O200, rosemary free algal vegetable oil, minimum 35% DHA; DSM, Columbia, MD) (**Table II-3.1-1**). The MVs contained folic acid (1.3 mg/kg feed), pyridoxine (1.0 mg/kg feed), B-12 (0.015 mg/kg feed), riboflavin (3.75 mg/kg feed). Throughout the entire study period, all groups received the same amounts of MVs, choline, and DHA, incorporated into the gestation diet allotment for each pregnant pig just

before the morning feeding each day. Before breeding, all pigs received a gestation diet for 2 weeks at the standard rate of 2.5 kg feed/d. After insemination, the F group of pregnant pigs were fed 2.0 kg feed/d (the standard rate for gestating pigs) for the whole gestation period. While the pregnant pigs in the R group received 1.0 kg diet/d (50% intake restriction relative to 2.0 kg feed intake) for 35 days (**Table II-3.1-2**). After the first ultrasounds confirmation (performed on d 35 after insemination), the pregnant pigs in R group were fed 0.6 kg/d (70% feed restriction relative to 2.0 kg feed intake) for the rest of gestation period. Full term fetuses were obtained via C-section and hepatic tissues were collected immediately after being euthanized. The liver samples were immediately frozen in liquid nitrogen, and then stored at -80°C for future analyses to evaluate the effects of maternal undernutrition on RNA profiles in full-term fetal pigs. All procedures were approved by the Animal Care and Use Committee of North Carolina State University.

II-3.2. mRNA and miRNA Sequencing

Hepatic total RNA was isolated (Hicks, et al., 2017) from 16 full-term fetal pigs. Four litters were randomly chosen from the F group and R group, and two full-term fetal pigs' liver were collected from each litter for RNA sequencing, so a total $n = 8$. The library was prepared using Ion Total RNA-Seq Kit v2 (ThermoFisher 4479789, Waltham, MA, USA) and the barcode indices were designed following the manufacturer's instructions. mRNA and miRNA were sequenced at the NCSU Genomic Sciences Laboratory using an Illumina Genome Analyzer IIX (GAIIx).

II-3.3. RNA-seq and miRNA Data Analysis

The CLC Genomics Workbench (Qiagen, Hilden, Germany) was used for processing and analyzing all sequencing data. We imported RNA-seq raw data (FASTQ files) into the CLC

Genomics Workbench software for mRNA sequencing analysis. All residual adaptor sequences and low-quality sequences (Phred < 20) were removed by the NGS trim tool. Then, reads were mapped to the *Sus scrofa* reference genome (*Sus scrofa* 11.1) and normalized using the trimmed mean of M values (TMM) method. The RNA-seq analysis tool was used for mRNA expression analysis and the Differential Expression in Two Groups was used to identify differentially expressed genes (DEGs). The expression level of each gene was evaluated as the number of counts per million reads (CPM).

The miRNA sequencing analysis was processed using the small RNA (less than 200 nucleotides in length, miRNAs are a class of small RNA molecules) Analysis suite. Briefly, the raw data was imported to CLC Genomics Workbench. The Extract and Count function was used to create the small RNA samples. Then the Annotate and Merge Counts function was used to annotate and merge small RNA samples based on reference database miRBase 22.1 and normalized using the transformation and normalization tool. The differential expression analysis was carried out using Empirical Analysis of the DGE tool.

II-3.4. Gene Ontology Functional Analysis

Gene Ontology (GO) functional analysis was carried out for all the DEGs with a fold change > 1.5 or < -1.5 and a $p < 0.05$. The DAVID Functional Annotation Tool version 6.8 (URL: <https://david.ncifcrf.gov/>) was used to identify the Biological Processes from GO database. The up- and downregulated gene lists were uploaded using *Sus scrofa* as background. Using Benjamin's correction, the term enrichment was evaluated, and corrected $p < 0.05$ was considered significant.

II-3.5. Ingenuity Pathways Analysis and mi-mRNA Correlation Analysis

Within the Ingenuity Pathways Analysis (IPA) software, the Core Analysis function was

performed on DEGs ($p < 0.05$ and fold change difference > 1.5) data to investigate modified pathways. Because we were looking for subtle changes affected by nutrition, z-score > 1.6 was considered a meaningful potential pathway. The miRNA-mRNA correlation analysis was constructed using a microRNA Target Filter. Briefly, miRNA data with $p < 0.05$ were uploaded into IPA, run through the miRNA Target Filter, and we associated it with DEGs data above. Then a mi-mRNA correlation list was generated. Both experimentally validated and “highly predicted” mi-mRNA correlations were chosen in the analysis. Additionally, both negative and positive correlation expression pairings were included. The Core Analysis was again performed using the miRNA-targeting mRNA list to investigate potential modified pathways involving miRNA regulation.

II-3.6. RNA Expression Level Analysis

TRI Reagent (Sigma-Aldrich T9424, St. Louis, MO, USA) was used to lyse liver tissue, and chloroform was used to separate RNA from other cellular components. Isopropanol was used to precipitate RNA, and 70% ethanol was used to purify and clean RNA molecules. Total RNA extracted from organoids was used to synthesize cDNA by QuantiTect Reverse Transcription Kit (Qiagen 205313, Hilden, Germany). While the miScript II RT Kit (Qiagen 218161, Hilden, Germany) was used for miRNA cDNA synthesis. We validated 4 mRNAs including, *NDUF A1*, *NDUF A11*, *NDUFB10*, *NDUFS7* and 5 miRNAs including, miR-221, miR-103, miR-107, miR-4497, and miR-184 (**Table II-3.6**). Both forward and reverse primers of mRNA was created using Primer Designing Tool (<https://www.ncbi.nlm.nih.gov/tools/primer-blast/>), and synthesized by Sigma-Aldrich (St. Louis, MO, USA). All primers have a GC% in the range of 40% to 60%, a melting temperature between 58°C and 64°C, and do not have the potential for hairpin formation. Forward primer of miRNA was also synthesized by Sigma-Aldrich (St. Louis,

MO, USA), reverse primer was miScript Universal Primer provided from miScript II RT Kit. RT-qPCR was conducted using iQ™ SYBR® Green Supermix (Bio-Rad 1708886, Hercules, CA, USA) and CFX Connect Real-Time PCR Detection System (Bio-Rad 1855201, Hercules, CA, USA). *GAPDH* gene and *U6* snRNA (**Table II-3.6**) were used as the housekeeping gene to normalize mRNA and miRNA expression, respectively. Relative gene expression was calculated using the $2^{-\Delta\Delta CT}$ method.

II-3.7. Statistical Analysis

RT-qPCR data were analyzed with GraphPad Prism 5 software using unpaired Student's t-test and expressed as the mean \pm SEM. Correlational analysis was also performed with GraphPad Prism software. The statistics of bioinformatics analysis were carried out with built-in packages in IPA and CLC Workbench. In all analyses, p -values ≤ 0.05 were considered statistically significant.

II-4. Results

II-4.1. Expression Profiling of mRNA

Two cDNA libraries of fetal liver tissues from the F group and R group were sequenced. A total of 62,304,048 (F), and 28,153,954 (R) raw reads were acquired from mRNA sequencing. After removing the adaptors and low copy reads, then 62,296,238 (99.99%) and 28,151,683 (99.99%) clean reads were maintained in these two groups, respectively. It was found that 87.69% (F) and 81.16% (R) of the clean reads were mapped to the *Sus scrofa* reference genome (*Sus scrofa* 11.1). In total 10,426-11,556 (F) and 10,368-11,170 (R) expressed mRNAs (RPKM ≥ 0.5) were observed in these two groups, respectively. orosomuroid 1 (*ORM1*), serpin family A member 1 (*SERPINA1*), alpha 2-HS glycoprotein (*AHSG*), cytochrome c oxidase subunit 1 (*COX1*), subunit 2 (*COX2*), and subunit 3 (*COX3*), apolipoprotein C3 (*APOC3*), ATP synthase F0 subunit 6 (*ATP6*)

were the most abundant protein coding mRNAs in the fetal liver.

II-4.2. Full-nutrition Group vs. Restricted-nutrition Group mRNA Expression Profile

A total of 1189 genes were differentially expressed between F and R groups, based on absolute fold change > 1.5 and *p*-value < 0.05. Of these, 576 mRNAs were upregulated in R group with categorization such as ribosomal protein: ribosomal protein L14 (*RPL14*), L14 (*RPL18*), L19 (*RPL19*), S10 (*RPS10*), and S12 (*RPS12*), oxidative phosphorylation: NADH:ubiquinone oxidoreductase subunit A1 (*NDUFA1*), subunit A7 (*NDUFA7*), subunit A11 (*NDUFA11*), subunit B10 (*NDUFB10*), and subunit S5 (*NDUFS5*), cardiac muscle contraction: actin alpha cardiac muscle 1 (*ACTC1*), cytochrome c oxidase subunit 5B (*COX5B*), myosin heavy chain 7 (*MYH7*), troponin I3, cardiac type (*TNNI3*), troponin T2, cardiac type (*TNNT2*). Reciprocally, 613 mRNAs were downregulated in R group with classification such as alpha-beta T cell receptor complex: CD247 molecule (*CD247*), CD3 delta subunit of T-cell receptor complex (*CD3D*), and CD3 gamma subunit of T-cell receptor complex (*CD3G*), mitotic nuclear division: WEE1 G2 checkpoint kinase (*WEE1*), cell division cycle 20 (*CDC20*), cell division cycle 25C (*CDC25C*), PTTG1 regulator of sister chromatid separation, securing (*PTTG1*), inorganic anion exchanger activity: solute carrier family 4 member 7 (*SLC4A7*), solute carrier family 4 member 4 (*SLC4A4*), solute carrier family 4 member 11 (*SLC4A11*), C2H2 zinc finger protein: zinc finger protein 175 (*ZNF175*), zinc finger protein 195 (*ZNF195*), zinc finger protein 316 (*ZNF316*), GLI family zinc finger 1 (*GLI1*). The volcano plot is presented in **Figure II-4.2A**, and the heatmap of mRNAs are shown in **Figure II-4.2B**.

GO functional annotation and IPA pathway analysis were carried out to explore the potential functions of DEGs and pathways regulated by them. The upregulated genes in R group were significantly associated with 15 GO biological process terms (**Figure II-4.2C**), including

translation, cytoplasmic translation, ribosomal small subunit assembly, ventricular cardiac muscle tissue morphogenesis, and regulation of muscle contraction. Downregulated genes in R group (**Figure II-4.2D**) are catalogued as mitotic nuclear division, cell division, regulation of intracellular pH, trachea gland development, toll-like receptor signaling pathway, and positive regulation of protein secretion.

Results from the IPA analysis showed that 9 canonical pathways (**Table II-4.2**) were changed with a criterion of $p < 0.05$ and absolute z-score > 1.65 , with 2 of them were inhibited (z-score < -1.65 , z-score is a statistical measure of the match between expected relationship direction and observed gene expression), including sirtuin signaling and the Th2 pathway. The 7 stimulated pathways (z-score > 1.65) included oxidative phosphorylation, EIF2 signaling, production of nitric oxide and reactive oxygen species in macrophages, actin cytoskeleton signaling, signaling by Rho family GTPases, tumor microenvironment pathway, and death receptor signaling.

II-4.3. Differentially Expressed miRNAs Between Full-nutrition Group and Restricted-nutrition Group

In comparing the differentially expressed miRNAs among F and R, there were 360 mature miRNAs identified from F and R groups (**Figure II-4.3**). Of these, 34 known miRNAs were differentially expressed, p -value < 0.05 , and 27 were detected by IPA database. 13 miRNAs were upregulated, including miR-144, miR-200c, miR-221, let-7i, miR-151b, and 14 were downregulated, including miR-206, miR-133b, miR-4492, miR-4497, miR-503.

II-4.4. Canonical Pathway Regulated by miRNAs

When the miRNA target filter was used to filter out differentially expressed mRNA ($p < 0.05$ & fold change difference > 1.5) regulated by differentially expressed miRNAs ($p < 0.05$)

between F and R groups, 245 mRNAs were filtered out based on high predicted and positive or negative correlations. The filtered DEGs were then subjected to canonical pathway analysis. The results showed that oxidative phosphorylation, death receptor signaling, neuroinflammation signaling pathway, and estrogen receptor signaling changed (**Table II-4.4**).

II-4.5. miRNA-mRNA Correlation in miRNA-regulated Pathways

The result showed that the oxidative phosphorylation pathway was stimulated ($p < 0.01$) with a z-score of 2.236, and the differentially expressed miRNA including: miR-1843, miR-221, miR-4497, miR-103, miR-107, and miR-184 were predicted to target genes *NDUFA1*, *NDUFA11*, *NDUFB10*, *NDUFS7*, and ATP synthase F1 subunit gamma (*ATP5F1C*) in this pathway. In death receptor signaling ($p < 0.05$, z-score = 2.0), miR-92a, miR-27a, let-7i were predicted to target genes *ACTC1*, FAS-associated via death domain (*FADD*), FAS-cell surface death receptor (*FAS*), LIM domain kinase 1 (*LIMK1*). The neuroinflammation signaling pathway was stimulated ($p < 0.05$, z-score = 2.236), miR-151b, miR-1843, let-7i, miR-221, miR-424, miR-4492, miR-133b, miR-27a were predicted to target genes aph-1 homolog A, gamma-secretase subunit (*APH1A*), CD200 receptor 1 (*CD200R1*), *FAS*, Fos proto-oncogene, AP-1 transcription factor subunit (*FOS*), gamma-aminobutyric acid type B receptor subunit 1 (*GABBR1*), major histocompatibility complex, class II, DO beta (*HLA-DOB*), solute carrier family 6 member 1 (*SLC6A1*). In estrogen receptor signaling ($p < 0.05$, z-score = 2.0), miR-1843, miR-424, miR-200c, miR-221, miR-27a, miR-4497, miR-221, miR-184 were predicted to target genes *ATP5F1C*, calcium channel, voltage-dependent, alpha2/delta subunit 1 (*CACNA2D1*), cofilin 2 (*CFL2*), *FOS*, LIM domain kinase 1 (*LIMK1*), *NDUFA11*, *NDUFB10*, *NDUFS7*. All these correlations are listed in **Table II-4.5**.

II-4.6. RT-qPCR Validation of miRNAs and mRNAs in Oxidative Phosphorylation Pathway

RT-qPCR was used to validate those mRNAs and miRNAs in oxidative phosphorylation

pathway (**Figure II-4.6A-E**). Of these, *NDUFA1*, *NDUFA11*, *NDUFB10*, and *NDUFS7* were significant upregulated ($p < 0.05$). miR-221 was significant upregulated ($p < 0.05$). miR-103, miR-107, miR-4497 and miR-184 were significant downregulated ($p < 0.05$). Then, the correlational analysis is performed to clarify the correlation between mRNAs and miRNAs expression (**Figure II-4.6F-J**). Results from this analysis showed that miR-221 is positively correlated with *NDUFA1* ($R^2 = 0.5262$, $p < 0.05$) and *NDUFB10* ($R^2=0.8821$, $p < 0.001$), miR-103 negatively correlated with *NDUFB10* ($R^2 = 0.7262$, $p < 0.01$), miR-107 negatively correlated with *NDUFB10* ($R^2 = 0.5329$, $p < 0.05$), and miR-4497 negatively correlated with *NDUFA11* ($R^2 = 0.6950$, $p < 0.05$), but there is no significant correlation between miR-184 and *NDUFS7* ($R^2 = 0.4008$, $p = 0.092$).

II-5. Discussion

It has been demonstrated that maternal nutrition status has great impacts on many metabolic systems, resulting in adverse health outcomes on offspring, such as stunting, wasting and low birthweight (Black, et al., 2008). However, the possible impairments on fetal metabolic pathways have not been well investigated. In this study, by applying mRNA sequencing and miRNA sequencing, we found that hundreds of genes expressed differentially in liver of the term fetuses from dams with R compared to F. These genes are involved in regulating gene expression, protein translation, wound healing, spreading of cells, DNA repair, oxidative stress, and so on. By using IPA, the pathways of these mRNA regulated were classified as energy production, immune response, cell growth and proliferation. Among these genes, some are first time reported associated with maternal under nutrition, such as mRNAs *ACTC1*, *GLII*, fibroblast growth factor 21 (*FGF21*), carboxypeptidase M (*CPM*), TSPO associated protein 1 (*TSPOAP1*), integrin subunit alpha 3 (*ITGA3*), hydroxysteroid 11-beta dehydrogenase 1 (*HSD11B1*), flavin

containing dimethylaniline monooxygenase 5 (*FMO5*), Rho family GTPase 1 (*RND1*), mitochondrial ribosomal protein S15 (*MRPS15*), charged multivesicular body protein 2A (*CHMP2A*), polo like kinase 3 (*PLK3*), ELMO domain containing 1 (*ELMOD1*), and cellular retinoic acid binding protein I (*CRABP1*).

In addition to the differential expressions of mRNA, we identified dozens of differentially expressed miRNAs in the same liver samples. Some miRNAs, such as miR-141, miR-4492, let-7i, miR-503, miR-151b, and miR-103 have not been reported to be modified by maternal undernutrition. Interestingly, miR-206, miR-133b, miR-200c, and miR-184 were identified as miRNAs that underwent significant changes in expression due to maternal undernutrition. Similar findings were also reported in mouse and rat with maternal low protein diet (Kanakakis, et al., 2021; Assalin, et al., 2019; Sene, et al., 2013), demonstrating that the changes in abundance of these 4 miRNAs were indeed associated with the protein level in maternal diet. Furthermore, we found that maternal undernutrition only induced modifications of 34 miRNAs' expression, but the modified miRNAs affected expression of 1189 mRNAs ($p < 0.05$). The miRNA-mRNA correlation analysis illustrated that oxidative phosphorylation, death receptor signaling, neuroinflammation signaling pathway, and estrogen receptor signaling were stimulated ($p < 0.05$, z-scores > 1.65) by the modified miRNA expressions. Among those pathways, oxidative phosphorylation pathway has the highest z-score of 2.236. It is well known that the electron transport chain is one of the components in oxidative phosphorylation pathway embedded in mitochondria, via which the ATP is produced by oxidative phosphorylation pathway consisting of 5 enzyme complexes. Among the five enzyme complexes, mitochondrial Complex I (or NADH-ubiquinone oxidoreductase) is the largest complex in the pathway and contains over 45 subunits (Carroll, et al., 2006). These 4 miRNA-targeting genes, *NDUFA1*, *NDUFA11*, *NDUFB10*, and

NDUFS7, were identified in this study as part of Complex I. Previous studies showed that *NDUFA1*, *NDUFA11*, *NDUFB10* and *NDUFS7* played a critical role in Complex I assembly and thus were crucial for the oxidative phosphorylation pathway. Downregulation or mutation on these genes would lead to Complex I deficiency and respiratory inhibition (Au, et al., 1999; Potluri, et al., 2009; Li, et al., 2021; Jang & Javadov, 2018). In the present study, we identified 4 mRNAs, 5 miRNAs and 6 mi-mRNA correlations (some mi-mRNA correlations have overlap) in oxidative phosphorylation pathway. Furthermore, these 4 mRNAs (*NDUFA1*, *NDUFA11*, *NDUFB10* and *NDUFS7*), 5 miRNAs (miR-221, 103, 107, 4497, and 184) and 5 mi-mRNA correlations (miR-221 targeting *NDUFA1*, miR-221 targeting *NDUFB10*, miR-103 targeting *NDUFB10*, miR-107 targeting *NDUFB10*, miR-4497 targeting *NDUFA11*) were successfully confirmed in the liver using RT-qPCR ($p < 0.05$). Importantly, all these correlations have not been reported before. Likewise, 'thrifty phenotype' hypothesis, we propose a potential reason for the stimulated oxidative phosphorylation pathway. Because the 4 upregulated miRNA-targeting genes are structural genes, we assume they will enhance oxidative phosphorylation and then improve the production of ATP or energy in the hepatocyte. Maternal undernutrition is a big stress factor for fetal pigs, and it causes overall metabolism or signaling pathway disruption. To compensate for these overall changes, mitochondria produce more ATP via oxidative phosphorylation to keep the cell function properly. These changes may be regulated by miRNA modification.

Neuroinflammation signaling pathway is another pathway regulated by miRNA with z-score = 2.236. Neuroinflammation refers to the inflammation of the nervous tissue, and is an immune response often initiated against a variety of harmful stimuli such as pathogens or injury (Milatovic, et al., 2017). In the liver, two autonomic nervous system: sympathetic and parasympathetic arms are present, both play key roles in the maintenance homeostasis and

several disease processes (Jensen, et al., 2013; Mizuno & Ueno, 2017). The change of neuroinflammation signaling pathway indicates an aberrant effect happens in liver nervous system due to maternal undernutrition and may subsequently impact homeostasis and other metabolic processes in liver. Here we found that miR-221 targeting *FOS* was the only one correlation that was reported previously (Sehgal, et al., 2015). However, miR-151b upregulating *APH1A*, let-7i downregulating *CD200R1*, miR-1843 downregulating *CD200R1*, let-7i upregulating *FAS*, miR-424 downregulating *GABBR1*, miR-4492 upregulating *HLA-DOB*, miR-133b downregulating *SLC6A1*, miR-27a downregulating *SLC6A1* were not reported in the literature. Furthermore, Death Receptor (all cell-surface receptors) Signaling had a z-score of 2. Death receptors belong to the Tumor necrosis factor (TNF) receptor superfamily and provide a rapid and efficient route to apoptosis (Kavurma, et al., 2008). In this pathway a negative correlation between *miR-27a* and *FADD*, a common adaptor involved in apoptosis, in HEK293T (human embryonic kidney) cell was observed (Chhabra, et al., 2009 Jun 09). However, a positive correlation was detected in liver in our study. Other correlations were observed in this study including: miR-27a targeting *LIMK1*, miR-92a targeting *ACTC1* and let-7i targeting *FAS*, that is the major receptor that mediates cell apoptosis. Together, both stimulation of neuroinflammation signaling and death receptor signaling pathways indicate increased inflammation-mediated hepatocyte apoptosis and liver impairment caused by maternal undernutrition.

The last pathway that had a z-score of 2 was the estrogen receptor signaling pathway. We found that miR-424 downregulating *CACNA2D1* and *CFL2*, miR-221 upregulating *FOS* were reported before, but the other 6 correlations were not reported, including miR-1843 upregulating *ATP5F1C*, miR-200c downregulating *CFL2*, miR-27a upregulating *LIMK1*, miR-4497 upregulating *NDUFA11*, miR-221 upregulating *NDUFB10*, and miR-184 upregulating *NDUFS7*.

Estrogen receptor signaling plays a variety of roles in the liver, including in cell proliferation, energy homeostasis, glucose metabolism, lipid metabolism and gene expression (Fuentes & Silveyra, 2019; Palmisano, et al., 2017; Rodrigo & Jan-Ake, 2011). In this study, most identified mRNAs (*ATP5F1C*, *NDUFA11*, *NDUFB10*, *NDUFS7*) overlap with mRNAs in oxidative phosphorylation pathway, which is related to energy homeostasis. Again, it indicates the compensation effect against energy depletion caused by maternal undernutrition.

In summary, our study using comprehensive mi-mRNA analyses revealed that oxidative phosphorylation, death receptor signaling, neuroinflammation signaling, and estrogen receptor signaling pathways may be associated with miRNA regulation. Those 4 pathways were reported to be associated with miRNA regulation for the first time. Nevertheless, additional functional studies are needed to explain the regulatory roles of certain miRNAs in the fetal hepatic pathway induced by maternal undernutrition.

II-6. References

- Ameres, S. L. & Zamore, P. D., 2013. Diversifying microRNA sequence and function. *Nature reviews. Molecular cell biology*, 14(8), p. 475–488.
- Assalin, H., Gontijo, J. & Boer, P., 2019. miRNAs, target genes expression and morphological analysis on the heart in gestational protein-restricted offspring. *PLoS One*, 14(4), p. e0210454.
- Au, H. et al., 1999. The NDUFA1 gene product (MWFE protein) is essential for activity of complex I in mammalian mitochondria. *Proc Natl Acad Sci USA*, Volume 96, p. 4354–9.
- Baker, D., 2008. Animal models in nutrition research. *J Nutr*, 138(2), pp. 391-6.
- Black, R. et al., 2008. Maternal and child undernutrition: global and regional exposures and health consequences. *The Lancet Journal*, 371(9608), pp. 243-60.
- Carroll, J. et al., 2006. Bovine complex I is a complex of 45 different subunits. *J Biol Chem*, 281(43), pp. 32724-7.
- Catalanotto, C., Cogoni, C. & Zardo, G., 2016. MicroRNA in Control of Gene Expression: An Overview of Nuclear Functions. *International journal of molecular sciences*, 17(10), p. 1712.
- Chhabra, R. et al., 2009 Jun 09. Upregulation of miR-23a-27a-24-2 cluster induces caspase-dependent and -independent apoptosis in human embryonic kidney cells. *PLoS One*, 4(6), p. e5848.
- Crocker, O., Trigg, N. & Conine, C., 2022. Cloning and Sequencing Eukaryotic Small RNAs. *Current protocols*, 2(8), p. e495.
- Fisher, D., Baird, J. & Payne, L., 2006. *Are infant size and growth related to burden of disease in adulthood? A systematic review of literature*. 35 ed. *Int J Epidemiol*: 1196–1210.
- Friedman, R. C., Farh, K. K.-H., Burge, C. B. & Bartel, D. P., 2009. Most mammalian mRNAs are conserved targets of microRNAs. *Genome research*, 19(1), p. 92–105.

Fuentes, N. & Silveyra, P., 2019. Estrogen receptor signaling mechanisms. *Adv Protein Chem Struct Biol*, Volume 116, pp. 135-170.

Gallou-Kabani, C. & Junien, C., 2000. Nutritional epigenomics of metabolic syndrome: new perspective against the epidemic.. *Diabetes*, Volume 54, p. 1899–1906.

George, L. et al., 2012. Early maternal undernutrition programs increased feed intake, altered glucose metabolism and insulin secretion, and liver function in aged female offspring. *Am J Physiol Regul Integr Comp Physiol*, 302(7), pp. R795-804.

Guo, Y. et al., 2014. A comparison of microRNA sequencing reproducibility and noise reduction using mirVana and TRIzol isolation methods. *International Journal of Computational Biology and Drug Design*, Volume 7, p. 102–112.

Hales, C. & Barker, D., 1992. Type 2 (non-insulin-dependent) diabetes mellitus: the thrifty phenotype hypothesis. *Diabetologia*, Volume 35, p. 595–601.

Harder, T. et al., 2007. Birth weight and subsequent risk of type 2 diabetes: a meta-analysis.. *Am J Epidemiol*, Volume 165, p. 849–857.

Hicks, J., Porter, T. & Liu, H., 2017. Identification of microRNAs controlling hepatic mRNA levels for metabolic genes during the metabolic transition from embryonic to posthatch development in the chicken. *BMC Genomics*, 18(1), p. 687.

Jang, S. & Javadov, S., 2018. Elucidating the contribution of ETC complexes I and II to the respirasome formation in cardiac mitochondria. *Sci Rep*, 8(1), p. 17732.

Jensen, K., Alpini, G. & Glaser, S., 2013. Hepatic nervous system and neurobiology of the liver. *Compr Physiol*, 3(2), pp. 655-65.

Kanakis, I. et al., 2021. Small-RNA Sequencing Reveals Altered Skeletal Muscle microRNAs and snoRNAs Signatures in Weanling Male Offspring from Mouse Dams Fed a Low Protein

Diet during Lactation. *Cells*, 10(5), p. 1166.

Kavurma, M. M., Tan, N. Y. & Bennett, M. R., 2008. Death receptors and their ligands in atherosclerosis. *Arteriosclerosis, Thrombosis, and Vascular Biology*, 28(10), p. 1694–1702.

Khorram, O. et al., 2010. Effect of maternal undernutrition on vascular expression of micro and messenger RNA in newborn and aging offspring. *Am J Physiol Regul Integr Comp Physiol*, 298(5), p. R1366–R1374.

Kimura, T. et al., 2018. Maternal undernutrition during early pregnancy inhibits postnatal growth of the tibia in the female offspring of rats by alteration of chondrogenesis.. *Gen Comp Endocrinol*, 1(260), pp. 58-66.

Kloesz, J. et al., 2001. Uteroplacental Insufficiency Alters Liver and Skeletal Muscle Branched-Chain Amino Acid Metabolism in Intrauterine Growth-Restricted Fetal Rats. *Pediatr Res* , 50(5), p. 604–610.

Kramer, M., 1987. Determinants of low birth weight: methodological assessment and meta-analysis. *Bull World Health Organ*, Volume 65, pp. 663-737.

Kramer, M. & Victora, C., 2001. Low birth weight and perinatal mortality. In: R. Semba & M. Bloem, eds. *Nutrition and health in developing countries*. s.l.:Humana Press, p. 57–69.

Li, B. et al., 2021. Cloperastine inhibits esophageal squamous cell carcinoma proliferation in vivo and in vitro by suppressing mitochondrial oxidative phosphorylation. *Cell death discovery*, 7(1), p. 166.

Lima, H. et al., 2017. Supplementation of Maternal Diets with Docosahexaenoic Acid and Methylating Vitamins Impacts Growth and Development of Fetuses from Malnourished Gilts. *Current developments in nutrition*, 2(3), p. nzx006.

Lim, L. et al., 2005. Microarray analysis shows that some microRNAs downregulate large

numbers of target mRNAs. *Nature*, Volume 433, p. 769–773.

McCombie, W., McPherson, J. & Mardis, E., 2019. Next-Generation Sequencing Technologies. *Cold Spring Harbor perspectives in medicine*, 9(11), p. a036798.

Milatovic, D. et al., 2017. Neuroinflammation and Oxidative Injury in Developmental Neurotoxicity. *Reproductive and Developmental Toxicology (Second Edition)*, Volume 55, pp. 1051-1061.

Mizuno, K. & Ueno, Y., 2017. Autonomic Nervous System and the Liver. *Hepatol Res*, Volume 47, p. 160– 165.

Moore, S. et al., 2004. Birth weight predicts response to vaccination in adults born in an urban slum in Lahore, Pakistan. *Am J Clin Nutr*, Volume 80, p. 453–459.

NCD Risk Factor Collaboration, 2016. Trends in adult body-mass index in 200 countries from 1975 to 2014: a pooled analysis of 1698 population-based measurement studies with 19.2 million participants. *Lancet*, 387(10026), p. 1377–1396.

Odle, J. et al., 2014. The suckling piglet as an agrimedical model for the study of pediatric nutrition and metabolism.. *Annu Rev Anim Biosci.*, Volume 2, pp. 419-44.

Ozsolak, F. & Milos, P., 2011. RNA sequencing: advances, challenges and opportunities. *Nature reviews. Genetics*, 12(2), p. 87–98.

Palmisano, B., Zhu, L. & Stafford, J., 2017. Role of Estrogens in the Regulation of Liver Lipid Metabolism. *Adv Exp Med Biol*, Volume 1043, pp. 227-256.

Pedrana, G. et al., 2020. Maternal undernutrition during pregnancy and lactation affects testicular morphology, the stages of spermatogenic cycle, and the testicular IGF-I system in adult offspring.. *J Dev Orig Health Dis*, pp. 11(5):473-483.

Potluri, P. et al., 2009. A novel NDUFA1 mutation leads to a progressive mitochondrial complex

I-specific neurodegenerative disease. *Molecular genetics and metabolism*, 96(4), p. 189–195.

Richards, M., Hardy, R., Kuh, D. & Wadsworth, M., 2002. Birthweight, postnatal growth and cognitive function in a national UK birth cohort.. *Int. J. Epidemiol*, Volume 31, p. 342–8.

Ritchie, W., Rajasekhar, M., Flamant, S. & Rasko, J., 2009. Conserved expression patterns predict microRNA targets. *PLoS computational biology*, 5(9), p. e1000513.

Ritchie, W., Rasko, J. & Flamant, S., 2013. MicroRNA target prediction and validation. *Adv Exp Med Biol*, Volume 774, pp. 39-53.

Rodrigo, B. & Jan-Ake, G., 2011 Sep 7. Estrogen Receptors and the Metabolic Network. *Cell Metab*, 14(3), pp. 289-99.

Sehgal, M. et al., 2015. IFN- α -Induced Downregulation of miR-221 in Dendritic Cells: Implications for HCV Pathogenesis and Treatment. *Journal of interferon & cytokine research : the official journal of the International Society for Interferon and Cytokine Research*, 35(9), p. 698–709.

Sene, L. et al., 2013. Involvement of renal corpuscle microRNA expression on epithelial-to-mesenchymal transition in maternal low protein diet in adult programmed rats. *PloS one*, 8(8), p. e71310.

Strauss, R., 2000. Adult functional outcome of those born small for gestation age: twenty-six-year follow-up of the 1970 British birth cohort. *JAMA*, Volume 283, p. 625–32.

Victora, C. et al., 2008. Maternal and child undernutrition: consequences for adult health and human capital. *Lancet*, 371(9609), pp. 340-57.

Vieau, D. et al., 2007. HPA axis programming by maternal undernutrition in the male rat offspring.. *Psychoneuroendocrinology*, Volume 32 Suppl 1, pp. S16-20.

Widdowson, E., 1971. Intra-Uterine Growth Retardation in the Pig. I. Organ Size and Cellular

Development at Birth and After Growth to Maturity. *Neonatology*, 19(4), p. 329–340.

Xue, Y. et al., 2019. Maternal undernutrition induces fetal hepatic lipid metabolism disorder and affects the development of fetal liver in a sheep model. *The FASEB Journal*, 33(9), pp. 9990-10004.

Zelko, I., Zhu, J. & Roman, J., 2019. Maternal undernutrition during pregnancy alters the epigenetic landscape and the expression of endothelial function genes in male progeny. *Nutr Res*, Volume 61, pp. 53-63.

Zhu, W. et al., 2021. Maternal undernutrition modulates hepatic MicroRNAs expression in the early life of offspring. *Experimental cell research*, 400(2), p. 112450.

Zhu, W. et al., 2016. Maternal undernutrition leads to elevated hepatic triglycerides in male rat offspring due to increased expression of lipoprotein lipase. *Mol Med Rep*, 13(5), pp. 4487-93.

CHAPTER II TABLES

Table II-3.1-1 Composition of the gestation diet and supplement[@].

Item	
Ingredients	%
Corn, yellow dent	89.34
Soy protein isolate ¹	7.26
Dicalcium phosphate 18.5%	1.84
Limestone	0.95
Salt	0.50
Basal vitamin premix ²	0.06
Trace mineral premix ³	0.05
Total	100.00
Supplement [@]	
Ingredients ⁴	mg/kg feed
folic acid	1.3
pyridoxine	1.0
B-12	0.015
riboflavin	3.75
Choline (donated by DSM, Heerlen, Netherlands)	1250
DHA (life's DHA S35-O200, rosemary free algal vegetable oil, minimum 35% DHA; DSM, Columbia, MD)	2420

¹From Archer Daniels Midland, Chicago, IL. Isolated soy protein was used instead of soybean meal in order to minimize the choline content of the basal diet.

²Basal vitamin premix provided vitamin A, 17.64 g/kg premix; vitamin D, 7.06 g/kg premix; vitamin E, 388.01 g/kg premix; menadione, 6.68 g/kg premix; biotin, 8.82 g/kg premix; niacin, 44.09 g/kg premix; pantothenic acid, 58.79 g/kg premix; thiamin, 4.79 g/kg premix.

³Trace mineral premix included manganese sulfate 6.00%, zinc sulfate 6.00%, ferrous sulfate 4.00%, copper sulfate 0.5%, calcium iodate 0.125%, cobalt sulfate 0.05%, and calcium carbonate as carrier.

⁴The diet was further supplemented with a mixture of methylating vitamins (MVs) containing folic acid (1.3 mg/kg feed), pyridoxine (1.0 mg/kg feed), B-12 (0.015 mg/kg feed), and riboflavin (3.75 mg/kg feed). Additionally, choline (1250 mg/kg feed, vitamins donated by DSM, Heerlen, Netherlands), and DHA (2420 mg/kg feed; life's DHA S35-O200, rosemary free algal vegetable oil, minimum 35% DHA; DSM, Columbia, MD) were included. MVs, choline, and DHA were pre-weighed, packaged, and stored in the dark at 4°C. Oil-based DHA was stored in an airtight container at 4°C. All of them were added to the basal diet allotments for each pregnant pig immediately prior to feeding each day.

Table II-3.1-2 Timeline of experimental events and nutritional treatments.

	Day of pregnancy				
	-14	0	35	56	109-114 [#]
Events	Estrus Synchronization	Insemination	First Ultrasound	Second Ultrasound	C-section
	Days of feed intake (kg)				
Treatments	From -14 to 0	From 0 to 35	From 35-56	From 56-109	From 109-114 [#]
Full nutrition (F)	2.5	2.0			
Restricted nutrition (R)	2.5	1.0	0.6		

[#]C-sections were performed on days of 109-114. All pigs received a mixture of MVs, choline and DHA during the whole gestation period.

Table II-3.6 The sequence of primers used for RT-qPCR.

RNAs	Sequence, 5'-3'	
	Forward primer	Reverse primer
<i>NDUFA1</i>	GGAATCAAAGTCGGGTCACC	GATGTGAGCAGTGGCCATTC
<i>NDUFA11</i>	GGCCAAGACGCTTCTTCACA	TGTGTACCGTCCTGTCCTTG
<i>NDUFB10</i>	CTGGGACAAGGACGTGTACC	GCGGAATTCCCGGTGATAGT
<i>NDUFS7</i>	AGCTGTGGTCTCCAAACCCA	AGCGGTCCATGTCGTAGCGT
<i>GAPDH</i>	GTCTGGAGAAACCTGCCAAA	CCCTGTTGCTGTAGCCAAAT
<i>U6</i>	GCTTCGGCAGCACATATACT	CGCTTCACGAATTTGCGTGTGCAT
miR-221	AGCTACATTGTCTGCTGGGTTT	miScript Universal Primer
miR-103	AGCAGCATTGTACAGGGCTATGA	miScript Universal Primer
miR-107	AGCAGCATTGTACAGGGCTATCA	miScript Universal Primer
miR-4497	CTCCGGGACGGCTGGGC	miScript Universal Primer
miR-184	TGGACGGAGAAGCTGATAAGGGT	miScript Universal Primer

NDUFA1: NADH:ubiquinone oxidoreductase subunit A1; *NDUFA11*: NADH:ubiquinone oxidoreductase subunit A11; *NDUFB10*: NADH:ubiquinone oxidoreductase subunit B10; *NDUFS7*: NADH:ubiquinone oxidoreductase core subunit S7; *GAPDH*: glyceraldehyde 3-phosphate dehydrogenase; *U6*: U6 snRNA

Table II-4.2 Canonical pathway analysis of genes differentially expressed between full-nutrition (F) group and restricted-nutrition (R) group.

Canonical Pathways	-log(<i>p</i>-value)	Ratio	z-score	Molecules
Oxidative Phosphorylation	3.43	0.119	3.606	ATP5F1C,COX17,COX5B,COX7A1,CYC1,NDUFA1,NDUFA13,NDUFB10,NDUFB11,NDUFB2,NDUFS5,NDUFS7,UQCR10
EIF2 Signaling	4.07	0.0982	2.309	ACTC1,ATF3,DDIT3,EIF2AK3,EIF3G,EIF3J,HRAS,RPL10,RPL19,RPL30,RPL34,RPL35,RPL7A,RPL8,RPLP2,RPS10,RPS12,RPS18,RPS26,RPS28,RPS5,RPS9
Production of Nitric Oxide and Reactive Oxygen Species in Macrophages	1.39	0.0681	1.897	APOD,CYBA,FOS,MAP3K5,NCF4,NFKB2,PPP1R12A,REL,RHOBTB2,RHOC,RHOD,RND1,RND3
Actin Cytoskeleton Signaling	2.38	0.0776	1.732	ABI2,ACTC1,ACTN3,CD14,CFL2,DIAPH2,FGF10,FGF17,FGF21,FGF6,HRAS,ITGA3,ITGA7,LIMK1,MYH7,PDGFD,PPP1R12A,TMSB10/TMSB4X,WAS

Table II-4.2 (continued).

Signaling by Rho Family GTPases	1.69	0.0672	1.732	ACTC1,CFL2,FOS,GNB1L,ITGA3,ITGA7,LIMK1,NEDD4,NFKB2,PPP1R12A,REL,RHOBTB2,RHOC,RHOD,RND1,RND3,SEPTIN4,WAS
Tumor Microenvironment Pathway	1.59	0.0726	1.732	FAS,FGF10,FGF17,FGF21,FGF6,FOS,HRAS,IL6,MMP11,MMP2,NFKB2,PDGFD,REL
Death Receptor Signaling	1.44	0.0833	1.633	ACTC1,CYC1,FADD,FAS,LIMK1,MAP3K5,NFKB2,REL
Th2 Pathway	1.34	0.073	-1.667	APH1A,BHLHE41,CD247,CD3D,CD3E,CD3G,CD86,HLA-DOB,IL12B,SOCS3
Sirtuin Signaling Pathway	1.9	0.0685	-1.732	ATP5F1C,CYC1,E2F1,MAP1LC3A,NAMPT,NDUFA1,NDUFA13,NDUFB10,NDUFB11,NDUFB2,NDUFS5,NDUFS7,NEDD4,NFKB2,PPARG,REL,SLC25A4,TIMM13,TIMM17B,TIMM22

Note: Canonical pathways according to Ingenuity core analysis of mRNAs differentially expressed ($p < 0.05$, absolute of fold change > 1.5). The “Ratio” represents the percentage of altered genes within the total number of genes in a given pathway. The “z-score” is a statistical measure of the match between expected relationship direction and observed gene expression. A positive z-score indicates activation, while a negative score indicates inhibition.

Table II-4.4 Canonical Pathways regulated by differentially expressed miRNAs.

Canonical Pathways	-log(p-value)	Ratio	z-score	Molecules
Oxidative Phosphorylation	2.41	0.0459	2.236	<i>ATP5F1C,NDUFA1,NDUFA11,NDUFB10,NDUFS7</i>
Neuroinflammation	1.5	0.0222	2.236	<i>APH1A,CD200R1,FAS,FOS,GABBR1,HLA-DOB,SLC6A1</i>
Signaling Pathway				
Death Receptor	1.88	0.0417	2	<i>ACTC1,FADD,FAS,LIMK1</i>
Signaling				
Estrogen Receptor	1.4	0.0198	2	<i>ATP5F1C,CACNA2D1,CFL2,FOS,LIMK1,NDUFA11,NDUFB10,NDUFS7</i>
Signaling				

Note: Canonical pathways according to Ingenuity core analysis of mRNAs differentially expressed ($p < 0.05$ & fold change difference > 1.5) which regulated by differentially expressed miRNA ($p < 0.05$). The “Ratio” represents the percentage of altered genes within the total number of genes in a given pathway. The “z-score” is a statistical measure of the match between expected relationship direction and observed gene expression. A positive z-score indicates activation, while a negative score indicates inhibition.

Table II-4.5 Differentially expressed miRNAs and their targeted differentially expressed genes in canonical pathway.

ID	Fold change	Confidence	ID	Fold Change
Oxidative phosphorylation pathway				
miR-1843	-2.667	High (predicted)	ATP5F1C	1.537
miR-221	1.835	High (predicted)	NDUFA1	1.928
miR-4497	-1.696	High (predicted)	NDUFA11	1.541
miR-221	1.835	High (predicted)	NDUFB10	2.005
miR-103	-1.323	High (predicted)	NDUFB10	2.005
miR-107	-1.424	High (predicted)	NDUFB10	2.005
miR-184	-1.368	High (predicted)	NDUFS7	1.989
Death receptor signaling				
miR-92a	1.235846	High (predicted)	ACTC1	27.341
miR-27a	1.265102	Experimentally Observed	FADD	1.618
let-7i	2.214461	High (predicted)	FAS	3.568
miR-27a	1.265102	High (predicted)	LIMK1	2.207
Neuroinflammation signaling pathway				
miR-151b	1.776933	High (predicted)	APH1A	1.595
let-7i	2.214461	High (predicted)	CD200R1	-3.620
miR-1843	-3.26313	High (predicted)	CD200R1	-3.620
let-7i	2.214461	High (predicted)	FAS	3.568
miR-221	1.323114	Experimentally Observed	FOS	9.520
miR-424	-1.26534	High (predicted)	GABBR1	-1.629

Table II-4.5 (continued).

miR-4492	-1.73463	High (predicted)	HLA-DOB	2.868
miR-133b	-6.2979	High (predicted)	SLC6A1	-3.204
miR-27a	1.265102	High (predicted)	SLC6A1	-3.204
Estrogen receptor signaling				
miR-1843	-3.26313	High (predicted)	ATP5F1C	1.537
miR-424	-1.26534	Experimentally Observed	CACNA2D1	-1.685
miR-424	-1.26534	Experimentally Observed	CFL2	-1.666
miR-200c	1.835944	High (predicted)	CFL2	-1.666
miR-221	1.323114	Experimentally Observed	FOS	9.520
miR-27a	1.265102	High (predicted)	LIMK1	2.207
miR-4497	-1.94776	High (predicted)	NDUFA11	1.544
miR-221	1.323114	High (predicted)	NDUFB10	2.006
miR-184	-1.8964	High (predicted)	NDUFS7	1.989

Note: Confidence in Higher levels suggests a stronger likelihood or reliability of the predicted miRNA-target gene interaction. “Experimentally Observed” typically refers to miRNA-target interactions that have been verified or validated through laboratory experiments or empirical studies.

CHAPTER II FIGURES

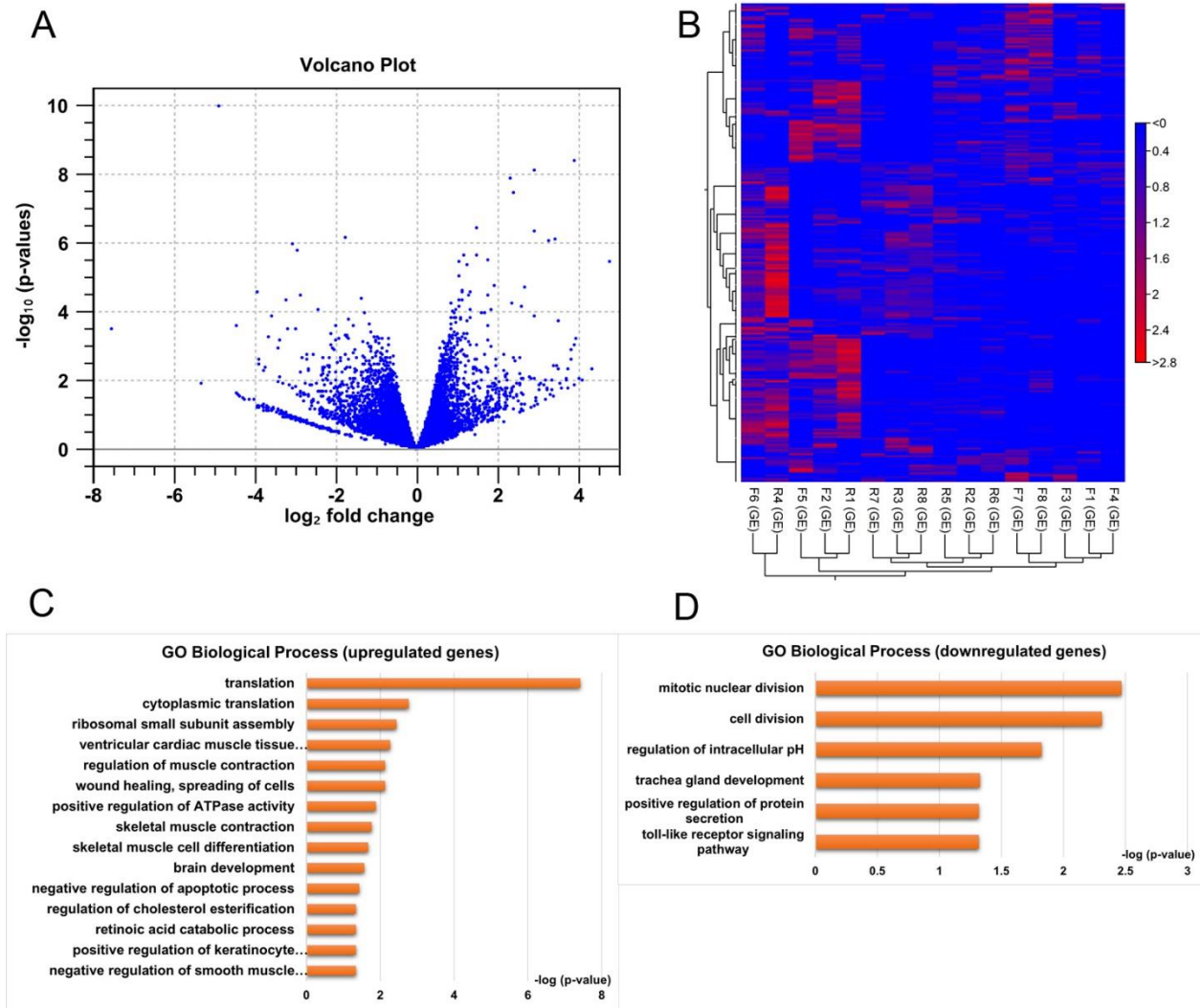


Figure II-4.2 mRNA profiles between full-nutrition (F) group and restricted-nutrition (R) group. (A) Full-nutrition group versus restricted-nutrition group mRNA volcano plot. (B) Heat map of mRNA profiles ($n = 8$) showing the top 250 differentially expressed mRNAs ($p < 0.05$, absolute fold change > 1.5) in fetal liver between full-nutrition group and restricted-nutrition group. Blue indicates low expression levels; while red reflects high expression levels. (C) Gene ontology (GO) biological process annotations for differentially expressed mRNAs ($p < 0.05$, absolute fold change > 1.5) in fetal liver between full-nutrition group and restricted-nutrition group. (C) showing the upregulated genes in R group, (D) showing the downregulated genes in R group.

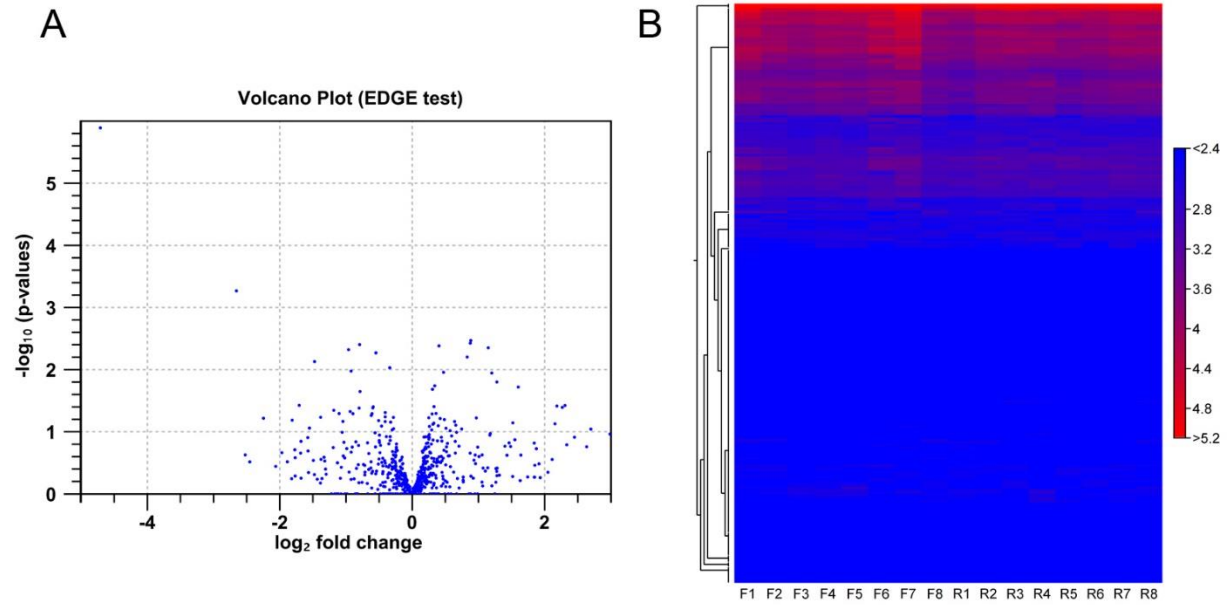


Figure II-4.3 miRNA profiles between full-nutrition (F) group and restricted-nutrition (R) group. Full-nutrition group versus restricted-nutrition group miRNA volcano plot ($n = 8$). (B) Heat map of miRNA profiles ($n = 8$) showing the miRNAs in fetal liver between full-nutrition group and restricted-nutrition group. Blue indicates low expression levels; while red reflects high expression levels.

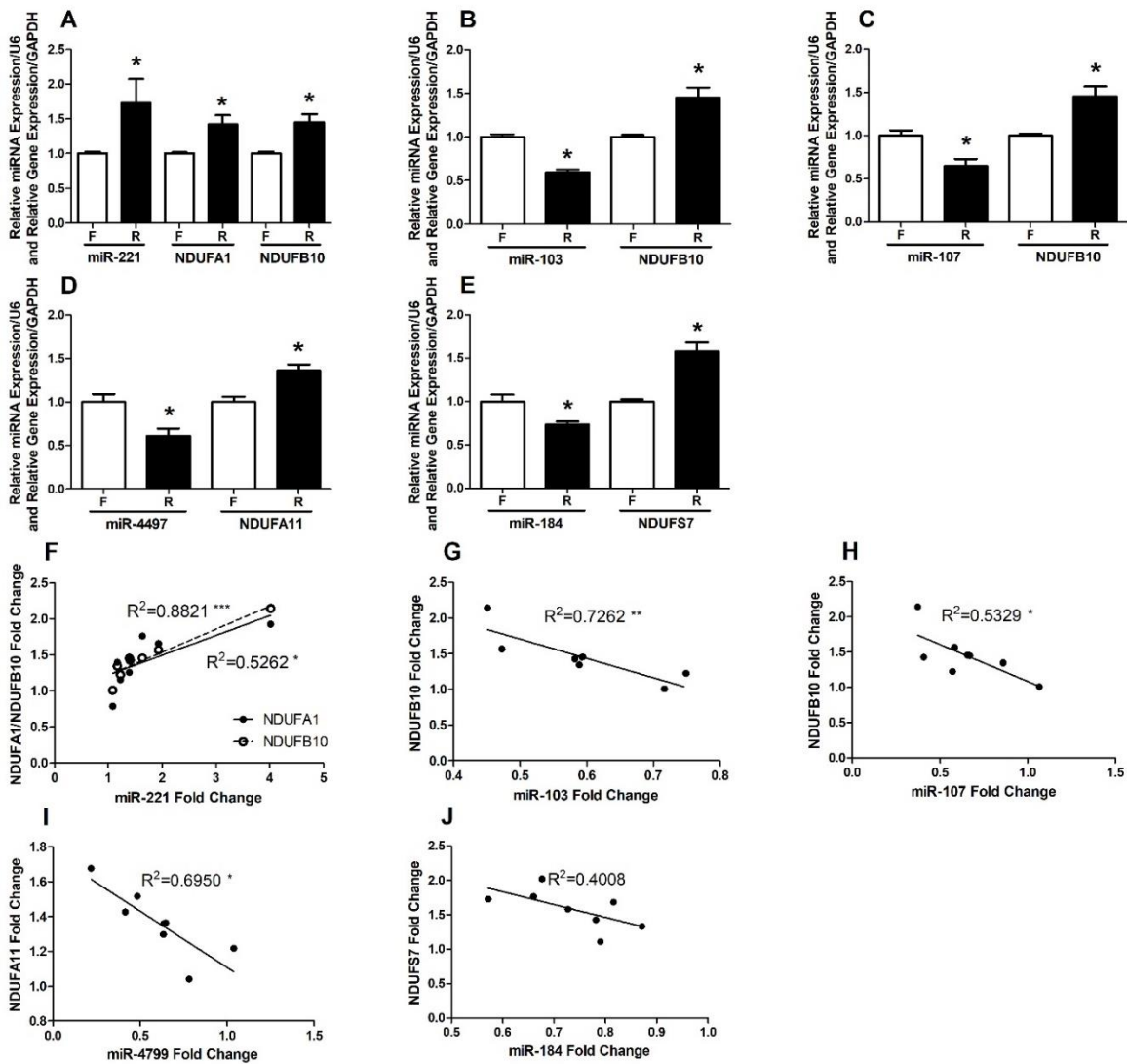


Figure II-4.6 Relative expression of miRNAs and genes and their correlational analysis in fetal liver in full-nutrition (F) group and restricted-nutrition (R) group ($n = 8$). The data are expressed as fold-change (mean \pm SEM). The significance level (*) was set at $p < 0.05$, (**) was set at $p < 0.01$, and (***) was set at $p < 0.001$, respectively. (A) shows miR-221 targeting *NDUFA1* and *NDUFB10*; (B) shows miR-103 targeting *NDUFB10*; (C) shows miR-107 targeting *NDUFB10*; (D) shows miR-4497 targeting *NDUFA11*; (E) shows miR-184 targeting *NDUFS7*; (F) shows correlation between miR-221 and *NDUFA1*/*NDUFB10*; (G) shows correlation between miR-103 and *NDUFB10*; (H) shows correlation between miR-107 and *NDUFB10*; (I) shows correlation between miR-4799 and *NDUFA11*; (J) shows correlation between miR-184 and *NDUFS7*.

Chapter III Dietary Choline and Docosahexaenoic Acid (DHA) Supplementation to Pregnant Pigs Experiencing Gestational Nutrition Restrictions Impacts Hepatic miRNA and mRNA Expression in Full-term Fetal Pigs

III-1. Abstract

Maternal undernutrition causes serious consequences for the developing fetus, and maternal choline and docosahexaenoic acid (DHA) supply are crucial for fetal health during gestation. Thus, we sequenced mRNA and miRNA on fetal liver samples obtained from pregnant pigs subjected to restricted feed intake, supplemented in a 2 (\pm choline) x 2 (\pm DHA) factorial design. This investigation aimed to explore the individual and interactive effects of choline and DHA during gestational nutrition restriction on the fetal liver. By conducting 2 x 2 factorial analysis, and following ingenuity pathways analysis (IPA), we identified 144 mRNAs and 1 miRNA (miR-503) that were altered by choline. Specifically, 5 pathways: cardiac hypertrophy signaling, IL-6 signaling, IL-3 signaling, Th1 pathway, and acute phase response signaling were inhibited by maternal supplementation of choline. 151 mRNAs and 6 miRNAs were altered by DHA. Specifically, 5 inositol-related pathways, 5 immune-related pathways, cardiac hypertrophy signaling, sphingosine-1-phosphate signaling, signaling by Rho family GTPases, thrombin signaling, actin nucleation by ARP-WASP complex, regulation of actin-based motility by Rho, and cholecystokinin/gastrin-mediated signaling were inhibited by maternal supplementation of DHA, whereas PPAR signaling and RhoGDI signaling were stimulated. Furthermore, 383 mRNAs and 25 miRNAs displayed a choline x DHA interaction effect; 17 mRNAs displayed a synergistic interaction which stimulated acute phase response signaling. In contrast, 204 mRNAs and 19 miRNAs displayed a choline x DHA antagonistic effect, with choline having the greater impact. Specifically, 4 pathways: sirtuin signaling pathway, tRNA splicing, PPAR α /RXR α

activation, and NAD signaling pathway were inhibited by this effect. 162 mRNAs and 6 miRNAs displayed the choline x DHA antagonistic effect, with DHA having the greater impact. RNA polymerase I transcription pathway was inhibited by this effect, while sirtuin signaling pathway was stimulated. Through miRNA target prediction analysis, we identified 20 miRNA-mRNA pairings. Validation using RT-qPCR confirmed the accuracy of 10 of these miRNA-mRNA pairs, aligning with the findings from the initial sequencing data. They are miR-503 targeting *LIPG* and *SPOUT1*, miR-221 targeting *TIMP3* and *TM4SF1*, miR-31 targeting *CASR* and *FLOT1*, Let-7f targeting *DUSP16* and *CDKN1A*, miR-26b targeting *FAM98A*, and miR-144 targeting *PLAT*. In conclusion, our study empowered the significant influence of maternal choline and DHA supplementation during gestational feed restriction on the hepatic expression patterns of miRNA and mRNA in offspring. Utilizing statistical and pathway analyses, we described the specific effects of maternal choline or DHA supplementation, as well as their interactions on distinct genes, biological processes, and metabolic and signaling pathways. Furthermore, we successfully identified and validated a subset of miRNA-mRNA pairings that could potentially play a role in the regulatory mechanisms induced by maternal supplementation with choline or DHA during feed restriction.

III-2. Introduction

Choline, an essential micronutrient for fetal development, serving as a precursor of acetylcholine and a constituent of key phospholipids in the central nervous system (phosphatidylcholine and sphingomyelin) (Blusztajn, et al., 1987). Additionally, acting as a supplier of methyl groups via its derivative betaine, choline plays a role in generating the universal methyl donor S-adenosylmethionine (SAM) (Spoelstra, et al., 2023). The presence of SAM affects the DNA methylation status, thereby influencing gene expression during fetal development (Zeisel, 2017).

Maternal supplementation of choline during pregnancy is anticipated to impact the epigenetic status of the developing fetal brain and liver. Evidence from studies with rats and mice reveals that maternal dietary choline intake significantly influences neurogenesis (Craciunescu, et al., 2003) and angiogenesis (Mehedint, et al., 2010). A maternal diet deficient in choline has been shown to decrease these processes in the fetal hippocampus by regulating DNA methylation, leading to increased apoptosis in this brain region (Craciunescu, et al., 2003; Mehedint, et al., 2010; Niculescu, et al., 2006). Specifically, the gene encoding cyclin-dependent kinase (Cdkn3) showed hypomethylation in its promoter, resulting in increased gene expression and downstream signaling associated with reduced cell cycling, consistent with decreased neurogenesis (Niculescu, et al., 2006). These structural changes in the fetal brain due to maternal choline intake during pregnancy have enduring effects on brain function throughout life, including sustained alterations in hippocampal function (memory) in adult offspring. Notably, choline supplementation in pregnant rats has been found to enhance memory in their offspring, with this improvement persisting into old age (Meck & Williams, 1997). Conversely, offspring from mothers on a choline-deficient diet exhibited contrasting outcomes (Meck & Williams,

1997).

Liver is a central hub for choline metabolism, orchestrating various metabolic pathways essential for maintaining cell functions (Smallwood, et al., 2016). The significance of maternal choline in fetal liver development was reported by Carolan-Olah *et al* (2015). They employed a toxic milk (tx-j) mouse model of Wilson's Disease. Wilson disease (WD), which is caused by autosomal recessive mutations in *ATP7B* encoding a biliary copper transporter, is characterized by excessive hepatic copper accumulation. In contrast to control group, the fetal livers of tx-j mice exhibited significantly reduced copper concentrations and lower transcript levels of genes associated with methionine (*MAT2A*, *MTR*, *SAHH*), lipid metabolism (*CPT1A*, *PPAR α*), DNA methylation (*DNMT1*, *DNMT3A*, *DNMT3B*) and cell cycle (*Cyclin D1*). Maternal choline supplementation effectively mitigated all the down-regulated genes in fetal tx-j livers. Notably, global DNA methylation in tx-j fetal livers increased by 17% following maternal choline supplementation ($p < 0.05$). This study underscores the significance of maternal choline during fetal development.

Additionally, Yan *et al.* (2014) discovered that maternal choline supplementation resulted in an improved hepatic phosphatidylethanolamine N-methyltransferase (PEMT) activity, contributing to sustained cognitive benefits in the Ts65Dn mouse model of Alzheimer's disease. Adult Ts65Dn offspring born to dams supplemented with choline showed a 60% increase in hepatic PEMT activity and a higher content of PEMT-derived metabolites compared to those born to dams without choline supplementation. PEMT plays a role in *de novo* choline synthesis, leading to the production of phosphatidylcholine enriched in docosahexaenoic acid (DHA). These data demonstrate that maternal supplementation of choline can enhance the activity of the PEMT pathway in adult Ts65Dn mice. Furthermore, phosphatidylcholine can combine with

DHA to form phosphatidylcholine- DHA, although its specific benefits are not extensively studied (Patrick, 2019).

Hence, recognizing the crucial role of choline in fetal liver development, researchers have been initiated to explore the potential benefits of supplementing maternal choline to mitigate the adverse effects associated with maternal undernutrition. Choline supplementation during pregnancy had a positive impact on fetal liver DNA methylation in pigs experiencing maternal undernutrition (Lima, et al., 2017). Pregnant pigs experienced a gradual reduction in feed intake by 50% to 70% from day 35 until delivery. This resulted in a significant increase in DNA methylation in the livers of their LBW offspring. Intriguingly, maternal choline supplementation was able to mitigate the elevated DNA methylation levels. However, the epigenetic role of choline in the fetal liver, particularly under conditions of maternal undernutrition, remains less understood, and this is one of the objectives of our study.

DHA, an omega-3 fatty acid, is another important nutrient we focused on not only because of its role in fetal health, but also because there are interactions between choline and DHA and synergistic effects on metabolism (Mun, et al., 2019). DHA is distributed in different tissues of the body (Lacombe, et al., 2018), with a notable concentration in the brain and retina. The liver contributes to the storage and release of DHA, ensuring the maintenance of sufficient levels throughout the body. DHA plays an important role in fetal brain and eye development, as DHA is present in high levels in both retinal and synaptic membrane phospholipids (Carlson & Colombo, 2016). Research demonstrates that taking DHA supplements during pregnancy could result in beneficial outcomes for offspring, such as improved cognitive and visual development (Lauritzen L, 2016; Koletzko, et al., 2008). In gestating ewes, DHA supplementation caused alterations not only in the growth of offspring (Nickles, et al., 2019), but also in the mRNA

expression of DNA methyltransferase (DNMT)-3A and free fatty acid receptor (FFAR)-4 in placenta (Roque-Jimenez, et al., 2020). Moreover, the addition of DHA supplements increased basal concentrations of resolvins, which are lipid mediators with anti-inflammatory and pro-resolution properties. It also upregulated the mRNA expression of lipoxygenases (ALOX), which are enzymes involved in the synthesis of resolvin D1 (RvD1) in rat placenta (Serhan, et al., 2002).

The interaction between choline and DHA involves their collaborative influence on various metabolic processes (Waterland & Rached, 2006). The addition of DHA significantly raised cellular choline uptake in human retinal cells, in comparison to cultured cells without DHA supplementation (Jones, et al., 2013). DHA also stimulated choline acetyltransferase (ChAT) activity and support neural cell growth and function in neural cell culture studies (Treen, et al., 1992). In addition, result from an *in-vivo* study with phosphatidylethanolamine N-methyltransferase (PEMT) gene knockout mouse model demonstrated the interaction of DHA and choline, in which PEMT enzyme facilitated endogenous hepatic synthesis of phosphatidylcholine from phosphatidylethanolamine, and maternal dietary DHA supplementation could reverse disrupted fetal hippocampal development caused by PEMT deficiency (Machová, et al., 2006). Moreover, supplementation of choline with DHA during pregnancy has many beneficial effects on fetal health, such as decreasing lipopolysaccharide (LPS)-induced neuroinflammation in microglia neuronal cells (da Costa, et al., 2010), reducing brain oxidative stress in a perinatal maternal separation stress rodent model (Fourrier, et al., 2017), and supporting brain development of offspring in rats, dogs, and pigs (Almeida, et al., 2018; Rajarethnem, et al., 2017; Zicker, et al., 2012). Nevertheless, the specific contributions of DHA and choline, as well as their interplay in the context of fetal liver development under

conditions of maternal undernutrition, remain uncertain. Our research investigation focuses on addressing this question.

III-3. Materials and Methods

III-3.1. Experimental Design

The experimental design was described previously by Lima *et al.* (2017). In brief, pregnant pigs (Landrace x Yorkshire x Duroc) with first parity were housed individually at the Swine Educational Unit located within North Carolina State University. All protocols were reviewed and approved by the North Carolina State University Animal Care and Use Committee. Pigs were randomly allocated to 4 dietary treatment groups following a 2 (\pm choline) x 2 (\pm DHA) factorial design. They are Choline-DHA-, Choline+DHA-, Choline-DHA+, and Choline+DHA+ groups. They received a standard gestational diet formulated with corn-plus-isolated-soyprotein as the primary component, and the diet (**Table III-3.1-1**) met all nutrient requirements for gestating pigs as outlined by the National Research Council (NRC, 2012). Prior to breeding, all pigs were fed gestation diet for 2 weeks at a standard rate of 2.5 kg feed per day, which included choline and DHA (**Table III-3.1-2**). After insemination, all four groups of pregnant pigs were fed 1.0 kg per day (which is a 50% intake restriction relative to 2.0 kg standard feed intake) supplemented with or without either choline or DHA, every morning for 35 days. Following the first confirmation of pregnancy via ultrasound (performed on day 35 after insemination), the feed allotment was further reduced to 0.6 kg per day (a 70% feed restriction) for the remaining gestation period. Full term fetuses were obtained via C-section and liver tissues were immediately collected. Samples were rapidly frozen in liquid nitrogen, and subsequently kept at -80°C .

III-3.2. RNA Sequencing

The total RNA of the liver was obtained from 32 full-term fetal pigs. In each treatment, four litters were selected, and then two fetal pigs were selected from each litter, resulting in $n=8$ replications per treatment. The Ion Total RNA-Seq Kit v2 (ThermoFisher 4479789, Waltham, MA, USA) was used to prepare the library and the barcode indices were designed according to the manufacturer's instructions. An Illumina Genome Analyzer IIX (GAIIX) was used to sequence both mRNA and miRNA at the NCSU Genomic Sciences Laboratory. The sequencing was completed with the same RNA extract for all the fetal liver samples.

III-3.3. Data Analysis for RNA-sequencing

We used the CLC Genomics Workbench (Qiagen, Hilden, Germany) for processing and analyzing all sequencing data. For mRNA sequencing analysis, we imported RNA-seq raw data (FASTQ files) into the software and removed all residual adaptor sequences and low-quality sequences (Phred < 20) using the NGS trim tool. The reads were then mapped to the *Sus scrofa* reference genome (*Sus scrofa* 11.1) and normalized using the TMM (trimmed mean of M values) method. To identify differentially expressed genes (DEGs), we utilized the RNA-seq analysis tool for mRNA expression analysis, and the Differential Expression in Two Groups feature. The expression level of each gene was measured in counts per million reads (CPM).

To analyze miRNA sequencing data, we utilized the Small RNA Analysis suite. Firstly, the raw data was imported into the CLC Genomics Workbench, where the Extract and Count function was used to create the small RNA samples. Next, the Annotate and Merge Counts function was applied to annotate and merge miRNA samples based on miRBase 22.1 reference database, followed by normalization using the transformation and normalization tool. Finally, we used the Empirical Analysis of the DGE tool for differential expression analysis. The expression value of each miRNA was used for statistical analysis.

III-3.4. 2 x 2 Factorial Analysis

In our study, we obtained sequencing data from 4 treatment groups following a 2 x 2 factorial design. We conducted a two-phase statistical analysis (candidate gene selection and 2 x 2 factorial analysis) to study the choline, DHA, and their interaction effect on the regulation of mRNA and miRNA expression. Phase one: among 4 treatment groups, multiple comparisons were conducted using a program in CLC Genomics Workbench (Qiagen, Hilden, Germany) called Differential Expression in Two Groups. We totally identified 812 differentially expressed mRNAs (FDR < 0.05) and 120 differentially expressed miRNAs ($p < 0.05$) among 4 treatment groups. Phase two: All of mRNAs and miRNAs were selected to perform the 2 x 2 factorial analysis (based on the CPM of mRNA or the expression value of miRNA) using GLM model in SAS software 9.4 (Cary, NC, USA). Firstly, we examined whether there were choline x DHA interaction effects on the expression of these genes. Secondly, for genes without interaction effect, we assessed the individual effects of choline and DHA on their expression. Thirdly, for genes with interaction effects, we further identified whether they were synergistic or antagonistic effects based on the comparison of CPM (representing mRNA expression value) between the Choline+DHA-, Choline-DHA+, or Choline+DHA+ group and the Choline-DHA- group. If the absolute CPM difference ($|\text{Choline+DHA+} - \text{Choline-DHA-}|$) was greater than the absolute CPM difference ($|\text{Choline-DHA+} - \text{Choline-DHA-}|$) and ($|\text{Choline+DHA-} - \text{Choline-DHA-}|$), it was classified as synergistic effects, which means the combined effect of choline and DHA was greater than they were individually. Otherwise, it was classified as antagonistic effects, which means the combined effect of the two factors was less than they would be individually. Finally, under antagonistic effects, our focus was on determining whether maternal choline or DHA had a greater effect on specific mRNA expression. To investigate this, we categorized the genes into

two groups based on the comparison of CPM between the Choline+DHA- or Choline-DHA+ group and the Choline-DHA- group. If the absolute CPM difference ($|\text{Choline+DHA-} - \text{Choline-DHA-}|$) was greater than the absolute CPM difference ($|\text{Choline-DHA+} - \text{Choline-DHA-}|$), it indicated that maternal choline had a more substantial impact on these genes compared to DHA. Conversely, if the absolute CPM difference ($|\text{Choline-DHA+} - \text{Choline-DHA-}|$) was greater than the absolute CPM difference ($|\text{Choline+DHA-} - \text{Choline-DHA-}|$), it suggested that maternal DHA had a greater influence on these genes than choline.

III-3.5. Gene Ontology Enrichment Analysis and Ingenuity Pathways Analysis

The DAVID Functional Annotation Tool v6.8 (available at <https://david.ncifcrf.gov/>) was used to identify the Biological Processes from the Gene Ontology (GO) database. We uploaded the gene lists with *Sus scrofa* as background and the analysis was conducted with a significance criterion of $EASE < 0.05$. A $p < 0.05$ was considered statistically significant. Ingenuity Pathways Analysis (IPA) software (Qiagen, Hilden, Germany) and Core Analysis function was used to explore modified pathways. Pathways with an absolute z-score > 2 and a $p < 0.05$ were considered significant. The z-score is a statistical measure of the match between expected relationship direction and observed gene expression. A positive z-score indicates activation, while a negative score indicates inhibition.

III-3.6. miRNA Target Prediction Analysis

The miRNA-mRNA target prediction was conducted using a miRNA Target Filter in IPA software. Briefly, we imported miRNAs data of each group (generated from 2 x 2 factorial analysis) into IPA, run the miRNA Target Filter, and associated it with corresponding mRNAs in the same statistical category from 2x2 factorial analysis. Then a miRNA-mRNA target prediction list was generated. Both experimentally verified and "highly predicted" miRNA-mRNA

correlations will be used. Moreover, it incorporated both positive and negative correlation expression pairings.

III-3.7. RT-qPCR Validation for miRNA-mRNA Pairings

After total RNA extraction, we utilized the QuantiTect Reverse Transcription Kit (Qiagen, Hilden, Germany) to synthesize mRNA cDNA, while miScript II RT Kit (Qiagen, Hilden, Germany) was used for miRNA cDNA synthesis. RT-qPCR was employed to determine mRNA and miRNA expression levels, using the CFX Connect Real-Time PCR Detection System (Bio-Rad). We validated the expressions of 20 mRNAs and 12 miRNAs. The primer sequences are provided in (**Table III-3.7**). *GAPDH* and *U6* were utilized to normalize the expression levels of target mRNAs and miRNAs, respectively.

III-3.8. Choline Content Measurement in Fetal Liver

Choline content in fetal liver sample was measured ($n = 8$) using Amplite® Choline Quantitation Kit according to the user's manual (AAT Bioquest 40007, Sunnyvale, CA, USA).

III-3.8. Statistical Analysis

Candidate gene selection (multiple comparisons among 4 treatment groups) for 2 x 2 factorial design was conducted using a program in CLC Genomics Workbench (Qiagen, Hilden, Germany) called 'Differential Expression in Two Groups'. mRNA with an FDR < 0.05 and miRNA with a p -value < 0.05 were selected. The 2 x 2 factorial analysis for mRNA and miRNA sequencing data were performed using General Linear Models (GLM) model in SAS software 9.4 (Cary, NC USA). For bioinformatics analysis, we utilized built-in packages within IPA and CLC Workbench. When $p < 0.05$ it was considered statistically significant in all the analyses.

III-4. Results

III-4.1. The Statistical Summary of mRNA and miRNA in 2 x 2 Factorial Design

Results of mRNAs from the statistical analysis with SAS GLM model following a 2 x 2 factorial design were listed in **Table III-4.1-1**. The expressions of 144 mRNAs were altered by choline, with no interactions (Choline $p < 0.05$; Choline x DHA interaction $p > 0.05$). Among them, 38 mRNAs' expressions were upregulated in response to maternal undernutrition when supplemented with choline compared to the condition without choline, while 106 mRNAs' expressions were downregulated. 151 mRNAs' expressions were altered by DHA, with no interactions (DHA $p < 0.05$; Choline x DHA interaction $p > 0.05$). Among them, 43 mRNAs' expressions were upregulated in response to maternal undernutrition when supplemented with DHA compared to the condition without DHA, while 108 mRNAs' expressions were downregulated. 383 mRNAs' expressions displayed a Choline x DHA interaction ($p < 0.05$). Of them, 17 mRNAs' expressions had synergistic effects, while 366 mRNAs' expressions had antagonistic effects. Among the mRNAs' expressions exhibiting antagonistic effects, 204 mRNAs' expressions showed a greater impact of choline, while 162 mRNAs' expressions showed a greater impact of DHA.

Likewise, miRNA results were listed in **Table III-4.1-2**. miR-503's expression was altered by choline, with no interaction (Choline $p < 0.05$; Choline x DHA interaction $p > 0.05$). 6 miRNAs (miR-221, 4677, 219a-2, 31, 26a-1, and 450a) were altered by DHA, with no interaction (DHA $p < 0.05$; Choline x DHA interaction $p > 0.05$). 25 mRNAs' expressions displayed a Choline x DHA interaction ($p < 0.05$), and they all had antagonistic effects. Of them, the expression of 19 miRNAs (miR-101-1, 101-2, 182, 218b, 218-1, 29a, 26b, 21, 205, 30b, 190a, let-7a-1, 7a-2, 7f-2, 7f-1, 7i, 7c, 7d, 7e) showed a greater impact of choline, while the expression of 6 miRNAs (miR-92a-1, 10b, 144, 582, 1260a, 183) showed a greater impact of DHA.

III-4.2. GO Enrichment Analysis and IPA Analysis for Genes Have the Choline Effect

We conducted GO enrichment analysis for 144 genes that showed a choline effect (without choline x DHA interaction effect). 106 downregulated mRNA expressions, induced by maternal choline supplementation, were related to 11 biological processes (**Figure III-4.2**). These processes were identified as: JAK-STAT cascade, negative regulation of glycolytic process, cell differentiation, cellular response to DNA damage stimulus, fatty acid elongation, monounsaturated fatty acid, circadian regulation of gene expression, fatty acid elongation, polyunsaturated fatty acid, fatty acid elongation, saturated fatty acid, ER overload response, positive regulation of miRNA mediated inhibition of translation, negative regulation of inflammatory response. There were 38 upregulated mRNA expressions, induced by maternal choline supplementation, that were not associated with any identified biological processes.

In IPA analysis, 5 canonical pathways (**Table III-4.2**) were changed with a criterion of $p < 0.05$ and absolute z-score > 2 , all of them were inhibited (z-score < -2). These pathways are cardiac hypertrophy signaling, IL-6 signaling, IL-3 signaling, Th1 pathway, acute phase response signaling.

III-4.3. GO Enrichment Analysis and IPA Analysis for Genes Have the DHA Effect

We conducted GO enrichment analysis for 151 genes that had a DHA effect (without choline x DHA interaction effect). 108 downregulated genes, induced by maternal DHA supplementation, were related to 7 biological processes (**Figure III-4.3**). These biological processes were identified as: response to glucose, establishment or maintenance of cell polarity, cell migration, negative regulation of defense response to bacterium, regulation of cell shape, negative regulation of cGMP-mediated signaling, and cellular response to arsenic-containing substance. There were 43 upregulated genes associated with protein localization to plasma

membrane and regulation of Rho protein signal transduction.

In IPA analysis, 19 canonical pathways (**Table III-4.3**) were modified with a criterion of $p < 0.05$ and absolute z-score > 2 . Among them, 17 pathways were inhibited (z-score < -2), including cardiac hypertrophy signaling, Tec kinase signaling, phospholipase C signaling, sphingosine-1-phosphate signaling, IL-6 signaling, 3-phosphoinositide biosynthesis, CXCR4 signaling, signaling by Rho family GTPases, superpathway of inositol phosphate compounds, thrombin signaling, systemic lupus erythematosus in T cell signaling pathway, hepatic fibrosis signaling pathway, actin nucleation by ARP-WASP complex, regulation of actin-based motility by Rho, cholecystokinin/gastrin-mediated signaling, D-myo-inositol (1,4,5,6)-tetrakisphosphate biosynthesis, and D-myo-inositol (3,4,5,6)-tetrakisphosphate biosynthesis; whereas, PPAR signaling and RhoGDI signaling were stimulated (z-score > 2).

III-4.4. GO Enrichment and IPA Analysis for Genes Having a Choline x DHA Interaction Effect *Genes Having a choline x DHA Synergistic Effect*

We conducted GO enrichment analysis for 17 genes that had the choline x DHA synergistic effect. 13 downregulated mRNA expressions were related to two biological processes: negative regulation by host of viral process and complement activation, classical pathway (**Figure III-4.4**). 4 upregulated mRNA expressions failed to associate with any identified biological processes.

In IPA analysis, acute phase response signaling was inhibited (z-score < -2) by maternal choline x DHA synergistic effect.

Genes Having a Choline x DHA Antagonistic Effect, with Choline Displaying the Greater Impact

We conducted GO enrichment analysis for 204 genes that display a choline x DHA antagonistic effect. 144 downregulated genes were related to 6 biological processes: negative

regulation of oxidative phosphorylation, cellular response to leukemia inhibitory factor, positive regulation of response to cytokine stimulus, negative regulation of gene expression, glutathione biosynthetic process, and 'de novo' pyrimidine nucleobase biosynthetic process. We identified 60 upregulated genes that were associated with intracellular protein transport.

In IPA analysis, 4 canonical pathways (**Table III-4.4**) were modified with a criterion of $p < 0.05$ and absolute z-score > 2 , all of them were inhibited (z-score < -2), including, sirtuin signaling pathway, tRNA splicing, PPAR α /RXR α activation, and NAD signaling pathway.

Genes Having a Choline x DHA Antagonistic Effect, with DHA Displaying the Greater Impact

We conducted GO enrichment analysis for 162 genes that displayed a choline x DHA antagonistic effect. 107 downregulated genes were related to 6 biological processes: cytoplasmic translational termination, protein methylation, regulation of translational termination, mitochondrion organization, N-terminal protein amino acid acetylation, and positive regulation of transcription, DNA-templated. We identified 55 upregulated genes that were associated with intracellular protein transport, and labyrinthine layer blood vessel development.

In IPA analysis, 2 canonical pathways (**Table III-4.4**) were modified with a criterion of $p < 0.05$ and absolute z-score > 2 . RNA Polymerase I Transcription was inhibited (z-score < -2), while sirtuin signaling pathway was stimulated (z-score > -2).

III-4.5. miRNA Target Prediction Analysis

By conducting miRNA target prediction analysis between miRNA and mRNA with the same statistical category from 2x2 factorial analysis, we found 20 miRNA-mRNA pairings (**Table III-4.5**). Of them, miRNA-503 was affected by choline, with no interaction effect (Choline $p < 0.05$, Choline x DHA interaction $p > 0.05$), and its predicted targeting mRNAs were endothelial lipase (LIPG), leucine rich adaptor protein 1-like (LURAP1L), growth arrest and

DNA damage inducible gamma (GADD45G), and SPOUT domain containing methyltransferase 1 (SPOUT1). MiR-221 and miR-31 were affected by DHA with no interaction effect (DHA $p > 0.05$, Choline x DHA interaction $p > 0.05$). MiR-221 was predicted to target phosphoinositide-3-kinase regulatory subunit 1 (PIK3R1), tissue inhibitor of metalloproteinases 3 (TIMP3), transmembrane 4 L six family member 1 (TM4SF1), and miR-31 was predicted to target calcium-sensing receptor (CASR), DEAD-box helicase 21 (DDX21), and flotillin-1 (FLOT1). In addition, we found that 10 miRNA-mRNA pairings displayed a Choline x DHA interaction $p < 0.05$, and they all were antagonistic. 8 of them choline has the greater impact, including: let-7f which was predicted to target cyclin-dependent Kinase Inhibitor 1A (CDKN1A), phosphatidylinositol glycan anchor biosynthesis class A (PIGA), and Dual-Specificity Phosphatase 16 (DUSP16); miR-182 was predicted to target solute carrier family 35 member G1 (SLC35G1) and transmembrane protein 42 (TMEM42); miR-218 was predicted to target solute carrier family 6 member 1 (SLC6A1); miR-26b was predicted to target family with sequence similarity 98 member A (FAM98A); miR-29a was predicted to target peptidylprolyl isomerase C (PPIC). For 2 of them DHA had the greater impact, including: miR-1260a which was predicted to target death domain-associated protein (DAXX) and miR-144 which was predicted to target tissue-type plasminogen activator (PLAT).

III-4.6. RT-qPCR Validation for miRNA-mRNA Pairings

RT-qPCR was conducted to validate those miRNA-mRNA pairings, and the relative miRNA and mRNA expression results were shown in **Table III-4.6**. 7 of 12 miRNA's results were consistent with sequencing data under 2 x 2 factory design, including: miR-503, 221, 31, 218, 26b, 144, and Let-7f. 14 of 20 mRNA's PCR results were consistent with sequencing data, including: *LIPG*, *SPOUT1*, *TIMP3*, *TM4SF1*, *CASR*, *FLOT1*, *DUSP16*, *CDKN1A*, *SLC35G1*,

TMEM42, *FAM98A*, *PPIC*, *DAXX*, and *PLAT*. Thus, 10 miRNA-mRNA pairings were validated, including: miR-503 targeting *LIPG* and *SPOUT1*, miR-221 targeting *TIMP3* and *TM4SF1*, miR-31 targeting *CASR* and *FLOT1*, Let-7f targeting *DUSP16* and *CDKN1A*, miR-26b targeting *FAM98A*, and miR-144 targeting *PLAT*.

III-5. Discussion

The significance of maternal choline and DHA in fetal liver development has received recent attention (Carolan-Olah, et al., 2015; Wahab, et al., 2022). Researchers have been initiated to explore the potential benefits of supplementing maternal choline and DHA to mitigate the adverse effects associated with maternal undernutrition (Lima, et al., 2017). However, their effect on fetal metabolic pathways has not been well investigated.

In this study, by applying mRNA sequencing and miRNA sequencing, we found that hundreds of genes expressed differentially in fetal liver from dams supplemented with choline and DHA during gestational undernutrition compared to un-supplemented dams. By conducting 2 x 2 factorial analysis on fetal liver mRNA expression, we found that maternal supplemental choline affected 144 genes. Some of them are first time reported associated with maternal choline, such as p21-activated kinase 4 (PAK4), cytochrome P450 family 4 subfamily A member 24 (CYP4A24), monoamine oxidase A (MAOA), elongation of very-long-chain fatty acids-like 2 (ELOVL2), glutaminase 2 (GLS2), lipin2 (LPIN2), and Argonaute RISC Catalytic Component 2 (AGO2). Through GO analysis, we found that choline has impact on the JAK-STAT signaling cascade, fatty acid metabolism, cell differentiation, and inflammatory response. In the IPA analysis, 4 pathways—IL-6 signaling, IL-3 signaling, Th1 pathway, and acute phase response signaling—are all observed to be inhibited by maternal choline supplementation. Interleukin (IL)-6 signaling is vital for the acute phase response, infection defense, and hepatocyte

homeostasis in the liver (Schmidt-Arras & Rose-John, 2016). Young mice fed a methionine-choline diet exhibit increased expression of the *IL-6* gene (Che, et al., 2020). Additionally, blocking IL-6 signaling in mice prevents the progression of steatohepatitis induced by a methionine-choline-deficient diet (Yamaguchi, et al., 2011; Yamaguchi, et al., 2010). Hence, there is a suggested association between the choline content in the liver and IL-6 signaling. However, the relationship between IL-6 signaling in fetal liver and maternal choline supplementation has not been thoroughly studied. The results of our study indicate that maternal choline supplementation inhibited IL-6 signaling in the fetal liver, along with 3 inflammation-related pathways (IL-3 signaling, Th1 pathway, and acute phase response signaling). Collectively, these findings underscore the critical role of maternal choline in regulating inflammatory status in fetal liver.

Next, we found that 151 genes were impacted by maternal supplemental DHA, some genes are first time reported associated with maternal DHA, such as flotillin-1 (FLOT1), PBX Homeobox 2 (PBX2), Solute Carrier Family 16 Member 1 (SLC16A1), Solute Carrier Family 7 Member 4 (SLC7A4), Rho Family GTPase 3 (RND3), peroxisome proliferator activated receptor delta (PPARD), and ubiquitin fold modifier 1 (UFM1). Through GO analysis, we found that DHA has an impact on maintaining cell polarity, cell migration, cell shape, cell signaling, and cellular response. In the IPA analysis, 5 pathways—phospholipase C signaling, 3-phosphoinositide biosynthesis, superpathway of inositol phosphate compounds, D-myo-inositol (1,4,5,6)-tetrakisphosphate biosynthesis, and D-myo-inositol (3,4,5,6)-tetrakisphosphate biosynthesis—are all related to inositol metabolism and observed to be inhibited by maternal DHA supplementation. Inositol phosphate, such as inositol trisphosphate (IP3) and diacylglycerol (DAG), function as secondary messengers in diverse cellular signaling pathways,

influencing processes such as insulin sensitivity, glucose uptake, and lipid metabolism (Shears, 2018). Additionally, inositol is a component of phospholipids, much like DHA, and both are integral components of cell membranes, contributing to cell structure and function (Tu-Sekine & Kim, 2022; Lauritzen L, 2016). To date, the regulation of inositol-related pathways by maternal DHA supplementation has not been extensively investigated. However, findings from McNamara *et al.* (2009) suggest that in female rats fed a nonfat diet (initiated 1 month before pregnancy) and whose offspring continued on a nonfat diet into adulthood, the prefrontal cortex of the brain exhibited a 65% decrease in DHA and a 21% decrease in inositol compared to the normal-fed group. Conversely, when offspring of mothers on a normal diet were switched to a nonfat diet from post-weaning to adulthood, DHA decreased by 27%, while inositol levels remained unchanged. This highlights the possibility that maternal supplemental DHA could impact inositol metabolism in their offspring, especially in situations of dietary fat deficiency. Together, our current study reveals the downregulation of 5 inositol-related pathways in the fetal liver due to maternal DHA supplementation under conditions of maternal feed-restriction. This suggests that DHA regulates inositol metabolism in fetal liver during maternal feed-restriction.

DHA also displayed an impact on 5 immune-related pathways, including IL-6 signaling, CXCR4 signaling, systemic lupus erythematosus in T cell signaling pathway, Tec kinase signaling (crucial in various cellular processes, particularly in immune cells), and hepatic fibrosis signaling pathway. More recent evidence demonstrated the role of DHA in controlling inflammatory responses (Djuricic & PC, 2021). It has been documented that DHA regulates *IL-6* expression in pancreatic acinar cells (Song, et al., 2017), *CXCR4* expression in colorectal cancer stem-like cells (Kalbkhani, et al., 2021), T cell inflammatory responses (Lee, et al., 2021; Talamonti, et al., 2023), and hepatic fibrosis in rats (He, et al., 2017). Furthermore, maternal

DHA supplementation has been reported to influence *IL-6* in rats' colon (Reddy & Naidu, 2016) and T cell in mouse spleen (Patel, et al., 2023). Notably, all 5 pathways are observed for the first time in the fetal liver due to maternal DHA supplementation under conditions of maternal feed-restriction. This underscores the pivotal role of DHA in immune response modulation.

Subsequently, we examined the interaction effect of maternal supplementation with choline and DHA on fetal hepatic gene expression. Currently, there is very limited research dedicated to this aspect. As a result, most of the genes, regardless of whether they exhibit synergistic or antagonistic effects, are being documented for the first time in our study. We found that acute phase response (APR) signaling displays a choline x DHA synergistic effect. The APR classically involves the swift reprogramming of gene expression and metabolism triggered by inflammatory cytokine signaling. Hepatocyte-derived acute phase proteins, integral components of the innate immune system, play a central role in restoring tissue homeostasis (Venteclef, et al., 2011). As mentioned earlier, both maternal choline and DHA impact the immune system. The synergistic effect observed on the APR signaling underscores their interaction and enhanced influence on immune response in the fetal liver when supplemented together.

Next, we observed inhibition in PPAR α /RXR α activation, indicating a choline x DHA antagonistic effect, with choline exhibiting a more substantial impact than DHA. PPAR α /RXR α activation refers to the activation of a specific nuclear receptor complex composed of two key proteins: Peroxisome Proliferator-Activated Receptor Alpha (PPAR α) and Retinoid X Receptor Alpha (RXR α). These receptors play crucial roles in regulating various physiological processes, especially those related to lipid metabolism and energy homeostasis (Tahri-Joutey, et al., 2021). Shen, et al. (2020) demonstrated that incubating LO2 hepatocytes with choline and non-esterified

fatty acids after 6 hours of serum starvation resulted in an increase in PPAR- α protein expression. Conversely, 10-week-old rats fed a methionine-choline-deficient diet for 10 weeks exhibited a downregulation in *PPAR α* gene expression in liver (Chen, et al., 2016). On the other hand, DHA is known as a PPAR α activator. Activated PPAR α then forms a heterodimer with RXR and binds regulatory elements in promoters of responsive genes, promoting the expression of genes involved in fatty acid oxidation and lipoprotein metabolism (Jump, et al., 2008). Both choline and DHA play a regulatory role in PPAR α /RXR α activation. Intriguingly, we found an antagonistic effect of maternal choline and DHA in the fetal liver, calling for further investigation in future research.

A choline x DHA antagonistic effect observed in another pathway, with choline exerting a greater impact, was the sirtuin signaling pathway, and it was inhibited. The sirtuin signaling pathway involves a group of proteins known as sirtuins (SIRT), which are a class of NAD⁺-dependent deacetylases and ADP-ribosyltransferases. They are involved in various biological processes, including metabolism, stress response (Lou, et al., 2021), longevity, and aging (Lee, et al., 2019). Xu *et al.*, (2019) demonstrated that choline mitigates cardiomyocyte remodeling and hypertrophy induced by abdominal aortic banding or angiotensin II in rats, with the assistance of SIRT3, a member of the sirtuin signaling pathway. Similarly, Song *et al.*, (2022) observed choline's alleviating effect on high-fat diet-induced hepatic lipid dysregulation with the involvement of SIRT3 in yellow catfish. On the other hand, Du *et al.*, (2022) discovered that dietary DHA-enriched phospholipids alleviate lipopolysaccharide-induced intestinal barrier injury in mice through the upregulation of sirtuin 1. Moreover, Shi *et al.*, (2019) found that DHA- phosphatidylcholine protects the kidneys from cisplatin-induced toxicity, and the upregulated sirtuin 1 may be an underlying mechanism in mice. Together, additional evidence

from our study affirmed the central roles of choline and DHA as key mediators in sirtuin signaling pathway regulation processes within the liver. The novel aspect of our investigation lies in its focus on maternal supplementation of choline and DHA and its antagonistic effect in liver during fetal development.

More intriguingly, our findings revealed that the sirtuin signaling pathway is subject to the antagonistic influence of choline and DHA. Specifically, we observed stimulation induced by DHA, whereas choline exhibited inhibitory effects on this pathway. The complexity of the sirtuin signaling pathway, which involves hundreds of genes and molecules, may contribute to the varied regulatory effects observed with choline and DHA. Different sections of the pathway likely have distinct regulatory mechanisms that respond differently to choline and DHA. The apparent contradictions in the observed effects underscore the intricate nature of the cellular regulatory network and the interplay between choline and DHA. Further in-depth studies are needed to unravel the specific mechanisms governing these interactions within the sirtuin signaling pathway.

As the last part of discussion, we propose a regulatory pathway based on the results from miRNA target prediction analysis and its RT-qPCR validation. We found that hepatic *LIPG* expression was modified by miR-503 (**Figure III-4.7-1, 2A**) in fetal pigs from dams with or without dietary choline supplementation during gestation. The *LIPG* expression decreased when the miR-503 expression increased, and a negative correlation was detected ($R^2 = 0.7$ and $p < 0.01$; **Figure III-4.7-2B**). Then, we observed a significant increase in choline content in the fetal liver due to maternal undernutrition, which subsequently decreased upon receiving maternal supplemental choline (**Figure III-4.7-3A**). This changes in choline content were consistent with changes in hepatic DNA methylations (**Figure III-4.7-3B**, data was reported previously by Lima

et al. (2017). Therefore, choline content in fetal liver may control gene expression (such as miR-503) by DNA methylation. Together, we hypothesize that choline regulates miR-503 expression in liver through DNA methylation. If methylation decreases in the promoter region of the miR-503 gene, it will lead to increased expression of miR-503. Released miR-503 can destabilize its target mRNA *LIPG* and repress *LIPG* translation, so that reduce the production of *LIPG* protein. Moreover, *LIPG* is a primary determinant of HDL-C level in circulation (Yu, et al., 2018), which help to reduce the risk of atherosclerotic cardiovascular disease (ASCVD) (Vitali, et al., 2017) (**Figure III-4.7-4**). Specifically, the epigenetic role of miR-503, identified from our study, in inhibiting expression/activity of hepatic *LIPG*, and increasing (or promoting) HDL-C level will be assessed under different choline concentrations. This may provide a new approach or idea in preventing the ASCVD development.

III-6. References

- Almeida, P. et al., 2018. Persistent attenuation of brain oxidative stress through aging in perinatal maternal separated rat pups supplemented with choline and docosahexaenoic acid or *Clitoria ternatea* aqueous root extract. *Folia Neuropathol*, Volume 56, p. 206–214.
- Blusztajn, J. et al., 1987. Phosphatidylcholine as a precursor of choline for acetylcholine synthesis. *Journal of Neural Transmission. Supplementum*, Volume 24, p. 247–259.
- Carlson, S. & Colombo, J., 2016. Docosahexaenoic Acid and Arachidonic Acid Nutrition in Early Development. *Adv Pediatr*, Volume 63, p. 453–471.
- Carolan-Olah, M., Duarte-Gardea, M. & Lechuga, J., 2015. A critical review: early life nutrition and prenatal programming for adult disease. *J Clin Nurs*, pp. 24(23-24):3716–29.
- Chen, J., Fan, X., Zhou, L. & Gao, X., 2016. Treatment with geraniol ameliorates methionine-choline-deficient diet-induced non-alcoholic steatohepatitis in rats. *Journal of gastroenterology and hepatology*, 31(7), p. 1357–1365.
- Che, Y. et al., 2020. Resveratrol prevents liver damage in MCD-induced steatohepatitis mice by promoting SIGIRR gene transcription. *The Journal of nutritional biochemistry*, Volume 82, p. 108400.
- Craciunescu, C. et al., 2003. Choline availability during embryonic development alters progenitor cell mitosis in developing mouse hippocampus. *The Journal of nutrition*, 133(11), p. 3614–3618.
- da Costa, K. et al., 2010. Dietary Docosahexaenoic Acid Supplementation Modulates Hippocampal Development in the *Pemt*^{-/-} Mouse. *J. Biol. Chem*, Volume 285, p. 1008–1015.
- Djuricic, I. & PC, C., 2021. Beneficial Outcomes of Omega-6 and Omega-3 Polyunsaturated Fatty Acids on Human Health: An Update for 2021. *Nutrients*, Volume 13, p. 2421.

Du, L. et al., 2022. DHA-Enriched Phospholipids and EPA-Enriched Phospholipids Alleviate Lipopolysaccharide-Induced Intestinal Barrier Injury in Mice via a Sirtuin 1-Dependent Mechanism. *Journal of agricultural and food chemistry*, 70(9), p. 2911–2922.

Fourrier, C. et al., 2017. Docosahexaenoic acid-containing choline phospholipid modulates LPS-induced neuroinflammation in vivo and in microglia in vitro. *J. Neuroinflam*, Volume 14, p. 170.

He, J. et al., 2017. Docosahexaenoic acid attenuates carbon tetrachloride-induced hepatic fibrosis in rats. *International immunopharmacology*, Volume 53, p. 56–62.

Jones, M. et al., 2013. Maternal dietary omega-3 fatty acid intake increases resolvin and protectin levels in the rat placenta. *J Lipid Res*, 54(8), p. 2247–2254.

Jump, D. et al., 2008. Docosahexaenoic acid (DHA) and hepatic gene transcription. *Chemistry and physics of lipids*, 153(1), p. 3–13.

Kalbkhani, F., Pirnejad, A., Sam, S. & Sam, M., 2021. The Safe Soluble Compound Dehydroascorbic Acid Inhibits Various Upstream and Downstream Effectors of PI3K and KRAS Signaling Pathways in Undruggable PIK3CA/KRAS-Mutant Colorectal Cancer Stem-Like Cells. *Nutrition and cancer*, 73(11-12), p. 2654–2664.

Koletzko, B. et al., 2008. The roles of long-chain polyunsaturated fatty acids in pregnancy, lactation and infancy: review of current knowledge and consensus recommenda. *Journal of perinatal medicine*, 36(1), p. 5–14.

Lauritzen L, B. P. M. A. H. L. C. V. A. C., 2016. DHA Effects in Brain Development and Function. *Nutrients*, 8(1), p. 6.

Lee, J. et al., 2021. Common and differential effects of docosahexaenoic acid and eicosapentaenoic acid on helper T-cell responses and associated pathways. *BMB Rep*, Volume 54, p. 27.

Lima, H. et al., 2017. Supplementation of Maternal Diets with Docosahexaenoic Acid and Methylating Vitamins Impacts Growth and Development of Fetuses from Malnourished Gilts.. *Current developments in nutrition*, pp. 2(3), nzx006..

Lou, T. et al., 2021. Targeting Sirtuin 1 signaling pathway by ginsenosides. *Journal of ethnopharmacology*, Volume 268, p. 113657.

Machová, E., Nováková, J., Lisá, V. & Dolezal, V., 2006. Docosahexaenoic acid supports cell growth and expression of choline acetyltransferase and muscarinic receptors in NG108-15 cell line. *J Mol Neurosci*, 30(1-2), pp. 25-6.

McNamara, R. et al., 2009. Perinatal n-3 fatty acid deficiency selectively reduces myo-inositol levels in the adult rat PFC: an in vivo (1)H-MRS study. *Journal of lipid research*, 50(3), p. 405–411.

Meck, W. & Williams, C., 1997. Perinatal choline supplementation increases the threshold for chunking in spatial memory. *Neuroreport*, Volume 8, p. 3053–9.

Mehedint, M., Craciunescu, C. & Zeisel, S., 2010. Maternal dietary choline deficiency alters angiogenesis in fetal mouse hippocampus. *Proc Natl Acad Sci USA*, Volume 107, p. 12834–9.

Mun, J., Legette, L., Ikonte, C. & Mitmesser, S., 2019. Choline and DHA in Maternal and Infant Nutrition: Synergistic Implications in Brain and Eye Health. *Nutrients*, 11(5), p. 1125.

Nickles, K., Hamer, L., Coleman, D. & Relling, A., 2019. Supplementation with eicosapentaenoic and docosahexaenoic acids in late gestation in ewes changes adipose tissue gene expression in the ewe and growth and plasma concentration of ghrelin in the offspring. *J Anim Sci*, Volume 97, p. 2631–2643.

Niculescu, M., Craciunescu, C. & Zeisel, S., 2006. Dietary choline deficiency alters global and gene-specific DNA methylation in the developing hippocampus of mouse fetal brains. *FASEB J*,

20(1), pp. 43-9.

Patel, D. et al., 2023. Maternal diet supplementation with high-docosahexaenoic-acid canola oil, along with arachidonic acid, promotes immune system development in allergy-prone BALB/c mouse offspring at 3 weeks of age. *European journal of nutrition*, 62(6), p. 2399–2413.

Rajarethnem, H. et al., 2017. Combined Supplementation of Choline and Docosahexaenoic Acid during Pregnancy Enhances Neurodevelopment of Fetal Hippocampus. *Neurol Res. Int.*, Volume 2017, p. 8748706.

Reddy, K. & Naidu, K., 2016. Maternal and neonatal dietary intake of balanced n-6/n-3 fatty acids modulates experimental colitis in young adult rats. *European journal of nutrition*, 55(5), p. 1875–1890.

Roque-Jimenez, J. et al., 2020. Eicosapentaenoic and docosahexaenoic acid supplementation during early gestation modified relative abundance on placenta and fetal liver tissue mRNA and concentration pattern of fatty acids in fetal liver and fetal central nervous system of sheep. *PlosOne*, Volume 15, p. e035217.

Schmidt-Arras, D. & Rose-John, S., 2016. IL-6 pathway in the liver: From physiopathology to therapy. *Journal of hepatology*, 64(6), p. 1403–1415.

Serhan, C. et al., 2002. Resolvins: a family of bioactive products of omega-3 fatty acid transformation circuits initiated by aspirin treatment that counter proinflammation signals. *J Exp Med*, 196(8), p. 1025–1037.

Shears, S., 2018. Intimate connections: Inositol pyrophosphates at the interface of metabolic regulation and cell signaling. *J Cell Physiol*, 233(3), pp. 1897-1912.

Shen, J. et al., 2020. Choline and methionine regulate lipid metabolism via the AMPK signaling pathway in hepatocytes exposed to high concentrations of nonesterified fatty acids. *Journal of*

cellular biochemistry, 121(8-9), p. 3667–3678.

Shi, H. et al., 2019. DHA-PC protects kidneys against cisplatin-induced toxicity and its underlying mechanisms in mice. *Food & function*, 10(3), p. 1571–1581.

Smallwood, T., Allayee, H. & Bennett, B., 2016. Choline metabolites: gene by diet interactions. *Curr Opin Lipidol*, 27(1), pp. 33-9.

Song, E., Lim, J. & Kim, H., 2017. Docosahexaenoic acid inhibits IL-6 expression via PPAR γ -mediated expression of catalase in cerulein-stimulated pancreatic acinar cells. *The international journal of biochemistry & cell biology*, Volume 88, p. 60–68.

Song, Y. et al., 2022. Dietary Choline Alleviates High-Fat Diet-Induced Hepatic Lipid Dysregulation via UPRmt Modulated by SIRT3-Mediated mtHSP70 Deacetylation. *International journal of molecular sciences*, 23(8), p. 4204.

Spoelstra, S., Eijsink, J., Hoenders, H. & Knegtering, H., 2023. Maternal choline supplementation during pregnancy to promote mental health in offspring. *Early intervention in psychiatry*, 17(7), p. 643–651.

Tahri-Joutey, M. et al., 2021. Mechanisms Mediating the Regulation of Peroxisomal Fatty Acid Beta-Oxidation by PPAR α . *Int J Mol Sci*, 22(16), p. 8969.

Talamonti, E., Jacobsson, A. & Chiurchiù, V., 2023. Impairment of Endogenous Synthesis of Omega-3 DHA Exacerbates T-Cell Inflammatory Responses. *Int J Mol Sci*, 24(4), p. 3717.

Treen, M. et al., 1992. Effect of docosahexaenoic acid on membrane fluidity and function in intact cultured Y-79 retinoblastoma cells. *Arch Biochem Biophys*, 294(2), pp. 564-70.

Tu-Sekine, B. & Kim, S., 2022. The Inositol Phosphate System-A Coordinator of Metabolic Adaptability. *Int J Mol Sci*, 23(12), p. 6747.

Venteclef, N., Jakobsson, T., Steffensen, K. & Treuter, E., 2011. Metabolic nuclear receptor

signaling and the inflammatory acute phase response. *Trends in endocrinology and metabolism: TEM*, 22(8), p. 333–343.

Vitali, C., Khetarpal, S. & Rader, D., 2017. HDL Cholesterol Metabolism and the Risk of CHD: New Insights from Human Genetics. *Curr Cardiol Rep*, Volume 19, p. 132.

Wahab, R., Jaddoe, V., Mezzoiuso, A. & Gaillard, R., 2022. Maternal polyunsaturated fatty acid concentrations during pregnancy and childhood liver fat accumulation. *Clinical nutrition (Edinburgh, Scotland)*, 41(4), p. 847–854.

Waterland, R. & Rached, M., 2006. Developmental establishment of epigenotype: a role for dietary fatty acids?. *Scand J Food Nutr*, Volume 50, p. 21–6.

Xu, M. et al., 2019. Choline ameliorates cardiac hypertrophy by regulating metabolic remodelling and UPRmt through SIRT3-AMPK pathway. *Cardiovascular research*, 115(3), p. 530–545.

Yamaguchi, K. et al., 2010. Blockade of interleukin-6 signaling enhances hepatic steatosis but improves liver injury in methionine choline-deficient diet-fed mice. *Laboratory investigation; a journal of technical methods and pathology*, 90(8), p. 1169–1178.

Yamaguchi, K. et al., 2011. Blockade of IL-6 signaling exacerbates liver injury and suppresses antiapoptotic gene expression in methionine choline-deficient diet-fed db/db mice. *Laboratory investigation; a journal of technical methods and pathology*, 91(4), p. 609–618.

Yan, et al., 2014. Maternal choline supplementation programs greater activity of the phosphatidylethanolamine N-methyltransferase (PEMT) pathway in adult Ts65Dn trisomic mice. *FASEB J*, 28(10), pp. 4312-23.

Yu, J., Han, S., Wolfson, B. & Zhou, Q., 2018. The role of endothelial lipase in lipid metabolism, inflammation, and cancer. *Histol Histopathol.*, 33(1), pp. 1-10.

Zeisel, S., 2017. Choline, Other Methyl-Donors and Epigenetics. *Nutrients*, 9(5), p. 445.

Zicker, S., Jewell, D., Yamka, R. & Milgram, N., 2012. Evaluation of cognitive learning, memory, psychomotor, immunologic, and retinal functions in healthy puppies fed foods fortified with docosahexaenoic acid-rich fish oil from 8 to 52 weeks of age. *J. Am. Vet. Med. Assoc.* , Volume 241, p. 583–594.

CHAPTER III TABLES

Table III-3.1-1 Composition of the gestation diet and supplement[@].

Item	
Ingredients	%
Corn, yellow dent	89.34
Soy protein isolate ¹	7.26
Dicalcium phosphate 18.5%	1.84
Limestone	0.95
Salt	0.50
Basal vitamin premix ²	0.06
Trace mineral premix ³	0.05
Total	100.00
Supplement [@]	
Ingredients ⁴	mg/kg feed
folic acid	1.3
pyridoxine	1.0
B-12	0.015
riboflavin	3.75
Choline (donated by DSM, Heerlen, Netherlands)	1250
DHA (life's DHA S35-O200, rosemary free algal vegetable oil, minimum 35% DHA; DSM, Columbia, MD)	2420

¹From Archer Daniels Midland, Chicago, IL.

²Basal vitamin premix provided vitamin A, 17.64 g/kg premix; vitamin D, 7.06 g/kg premix; vitamin E, 388.01 g/kg premix; menadione, 6.68 g/kg premix; biotin, 8.82 g/kg premix; niacin, 44.09 g/kg premix; pantothenic acid, 58.79 g/kg premix; thiamin, 4.79 g/kg premix.

³Trace mineral premix included manganese sulfate 6.00%, zinc sulfate 6.00%, ferrous sulfate 4.00%, copper sulfate 0.5%, calcium iodate 0.125%, cobalt sulfate .05%, and calcium carbonate as carrier.

⁴Other supplemental ingredients (illustrated in Table II-3.1-1) included folic acid, pyridoxine, B-12, and riboflavin were added to all treatment groups every morning with the same amount, whereas choline and DHA were supplemented as different treatment groups.

Table III-3.1-2 Timeline of experimental events and nutritional treatments.

	Day of pregnancy				
	-14	0	35	56	109-114 [#]
Events	Estrus Synchronization	Insemination	First Ultrasound	Second Ultrasound	C-section
	Days of feed intake (kg/d)				
Treatments	From -14 to 0	From 0 to 35	From 35-56	From 56-109	From 109-114 [#]
Choline-DHA-	2.5	1.0	0.6		
Choline+DHA-	2.5	1.0	0.6		
Choline-DHA+	2.5	1.0	0.6		
Choline+DHA+	2.5	1.0	0.6		

[#]C-sections were performed on days of 109-114.

Table III-3.7 The sequence of primers used for RT-qPCR.

RNAs	Sequence, 5'-3'	
	Forward primer	Reverse primer
<i>LIPG</i>	CTGAGGACCCAGAGCATGAA	GACACGAGTTTGTACAGCCA
<i>LURAP1L</i>	CGACCTTCTCTACCGCTGAC	CCG TTCACATCCCATCGCTA
<i>GADD45G</i>	GGGCTGATCTCTCTTCGCTC	CCGTGCTTTCTGGAACCGTA
<i>SPOUT1</i>	ACAGGTCACCCGGAACAGACA	GCTGCTCTTTGTGCCGAATATC
<i>PIK3R1</i>	TTTACCTGAGGAGAGCTGCTG	GGTCCTCCTCCAACCTTCTTC
<i>TIMP3</i>	GGGTCAACTCCACTCACACA	AAGCTCAAAAACCGCCCTCT
<i>TM4SF1</i>	CACAAACAGGCACGCTTTCA	GCTACGATACAGAGGACGGC
<i>CASR</i>	TCACTGTTGTGCTCCCCATCC	TCAGGGCATTATCACAGGCA
<i>DDX21</i>	GCAGCAGTTATCGGGGATGT	TGTAACGACTGGGCATCCTG
<i>FLOT1</i>	TGGTGGTCTCTGGTTTCTGC	TCTGGCCCTGGATTTTCACC
<i>DUSP16-F</i>	CCTCGCCTGTCTCCTCCTTTC	TCAGGAAACTTCAAGCGCGG
<i>CDKN1A</i>	ACACCAATCAACGCCTGGAA	TAGCCCTCTTAGTGTGCCCT
<i>PIGA</i>	GCCATGGGACTAGCCGGTAT	AGACTTCCAGGGCTGACAGA
<i>SLC35G1</i>	GATCCTTATTGTGAGGCCACC	GATCCTTATTGTGAGGCCACC
<i>TMEM42</i>	TGTGTTGTACGGAGAGTGCC	AGTCGCCACCACTGTCTTTC
<i>SLC6A1</i>	CCTGGTGGTCAAGGTGCAGA	AGGAAGGCTCCACCACCGTT
<i>FAM98A</i>	TGTGCTTGGTTGGTGTCTGA	GCTTGGTCACATCCCAGAT
<i>PPIC-F</i>	GGTTGCTGACTGGTGATCCA	TCCTGTGATCTGGGGTGGAA
<i>DAXX</i>	GAAGGAAGGCGGAGGGAAC	ACGATGATGCTGTTAGCGGT
<i>PLAT</i>	GTATCACCTACAGGGGCACG	CCAGGGCTTCGAGTCTTTGT

Table III-3.7 (continued).

<i>GAPDH</i>	GTCTGGAGAAACCTGCCAAA	CCCTGTTGCTGTAGCCAAAT
<i>U6</i>	GCTTCGGCAGCACATATACT	CGCTTCACGAATTTGCGTGTCA T
mir-503	TAGCAGCGGGAACAGTACTGCAG	miScript Universal Primer
miR-221	AGCTACATTGTCTGCTGGGTTT	miScript Universal Primer
miR-31	AGGCAAGATGCTGGCATAGCTG	miScript Universal Primer
let-7f	TGAGGTAGTAGATTGTATAGTT	miScript Universal Primer
miR-182	TTTGGCAATGGTAGAACTCACACT	miScript Universal Primer
miR-218	TTGTGCTTGATCTAACCATGT	miScript Universal Primer
miR-26b	TTCAAGTAATTCAGGATAGGTT	miScript Universal Primer
miR-29a	ACTGATTTCTTTTGGTGTTCAG	miScript Universal Primer
miR-1260a	ATCCACCTCTGCCACCA	miScript Universal Primer
miR-144	GGATATCATCATATACTGTAAG	miScript Universal Primer

LIPG: endothelial lipase; *LURAP1L*: leucine rich adaptor protein 1-like; *GADD45G*: growth arrest and DNA damage inducible gamma; *SPOUT1*: SPOUT domain containing methyltransferase 1; *PIK3R1*: phosphoinositide-3-kinase regulatory subunit 1; *TIMP3*: tissue inhibitor of metalloproteinases 3; *TM4SF1*: transmembrane 4 L six family member 1; *CASR*: calcium-sensing receptor; *DDX21*: DEAD-box helicase 21; *FLOT1*: flotillin-1; *CDKN1A*: cyclin-dependent Kinase Inhibitor 1A; *PIGA*: phosphatidylinositol glycan anchor biosynthesis class A; *DUSP16*: Dual-Specificity Phosphatase 16; *SLC35G1*: solute carrier family 35 member G1; *TMEM42*: transmembrane protein 42; *SLC6A1*: solute carrier family 6 member 1; *FAM98A*: family with sequence similarity 98 member A; *PPIC*: peptidylprolyl isomerase C; *DAXX*: death domain-associated protein; *PLAT*: tissue-type plasminogen activator; *GAPDH*: glyceraldehyde 3-phosphate dehydrogenase; *U6*: U6 snRNA

Table III-4.1-1 Statistical result of mRNAs in 2 x 2 Factory Design.

Gene	Treatment				SEM	<i>p</i> -value		
	Cholin e- DHA-	Cholin e+DH A-	Choline- DHA+	Cholin e+DH A+		Choli ne	DHA	Cholin e x DHA
mRNAs displaying a choline effect, without choline x DHA interaction (144 mRNAs)								
ENSSSCG00000034976	8.10	1.84	4.40	2.06	0.92	0.001	0.080	0.050
TRAPPC1	4.80	10.91	6.33	12.58	1.08	0.001	0.169	0.949
MAPKAPK2	33.73	20.60	25.90	17.36	2.80	0.001	0.064	0.429
SPC24	9.87	22.96	14.90	21.07	2.47	0.001	0.545	0.187
ENSSSCG00000000908	9.52	3.50	6.73	5.00	1.03	0.001	0.551	0.055
CKMT2	3.21	0.67	3.99	1.92	0.68	0.001	0.123	0.719
ISOC1	22.78	12.08	18.68	12.76	2.23	0.001	0.466	0.309
PGGHG	18.57	43.10	31.00	38.10	4.77	0.002	0.423	0.067
ENSSSCG00000032605	3.51	0.68	3.69	2.08	0.62	0.002	0.229	0.349
ZNF691	3.55	8.94	5.92	7.55	0.99	0.002	0.637	0.078
S1PR1	56.86	31.84	48.04	37.01	5.05	0.002	0.733	0.197
MFHAS1	64.00	37.70	54.29	35.21	7.23	0.002	0.370	0.594
FYB2	2.45	0.34	1.14	0.31	0.42	0.002	0.137	0.152
PAK4	16.36	26.90	22.91	27.53	2.34	0.003	0.127	0.205
ENSSSCG00000012508	2.70	11.19	7.09	9.25	1.57	0.003	0.460	0.063
APOA5	57.42	8.26	25.53	14.03	9.58	0.004	0.184	0.060
CRISPLD2	25.47	13.99	19.30	11.25	3.07	0.005	0.170	0.590
ZNF394	22.88	43.32	37.53	42.26	4.12	0.006	0.113	0.070
TCEA2	7.56	16.57	9.85	13.15	2.04	0.006	0.782	0.172
RNF4	65.27	37.56	45.19	36.24	5.97	0.006	0.090	0.134
SPTLC1	17.12	6.83	10.84	7.64	2.34	0.007	0.242	0.133
SLC23A3	0.45	2.64	1.44	2.14	0.48	0.008	0.631	0.149
ENSSSCG00000008935	5.82	0.52	1.96	0.68	1.18	0.009	0.120	0.094
CYP4A24	111.16	332.29	277.58	316.15	44.64	0.009	0.112	0.056
FAM126B	17.19	6.25	9.38	6.60	2.30	0.009	0.137	0.105
SPOUT1	9.51	17.63	12.57	15.47	1.98	0.009	0.820	0.193
IGFBP3	34.53	59.98	51.47	64.97	7.13	0.011	0.132	0.404
MARCH2	7.97	16.01	11.67	17.30	2.43	0.011	0.323	0.632
SELENOS	39.88	18.01	27.81	22.04	4.86	0.011	0.431	0.121
MAOA	40.80	20.37	31.40	24.84	5.23	0.012	0.626	0.177
ENSSSCG00000040980	161.66	52.87	71.24	51.07	23.13	0.012	0.065	0.076
ENSSSCG00000010077	0.10	1.42	0.63	1.12	0.34	0.013	0.746	0.237
ELK4	17.36	4.17	8.28	6.30	2.79	0.014	0.238	0.062
ELOVL2	106.20	45.50	78.28	56.94	16.19	0.014	0.601	0.217

Table III-4.1-1 (continued).

GLS2	168.95	91.20	112.48	75.35	21.23	0.015	0.111	0.362
LPIN2	298.44	72.40	88.41	82.45	54.32	0.017	0.090	0.064
ZFP28	20.31	11.18	13.73	9.81	2.61	0.017	0.133	0.319
ENSSSCG00000040088	149.19	46.98	86.04	43.34	27.07	0.017	0.251	0.305
MTPAP	22.25	9.52	11.86	9.56	2.81	0.018	0.092	0.089
LRRC59	159.33	93.86	110.31	91.77	17.85	0.018	0.134	0.168
CD86	9.14	2.69	4.16	2.81	1.51	0.018	0.126	0.110
GABARAPL1	315.43	134.43	153.94	135.88	38.05	0.020	0.057	0.053
USP53	12.97	5.75	7.41	6.27	1.69	0.021	0.150	0.085
AIFM2	5.00	13.68	8.42	11.83	2.49	0.021	0.751	0.292
MPDZ	48.53	19.29	35.07	29.19	6.77	0.021	0.806	0.115
ENSSSCG00000039341	41.10	2.70	8.02	3.54	8.74	0.022	0.077	0.064
FAM228B	16.63	7.48	9.94	6.98	2.44	0.024	0.167	0.233
ENSSSCG00000039538	40.55	18.75	22.28	18.73	5.08	0.025	0.097	0.097
FEM1B	36.35	17.50	21.22	19.68	4.11	0.025	0.142	0.053
FAM160A2	32.13	15.48	20.16	18.45	3.78	0.025	0.254	0.064
MARCH1	4.24	2.17	5.02	2.94	0.83	0.026	0.385	0.991
CRABP1	8.36	24.77	22.43	26.98	4.38	0.026	0.078	0.193
ETS2	78.54	46.49	52.37	42.24	8.73	0.026	0.101	0.231
ENSSSCG00000014361	23.27	11.57	13.69	11.21	2.93	0.027	0.111	0.138
FMNL2	10.01	4.18	7.26	6.45	1.42	0.027	0.867	0.087
YTHDF2	41.91	23.56	27.25	23.38	4.65	0.028	0.131	0.140
NUPR1	78.39	34.03	46.44	37.87	10.95	0.028	0.227	0.127
MEIOB	4.23	10.82	8.29	8.94	1.61	0.030	0.494	0.071
LURAP1L	12.47	4.10	5.92	5.39	1.85	0.031	0.188	0.054
DESI2	29.05	21.38	22.88	14.17	3.50	0.031	0.073	0.885
G2E3	7.46	1.84	4.80	3.55	1.44	0.032	0.756	0.160
ITPR3	16.90	4.86	5.60	4.42	2.89	0.033	0.056	0.076
ACSM3	24.54	6.76	12.82	7.01	5.58	0.033	0.284	0.264
PLIN4	6.89	1.93	3.80	2.36	1.47	0.034	0.358	0.229
ENSSSCG00000036836	4.94	0.41	0.85	0.33	1.10	0.034	0.075	0.086
PCK1	1410.5	105.95	185.61	62.14	304.2	0.036	0.060	0.078
	9				2			
NNMT	65.31	10.10	12.93	9.35	14.23	0.036	0.056	0.063
ERRFI1	153.25	39.36	50.84	44.89	25.85	0.037	0.086	0.058
AGO2	23.36	9.11	12.99	8.60	4.04	0.038	0.211	0.256
GALNS	22.87	46.79	30.80	33.52	5.80	0.038	0.664	0.093
GYS2	181.74	62.98	68.82	63.83	27.72	0.038	0.058	0.055
ETNPPL	52.38	1.83	4.66	2.52	11.54	0.040	0.064	0.057
LTBP2	21.73	35.91	31.44	52.55	7.84	0.040	0.118	0.673

Table III-4.1-1 (continued).

IHH	8.05	20.04	19.51	21.98	3.18	0.040	0.056	0.167
SGK1	286.33	71.14	76.69	67.44	49.44	0.041	0.051	0.059
ELMSAN1	32.23	8.99	13.35	10.50	5.79	0.042	0.165	0.106
FABP1	205.04	431.94	304.98	314.23	55.35	0.042	0.873	0.059
TMSB10	158.29	284.89	273.61	281.88	31.99	0.042	0.086	0.072
ID2	80.06	39.49	56.84	45.81	12.49	0.043	0.490	0.233
NOCT	56.49	4.11	5.13	3.51	12.57	0.043	0.050	0.056
STAT3	189.85	92.48	112.88	103.75	25.45	0.043	0.200	0.089
HSPA5	791.87	439.09	472.06	443.15	84.73	0.043	0.091	0.083
C1orf131	11.88	4.95	5.70	5.05	1.72	0.044	0.102	0.092
TTPAL	17.00	3.43	5.17	4.17	3.30	0.045	0.120	0.080
ENSSSCG00000008115	16.15	2.87	8.98	2.61	4.68	0.045	0.431	0.464
ENSSSCG00000035347	143.46	8.56	14.69	12.55	31.43	0.045	0.066	0.052
ENSSSCG00000010703	7.79	13.32	12.64	19.87	3.04	0.047	0.074	0.782
MARVELD3	4.44	1.73	7.51	3.77	1.49	0.047	0.110	0.743
ILK	66.82	115.81	99.92	102.15	12.71	0.048	0.437	0.069
LIPG	26.94	0.89	1.53	0.71	6.57	0.049	0.063	0.066
ENSSSCG00000032591	5.74	1.81	1.93	1.05	1.12	0.049	0.060	0.200
ENSSSCG00000010546	403.44	145.33	219.35	174.18	70.47	0.049	0.300	0.159
TCP11L1	36.66	24.07	24.56	20.43	4.09	0.049	0.063	0.306
NR1D2	23.81	9.16	10.15	9.64	3.53	0.050	0.086	0.066
HAMP	212.94	16.93	17.54	13.75	48.52	0.049	0.050	0.058
PPP3CC	278.46	110.77	156.75	130.44	44.75	0.039	0.264	0.125
PDE4B	21.17	6.64	12.11	10.71	3.60	0.035	0.493	0.079
NOLC1	105.45	50.59	59.36	48.99	14.47	0.032	0.111	0.135
JAK1	200.68	103.62	126.83	113.28	25.64	0.040	0.221	0.115
GADD45G	26.87	6.96	10.29	9.03	5.06	0.046	0.162	0.076
MCL1	152.74	72.22	79.84	76.87	20.23	0.049	0.103	0.066
IL1RAP	37.51	11.15	13.72	11.85	6.27	0.033	0.076	0.061
NAPEPLD	1.14	8.68	2.18	2.88	1.94	0.043	0.230	0.088
ELOVL6	168.43	106.35	125.44	103.18	10.61	0.001	0.047	0.084
MTMR9	14.58	6.53	7.60	5.45	1.44	0.002	0.013	0.063
ATP2B1	46.55	32.02	34.17	26.92	3.50	0.004	0.016	0.294
GPR156	48.37	85.56	93.48	108.65	8.12	0.005	0.001	0.207
UBE2J1	35.03	23.12	24.64	20.83	2.49	0.006	0.022	0.132
EHD3	47.87	66.60	69.51	80.92	5.33	0.007	0.002	0.484
MTFR1	30.78	19.11	17.95	13.88	2.64	0.007	0.003	0.171
DYSF	9.74	18.40	20.25	24.62	2.34	0.008	0.001	0.352
HELB	5.55	2.66	2.98	1.84	0.76	0.009	0.026	0.234
NDUFAF4	7.05	2.60	2.98	1.96	0.97	0.010	0.025	0.094

Table III-4.1-1 (continued).

SMPDL3B	12.68	5.55	6.20	4.14	1.60	0.010	0.026	0.140
DPF3	5.14	8.03	7.72	12.71	1.43	0.011	0.018	0.469
UGT2B31	59.86	18.36	24.45	15.24	8.72	0.011	0.047	0.092
HNF4A	495.99	279.42	284.38	236.35	46.57	0.012	0.015	0.095
AAAS	11.34	17.37	17.53	20.96	1.74	0.013	0.011	0.470
RANBP2	134.56	76.24	82.80	75.06	12.10	0.014	0.044	0.053
BCR	28.27	41.10	43.00	47.72	3.27	0.016	0.004	0.244
ENSSSCG00000004573	9.99	3.06	2.28	1.41	1.49	0.018	0.006	0.061
MISP	4.60	0.28	0.64	0.06	0.95	0.020	0.044	0.068
WDR81	54.76	89.90	88.76	98.81	8.95	0.021	0.028	0.185
GCH1	17.28	6.19	7.11	5.09	2.68	0.023	0.047	0.105
WDR37	51.38	21.55	23.53	19.33	7.22	0.024	0.044	0.083
CSF2RB	23.42	13.54	10.94	9.35	2.54	0.026	0.002	0.100
DDX5	202.08	101.94	103.24	93.64	22.39	0.028	0.031	0.065
PSEN2	107.00	51.02	49.13	37.87	16.07	0.028	0.021	0.133
TIGAR	23.52	12.53	10.81	6.78	3.10	0.029	0.009	0.295
GNA13	32.91	20.09	18.93	17.92	2.86	0.030	0.012	0.060
KYAT1	25.02	50.01	50.08	55.19	6.44	0.030	0.030	0.142
NAMPT	60.79	17.28	15.69	13.14	9.59	0.032	0.022	0.054
HAL	178.47	45.45	51.66	42.75	30.67	0.032	0.048	0.057
CKAP4	60.33	29.74	27.92	24.04	7.79	0.035	0.021	0.096
ST6GALNAC2	33.78	50.09	56.96	60.69	4.79	0.035	0.001	0.174
IL1R2	4.58	0.59	0.54	0.26	1.00	0.038	0.034	0.068
WSCD1	16.69	25.96	26.24	32.45	3.40	0.038	0.032	0.669
ENSSSCG00000000854	198.73	308.58	333.40	359.93	31.01	0.038	0.006	0.194
BRI3BP	35.50	28.67	23.35	17.55	2.77	0.039	0.001	0.859
PPA1	39.14	18.83	19.32	18.24	4.84	0.041	0.050	0.064
SLC5A3	3.35	1.35	1.21	0.82	0.54	0.041	0.024	0.156
PLK2	56.50	27.84	27.27	24.74	6.91	0.043	0.036	0.086
PBDC1	22.75	16.17	12.90	11.35	1.98	0.045	0.001	0.203
ENSSSCG00000000021	4.10	4.36	5.91	9.47	0.98	0.050	0.001	0.087
mRNAs displaying a DHA effect, without choline x DHA interaction (151 mRNAs)								
PPIL4	7.23	4.84	2.88	2.55	0.73	0.079	0.001	0.180
HDDC3	11.43	14.82	21.15	18.26	1.64	0.884	0.001	0.075
PACS1	24.32	34.84	44.01	45.52	3.87	0.144	0.001	0.270
REL	9.14	5.07	3.46	3.48	0.97	0.055	0.001	0.053
FLT4	27.02	37.07	51.13	45.20	4.63	0.660	0.002	0.098
TIMELESS	7.94	12.39	18.63	16.96	2.34	0.535	0.002	0.178
CREB3L3	128.17	160.43	223.56	190.80	19.36	0.990	0.003	0.096
ENSSSCG00000003248	0.50	0.48	1.21	2.96	0.52	0.086	0.003	0.082

Table III-4.1-1 (continued).

B4GALT1	60.77	48.21	38.73	36.98	5.12	0.169	0.003	0.295
SMG6	21.77	34.61	44.88	40.49	4.30	0.351	0.003	0.064
FAM173B	4.27	8.80	10.37	11.01	1.28	0.057	0.004	0.145
SRSF7	41.96	32.07	24.98	23.52	4.11	0.168	0.004	0.302
ENSSSCG00000031580	13.58	9.67	5.35	7.30	1.64	0.570	0.005	0.097
FLOT1	22.44	32.56	37.80	37.51	3.14	0.145	0.005	0.124
CCL14	7.61	10.15	11.81	15.02	1.46	0.069	0.006	0.828
ANXA5	30.66	21.35	14.59	15.73	3.62	0.280	0.007	0.171
PBX2	49.70	68.64	83.41	85.90	8.28	0.230	0.007	0.354
UFM1	19.21	12.91	9.89	8.87	2.25	0.128	0.008	0.268
FAM81A	13.00	20.58	23.19	25.98	2.97	0.073	0.009	0.395
ENSSSCG00000009213	3.66	1.35	0.67	0.17	0.71	0.071	0.010	0.235
GLYCTK	63.76	100.68	112.33	127.01	13.50	0.067	0.010	0.416
GAR1	4.11	3.28	1.29	2.00	0.72	0.937	0.011	0.315
PDE10A	4.56	2.10	1.20	1.47	0.78	0.146	0.011	0.074
PLEK2	30.28	20.81	15.91	15.76	3.39	0.187	0.011	0.201
IFRD1	23.65	11.10	6.72	8.68	3.38	0.148	0.012	0.051
SPON2	17.14	11.34	8.10	10.06	1.90	0.320	0.012	0.051
PSMD7	52.96	34.75	30.24	29.27	4.98	0.078	0.012	0.111
ENSSSCG00000012832	5.15	9.28	16.59	10.77	2.31	0.729	0.013	0.050
SAMSN1	3.19	1.86	1.50	0.55	0.54	0.052	0.013	0.739
ENDOV	1.96	3.59	4.92	5.26	0.83	0.267	0.013	0.463
ENSSSCG00000039926	1.05	3.78	8.98	5.36	1.77	0.812	0.016	0.097
SLC16A1	100.69	66.49	57.51	61.58	9.16	0.119	0.016	0.051
PPARD	26.97	19.13	17.02	14.22	2.83	0.078	0.017	0.392
DBR1	8.67	5.30	3.33	4.12	1.23	0.321	0.017	0.114
HRASLS5	0.78	0.83	1.77	4.24	0.86	0.157	0.018	0.175
KPNA4	29.34	17.31	12.08	14.54	3.80	0.239	0.018	0.080
KLHL22	7.42	11.01	18.10	13.28	2.56	0.812	0.019	0.115
RND3	14.49	6.91	5.77	5.78	1.88	0.065	0.019	0.065
SLC7A4	0.79	2.03	3.15	3.93	0.84	0.247	0.019	0.787
GADD45B	11.17	5.63	3.25	3.51	1.96	0.203	0.020	0.163
PXDC1	21.77	8.84	6.54	5.64	3.51	0.073	0.020	0.117
ATF4	224.58	157.49	135.70	127.68	23.20	0.128	0.020	0.227
IMPAD1	53.42	34.50	30.64	29.95	5.35	0.089	0.021	0.113
ENSSSCG00000024983	37.36	22.65	20.09	20.09	3.85	0.081	0.022	0.081
RPS6KA3	64.05	40.77	29.98	28.66	9.05	0.205	0.022	0.256
SESN2	54.80	26.95	22.29	21.48	7.81	0.077	0.022	0.094
DNTTIP2	59.42	37.11	31.14	32.88	6.32	0.136	0.022	0.084
ENSSSCG00000017920	23.71	36.45	46.44	38.85	5.44	0.622	0.023	0.060
DYNC1LI2	28.08	18.55	14.35	17.27	3.11	0.297	0.023	0.056
C6orf222	4.56	1.34	0.54	0.81	0.91	0.130	0.023	0.077

Table III-4.1-1 (continued).

STARD7	27.00	15.72	9.06	14.23	4.04	0.456	0.024	0.052
ZFAND2A	18.83	7.17	4.90	5.19	3.14	0.097	0.024	0.082
TMEM186	6.25	12.45	13.37	14.27	1.79	0.068	0.024	0.167
ENSSSCG00000008284	5.70	2.07	1.71	1.10	1.06	0.054	0.026	0.163
HAVCR2	10.92	3.11	2.11	1.83	2.02	0.070	0.026	0.090
ENSSSCG000000032242	21.01	10.59	9.70	8.48	2.83	0.051	0.026	0.118
ACD	2.72	5.66	6.35	6.37	0.91	0.121	0.027	0.127
ARG2	22.13	13.45	7.70	4.21	4.90	0.240	0.028	0.613
ITGA3	19.00	6.35	5.18	3.96	3.62	0.057	0.028	0.113
ENSSSCG000000011290	31.91	11.20	8.29	9.59	5.12	0.085	0.028	0.053
NOD1	6.40	4.06	1.91	3.69	1.01	0.791	0.029	0.061
FOSL2	25.77	14.46	10.93	10.84	4.02	0.166	0.030	0.173
IMPA2	7.33	12.62	15.12	14.19	2.08	0.295	0.030	0.139
CASR	1.04	7.12	13.98	7.89	3.00	0.998	0.030	0.053
ENSSSCG000000003679	31.81	19.13	17.88	14.78	3.88	0.059	0.030	0.240
NTPCR	7.39	12.48	15.27	13.91	1.97	0.367	0.031	0.125
CAPN8	1.34	5.82	8.72	7.36	1.89	0.431	0.031	0.148
SLC6A6	35.41	19.16	15.04	12.78	6.02	0.127	0.031	0.244
USP31	9.19	6.15	4.39	3.47	1.59	0.239	0.032	0.526
MEA1	16.38	27.46	33.45	31.72	4.85	0.329	0.032	0.185
RHOD	9.81	4.42	1.97	3.42	1.96	0.322	0.032	0.092
BMP6	50.04	31.13	21.51	25.72	7.59	0.339	0.033	0.138
APCDD1	11.74	16.19	22.73	19.89	3.11	0.807	0.033	0.275
ENSSSCG000000038506	71.16	45.03	37.31	38.06	8.80	0.174	0.034	0.151
CTPS1	19.99	12.72	7.79	7.24	3.97	0.329	0.034	0.401
CYB5B	43.96	29.88	28.80	23.96	4.53	0.055	0.034	0.335
PNPLA3	28.27	18.45	9.57	6.21	6.52	0.348	0.034	0.643
ENSSSCG000000020872	130.12	215.44	233.98	261.63	32.50	0.106	0.035	0.400
THBS1	66.81	39.19	26.43	32.50	10.19	0.318	0.035	0.124
DDX21	88.59	45.83	42.08	43.47	10.51	0.073	0.036	0.057
EDA	9.35	1.47	1.01	0.97	2.02	0.058	0.036	0.061
PPP1R10	35.38	18.15	16.01	16.60	4.58	0.091	0.037	0.071
PARD6B	11.63	4.66	4.10	3.34	1.95	0.066	0.037	0.136
HDAC4	10.94	5.90	3.85	5.57	1.61	0.334	0.038	0.057
ENSSSCG000000029261	47.91	30.41	23.93	28.33	5.98	0.281	0.038	0.078
COQ10B	13.17	4.30	2.88	3.34	2.48	0.115	0.038	0.082
KLHDC8B	35.60	64.04	65.04	66.39	6.93	0.051	0.039	0.075
PTPN1	66.00	24.94	20.44	19.23	11.81	0.084	0.039	0.103
MKNK2	40.29	22.61	21.30	20.52	4.85	0.068	0.039	0.093
TNFRSF21	41.84	20.50	18.43	17.56	6.11	0.080	0.040	0.105
SLC16A6	63.40	6.91	3.56	5.12	13.45	0.065	0.040	0.052
NANOS1	2.95	0.88	0.38	0.48	0.68	0.160	0.040	0.125

Table III-4.1-1 (continued).

RPUSD2	8.32	5.73	2.63	5.10	1.41	0.968	0.040	0.096
KLHL15	12.80	6.04	5.84	5.19	1.73	0.052	0.041	0.104
RNF152	3.81	0.37	0.09	0.03	0.89	0.076	0.042	0.086
RHOU	58.44	26.74	24.16	24.15	8.64	0.077	0.042	0.077
PITPNC1	8.67	5.36	3.78	2.83	1.71	0.230	0.042	0.500
PPRC1	52.25	25.82	19.28	23.38	8.02	0.189	0.042	0.077
IL4R	127.95	70.86	49.75	57.20	21.66	0.262	0.043	0.147
BICDL2	3.36	0.91	0.36	0.54	0.83	0.166	0.044	0.110
ENSSSCG00000040056	54.07	32.57	25.17	28.75	7.47	0.256	0.044	0.116
TM4SF1	105.50	36.30	31.15	29.13	19.38	0.077	0.045	0.094
IL1R1	331.33	124.16	117.59	116.64	49.93	0.059	0.046	0.061
TIMP3	209.23	48.60	38.32	45.33	41.66	0.076	0.046	0.054
DDR2	3.82	3.35	2.02	1.01	0.98	0.461	0.047	0.786
DUSP1	151.28	40.09	28.82	31.27	31.61	0.096	0.047	0.083
EEPDI	13.26	3.88	3.16	3.06	2.52	0.083	0.048	0.089
PPP2R3A	30.21	12.81	12.57	12.69	4.31	0.054	0.049	0.051
KLHL38	0.75	1.91	3.82	2.25	0.82	0.806	0.049	0.111
PIK3R1	51.25	30.03	26.90	27.40	6.58	0.126	0.050	0.110
mRNAs displaying a choline x DHA synergistic effect (17 mRNAs)								
ELMOD1	0.10	0.35	0.24	3.12	0.40	0.001	0.001	0.0028
CEBPG	32.89	17.01	17.14	15.91	2.82	0.008	0.009	0.021
ENSSSCG00000012202	19.56	5.91	6.77	5.71	2.43	0.008	0.018	0.022
CDV3	62.34	29.40	26.10	25.06	6.28	0.016	0.005	0.023
CRP	30.70	13.28	14.29	13.19	3.29	0.012	0.024	0.026
SLA-5	1.21	1.83	1.67	8.28	1.30	0.011	0.014	0.031
CCNJ	16.49	4.82	5.07	2.78	2.05	0.003	0.004	0.034
EHMT2	19.03	35.25	38.56	39.37	3.51	0.022	0.002	0.036
CP	203.23	1.77	13.69	0.59	41.03	0.019	0.035	0.038
OSMR	39.35	13.76	15.75	13.06	4.97	0.012	0.028	0.038
TSKU	14.25	6.24	4.15	3.98	1.85	0.031	0.002	0.038
NPC1L1	13.04	2.06	2.90	1.95	2.18	0.016	0.035	0.039
SLC7A2	246.46	126.88	122.01	118.28	25.52	0.030	0.020	0.041
SGSH	17.11	32.03	31.94	32.15	3.32	0.037	0.039	0.042
APCS	440.97	104.83	117.50	94.33	75.31	0.023	0.033	0.045
CHKA	111.13	63.14	68.34	61.50	9.66	0.010	0.033	0.046
ZYG11B	60.28	17.45	17.75	16.99	9.56	0.041	0.044	0.048
mRNAs displaying a choline x DHA antagonistic effect, with choline having greater impact (204 mRNAs)								
FAM199X	11.69	3.63	4.06	6.02	1.00	0.005	0.015	0.0001
ABHD13	16.78	7.26	8.31	10.92	1.29	0.014	0.077	0.0001
PRKAA2	12.41	4.78	5.37	7.70	1.17	0.025	0.076	0.0001
LYVE1	50.71	22.70	23.82	33.69	3.75	0.028	0.052	0.0001

Table III-4.1-1 (continued).

ENSSSCG00000037609	42.92	25.39	25.60	34.63	2.26	0.077	0.091	0.0001
ENSSSCG00000003885	54.51	28.72	32.95	36.07	3.08	0.002	0.039	0.0002
ENSSSCG00000025060	24.09	13.43	14.97	14.64	1.31	0.000	0.004	0.0003
SLC41A2	17.41	6.97	7.33	12.32	1.79	0.154	0.214	0.0003
ENSSSCG00000010954	30.18	15.45	16.63	24.14	2.56	0.189	0.372	0.0003
ENSSSCG00000027421	19.27	5.69	6.45	10.50	2.31	0.051	0.098	0.0008
TOM1L1	49.35	23.42	30.68	30.75	3.34	0.001	0.115	0.0009
HIPK3	86.59	35.51	41.61	54.09	8.28	0.031	0.131	0.0009
NUSAP1	32.63	14.07	15.28	18.15	2.88	0.013	0.033	0.0012
TOB1	27.51	6.93	9.40	10.76	3.06	0.006	0.034	0.0020
CTDSPL2	28.55	12.88	13.32	17.46	2.76	0.056	0.076	0.0020
SF3B6	31.89	13.65	14.10	18.68	3.43	0.057	0.075	0.0027
DDAH1	126.64	58.40	60.96	83.13	13.38	0.105	0.147	0.0029
ANXA7	48.06	28.03	29.60	32.37	3.41	0.022	0.057	0.0035
SLC31A1	82.09	47.19	58.54	52.85	4.76	0.000	0.065	0.0041
LIFR	66.45	24.61	31.19	35.56	7.18	0.017	0.109	0.0041
PRNP	46.93	24.04	25.83	26.94	4.22	0.008	0.025	0.0042
STX11	6.38	1.67	2.17	2.86	0.84	0.027	0.090	0.0042
TMED5	58.52	31.17	31.47	32.52	4.32	0.008	0.009	0.0045
SMNDC1	18.85	8.46	10.50	10.39	1.64	0.004	0.066	0.0050
KIAA1551	41.18	16.16	17.29	22.21	4.80	0.050	0.079	0.0051
UBALD2	24.58	10.27	11.46	16.20	2.96	0.136	0.258	0.0052
BBS9	2.48	0.17	0.91	2.14	0.61	0.361	0.739	0.0054
ALCAM	74.48	32.41	34.72	37.08	6.94	0.012	0.025	0.0056
TFRC	101.87	24.98	38.67	39.00	12.26	0.006	0.065	0.0056
SOD2	116.45	68.41	72.09	83.46	9.48	0.073	0.148	0.0056
ENSSSCG00000029866	2.50	0.28	0.36	0.70	0.45	0.034	0.053	0.0057
FAM98A	23.54	10.87	13.00	16.06	2.61	0.077	0.315	0.0058
METTL16	14.19	4.41	4.71	5.54	1.71	0.019	0.027	0.0064
CD163	139.67	82.63	92.57	101.50	10.80	0.040	0.215	0.0065
NANP	8.07	2.44	4.57	3.58	0.75	0.000	0.144	0.0066
LARP4	48.09	24.95	25.21	34.19	5.19	0.204	0.221	0.0067
HSPA13	47.96	18.12	20.13	21.14	5.01	0.011	0.026	0.0068
FAF2	39.78	23.07	27.86	29.93	3.10	0.030	0.434	0.0068
ALDH6A1	96.65	59.62	73.84	78.23	6.85	0.029	0.768	0.0070
ASNSD1	21.31	5.58	7.68	8.99	2.77	0.021	0.092	0.0073
GRAMD2B	48.42	15.37	19.24	17.52	5.36	0.004	0.019	0.0076
ENSSSCG00000033340	16.95	6.46	7.19	7.90	1.88	0.019	0.042	0.0080
DDX58	12.68	4.00	7.69	7.43	1.47	0.005	0.598	0.0081
DEGS1	62.96	28.32	31.16	32.60	5.94	0.014	0.038	0.0083
NDFIP2	73.08	20.20	23.42	28.55	9.70	0.027	0.053	0.0085
WNK1	112.06	47.32	55.32	58.04	11.48	0.015	0.063	0.0086

Table III-4.1-1 (continued).

TIMM8A	36.03	15.56	22.46	20.78	3.33	0.003	0.219	0.0089
FGD4	14.15	4.40	5.32	9.46	2.37	0.265	0.452	0.0093
GOLGA4	78.12	37.24	44.92	37.66	6.02	0.001	0.012	0.010
NQO1	5.61	0.84	1.10	2.05	1.00	0.077	0.123	0.010
POLD3	9.48	3.33	5.34	6.17	1.29	0.048	0.617	0.011
NETO2	2.18	0.09	0.13	0.30	0.41	0.029	0.037	0.012
PDE4D	11.15	3.03	5.06	4.89	1.40	0.009	0.162	0.012
ARL8B	16.82	7.32	9.82	9.99	1.72	0.016	0.240	0.013
GNL3	54.32	27.68	29.65	29.39	4.81	0.011	0.028	0.013
TMEM170B	12.02	2.26	4.43	4.70	1.79	0.018	0.183	0.013
AZIN1	20.71	7.58	11.80	10.93	2.23	0.005	0.238	0.013
USF3	13.50	4.13	4.76	6.92	2.09	0.113	0.188	0.015
GCLM	49.48	14.26	20.53	17.16	6.51	0.004	0.042	0.015
DHX9	229.84	139.44	149.52	157.27	18.48	0.038	0.110	0.015
SEMA3A	5.07	0.82	2.32	1.98	0.76	0.005	0.300	0.015
TMEM229B	18.48	5.63	11.46	9.92	2.33	0.003	0.538	0.016
MFSD6	25.68	3.87	5.00	3.89	3.80	0.008	0.016	0.016
ENSSSCG00000004392	91.63	28.39	29.88	36.13	12.92	0.045	0.056	0.016
CSTF2T	33.43	19.03	22.09	21.82	2.68	0.013	0.132	0.016
DUSP16	43.65	21.03	24.09	27.60	4.95	0.072	0.213	0.017
ENSSSCG00000010549	24.52	3.67	4.45	6.81	4.29	0.052	0.073	0.017
SLC27A2	4.67	0.04	1.11	0.73	0.80	0.006	0.097	0.017
BCLAF1	104.65	45.94	59.12	56.22	10.35	0.009	0.120	0.017
LITAF	55.59	13.50	15.52	21.22	8.91	0.064	0.097	0.017
TSPAN13	31.87	13.28	17.65	17.74	3.54	0.019	0.199	0.018
THRAP3	155.81	96.39	103.97	104.16	11.60	0.019	0.073	0.018
HSPH1	29.84	14.85	14.95	15.13	3.04	0.021	0.023	0.018
SLC1A2	10.84	1.03	1.14	1.52	1.93	0.029	0.033	0.019
TMEM131	93.08	45.09	50.16	48.74	9.33	0.014	0.046	0.020
LONP2	128.85	72.62	85.12	83.84	10.93	0.016	0.156	0.021
PRPF40A	63.61	35.35	36.72	37.58	5.73	0.029	0.047	0.021
REV3L	24.17	10.34	12.50	13.65	2.89	0.047	0.181	0.021
NRBF2	19.58	8.81	13.70	14.37	2.20	0.040	0.948	0.021
PPARGC1A	43.00	15.16	18.55	19.38	5.64	0.030	0.097	0.022
SLC36A4	10.74	2.80	3.61	3.49	1.56	0.019	0.056	0.023
GPNMB	72.91	13.36	14.06	19.53	13.32	0.055	0.061	0.023
ABCA1	127.69	63.10	82.74	84.33	13.28	0.030	0.394	0.023
CPS1	2460.9	611.67	700.13	692.83	363.1	0.023	0.038	0.024
	9				9			
NEBL	10.77	3.79	3.87	4.06	1.45	0.032	0.035	0.024
CDKN1A	5.47	1.57	2.76	3.49	0.93	0.114	0.689	0.024
C2CD2	18.34	8.64	10.16	10.27	1.96	0.027	0.121	0.024

Table III-4.1-1 (continued).

SMPDL3A	16.12	3.39	4.17	4.35	2.88	0.029	0.054	0.025
PPIF	111.56	44.22	47.29	48.11	14.20	0.029	0.046	0.026
PIM3	10.20	3.04	5.25	6.26	1.64	0.086	0.621	0.026
QTRT2	15.20	5.64	6.08	8.27	2.37	0.150	0.202	0.026
HECW2	16.16	6.57	6.87	7.64	2.08	0.055	0.072	0.026
SLC35G1	31.74	11.44	12.05	14.15	4.56	0.066	0.085	0.026
TOR1AIP1	37.36	10.54	13.90	12.89	5.52	0.017	0.064	0.026
ENSSSCG00000014060	113.77	65.63	76.75	75.81	10.79	0.021	0.190	0.026
SLC25A15	133.78	54.29	63.92	52.91	14.94	0.005	0.022	0.027
URB2	37.48	18.84	19.05	21.17	4.67	0.074	0.081	0.027
ADGRG1	9.35	3.45	4.77	4.10	1.07	0.007	0.089	0.027
ACSM4	241.99	75.01	193.41	192.16	34.61	0.026	0.344	0.028
TP53INP1	180.50	40.61	44.18	51.71	31.33	0.047	0.060	0.029
NUFIP2	47.90	26.12	29.30	28.50	4.39	0.019	0.085	0.029
ENSSSCG00000023415	99.98	25.31	38.85	51.11	18.69	0.109	0.356	0.029
CBFB	20.13	7.56	7.86	8.12	2.80	0.036	0.045	0.029
TBC1D9	14.18	3.32	5.17	5.23	2.25	0.031	0.145	0.029
AASS	68.14	7.65	10.66	8.90	12.16	0.022	0.037	0.030
DNAJC2	26.89	13.34	16.50	15.01	2.61	0.008	0.108	0.030
FKBP5	141.98	35.41	39.45	36.79	22.49	0.023	0.035	0.030
ZFAND5	171.43	44.34	45.40	67.56	31.22	0.120	0.127	0.031
SSH2	23.11	7.58	11.25	14.14	3.97	0.129	0.516	0.031
TNFAIP1	125.80	75.29	82.94	85.00	11.54	0.045	0.162	0.031
SLC38A4	136.59	61.60	66.58	68.15	16.35	0.038	0.070	0.031
PON1	28.55	4.18	8.55	7.60	4.98	0.021	0.119	0.032
FICD	28.34	9.64	14.54	12.28	3.84	0.008	0.136	0.032
ABHD5	48.23	12.41	16.78	16.36	7.48	0.029	0.090	0.032
TBC1D1	88.91	42.78	44.94	46.16	10.00	0.042	0.064	0.033
ENSSSCG00000007253	34.39	19.00	19.50	20.95	3.56	0.073	0.095	0.033
CYCS	92.78	28.94	30.23	28.94	13.38	0.027	0.033	0.033
ENSSSCG00000029203	64.38	36.56	40.66	36.61	5.13	0.006	0.034	0.033
ENSSSCG00000032529	31.00	14.69	14.96	14.90	3.68	0.038	0.033	0.034
SUCO	40.12	7.71	10.20	10.04	6.79	0.032	0.066	0.034
RELB	5.34	1.43	2.40	2.12	0.83	0.015	0.173	0.034
PPAT	79.92	21.66	28.53	26.70	12.49	0.025	0.077	0.034
TRAM2	58.69	29.49	32.93	30.55	6.02	0.014	0.049	0.034
MAPK1IP1L	50.93	28.20	29.90	29.13	4.92	0.026	0.054	0.037
PIGA	39.70	15.86	17.36	19.36	5.70	0.074	0.121	0.037
SQSTM1	211.31	120.90	144.62	136.29	17.99	0.014	0.180	0.037
PIK3AP1	71.63	38.18	53.35	50.29	6.64	0.014	0.658	0.037
SLC25A16	7.71	3.35	5.14	4.60	0.88	0.009	0.456	0.037
SMIM12	8.83	4.16	5.33	4.13	0.82	0.001	0.034	0.037

Table III-4.1-1 (continued).

HGD	135.62	50.79	70.11	64.34	17.84	0.019	0.161	0.038
CYP2C49	156.90	14.19	21.20	20.45	33.20	0.039	0.061	0.041
ENSSSCG00000007642	67.43	4.79	8.36	6.14	15.22	0.030	0.052	0.042
CDC37L1	9.41	3.70	6.07	4.44	0.96	0.001	0.184	0.043
AFF4	43.21	20.64	26.39	26.05	4.96	0.038	0.285	0.043
SALL1	34.28	11.10	11.42	11.48	5.21	0.045	0.050	0.044
SARAF	90.13	50.07	55.91	53.16	8.37	0.022	0.089	0.044
CTH	158.95	23.59	34.28	26.10	28.84	0.025	0.054	0.045
ANKRD12	47.45	25.66	29.22	28.09	4.08	0.005	0.045	0.045
SKIL	23.83	11.11	16.24	15.80	3.10	0.033	0.623	0.046
PDE12	15.72	6.41	8.51	6.83	1.80	0.006	0.073	0.046
DSC3	29.10	10.41	14.28	16.32	4.70	0.105	0.377	0.047
ARG1	924.76	73.35	100.65	88.53	191.3	0.042	0.056	0.048
					1			
FMO5	55.13	19.78	29.72	37.97	9.96	0.209	0.734	0.049
SMPD3	44.15	19.43	19.78	24.45	6.79	0.172	0.187	0.050
ATXN10	48.06	82.25	72.81	64.58	4.67	0.011	0.460	0.0001
SCARB1	133.80	215.93	212.44	176.31	14.87	0.111	0.173	0.0003
MAPK3	24.54	40.13	30.33	28.08	2.14	0.005	0.165	0.0004
SLC1A4	65.91	138.61	131.98	130.00	8.90	0.001	0.005	0.0005
KIF12	7.66	20.12	13.86	12.67	1.69	0.003	0.721	0.0006
EXTL1	82.11	148.82	134.67	115.68	11.89	0.042	0.392	0.0007
PSRC1	29.89	55.24	45.65	39.07	4.04	0.035	0.961	0.0008
POLL	5.89	14.46	13.09	11.43	1.59	0.022	0.152	0.0013
ENSSSCG00000009770	26.11	49.25	43.22	39.51	4.31	0.019	0.352	0.0020
SERPINF1	808.58	1563.4	1340.36	1202.3	129.5	0.030	0.531	0.0027
		0		4	2			
ENSSSCG000000034164	1.25	5.99	4.83	1.99	1.38	0.415	0.855	0.0028
ENSSSCG000000033006	2.36	7.35	6.04	3.80	1.18	0.224	0.952	0.0031
ALS2CL	3.80	10.14	7.65	6.42	1.13	0.040	0.955	0.0036
SLC6A1	1.08	6.39	2.96	1.65	1.01	0.072	0.190	0.0045
VPS16	27.44	44.51	39.24	36.87	3.15	0.032	0.528	0.0061
ARL10	21.28	37.72	34.87	32.03	3.15	0.045	0.231	0.0061
G6PC3	7.06	19.16	13.36	11.04	3.06	0.053	0.710	0.0062
PGAP2	21.08	38.01	31.24	30.54	2.85	0.011	0.652	0.0063
SMARCB1	30.20	51.91	51.10	43.56	4.89	0.167	0.219	0.0070
PPIC	10.13	17.79	16.74	15.24	1.51	0.061	0.207	0.0072
INMT	106.40	202.13	183.72	167.33	19.04	0.052	0.284	0.0079
EFNA4	12.28	29.78	23.51	17.71	3.87	0.161	0.919	0.0081
TMEM42	6.04	12.71	12.16	10.43	1.40	0.104	0.201	0.0083
TSPAN4	20.78	37.83	34.52	30.68	3.83	0.083	0.375	0.0084
DUSP9	86.94	240.07	211.07	175.25	32.64	0.088	0.378	0.0084

Table III-4.1-1 (continued).

COQ8B	4.07	10.48	8.54	7.57	1.31	0.049	0.560	0.010
SNX17	34.94	53.49	53.46	52.89	3.44	0.016	0.016	0.011
B3GNT7	58.60	97.87	89.28	86.17	7.56	0.030	0.238	0.012
NENF	9.36	19.00	17.52	16.55	2.04	0.040	0.166	0.014
CERCAM	12.75	28.18	26.95	21.61	3.76	0.210	0.340	0.014
SYNPR	2.10	11.03	7.61	7.13	1.83	0.026	0.655	0.014
SOAT2	43.20	93.90	91.98	84.85	11.15	0.059	0.083	0.015
GINS4	6.75	14.93	12.95	9.60	2.15	0.281	0.845	0.015
MARC1	31.63	63.28	42.88	41.13	6.40	0.030	0.410	0.017
AGPAT1	13.42	26.68	20.42	20.30	2.68	0.021	0.907	0.019
METAP1D	7.74	15.73	13.81	14.89	1.38	0.003	0.072	0.020
ALKBH6	4.64	15.87	8.12	8.38	2.33	0.016	0.374	0.020
CPSF4	15.45	29.01	27.69	26.65	2.94	0.045	0.108	0.021
TM4SF5	20.81	61.25	45.83	43.11	8.90	0.045	0.704	0.024
VIPAS39	15.26	24.91	23.30	23.60	1.89	0.019	0.101	0.026
STYXL1	1.38	5.38	2.65	2.89	0.77	0.014	0.450	0.027
SLC41A3	9.69	19.69	13.34	13.46	1.99	0.024	0.546	0.027
ENSSSCG00000032748	7.65	16.49	14.51	15.91	1.52	0.004	0.061	0.028
ENSSSCG00000000734	17.90	39.31	38.12	35.01	5.17	0.098	0.147	0.030
ENSSSCG00000033041	8.53	36.61	20.52	24.41	5.11	0.006	0.984	0.030
MASP1	84.42	128.61	115.65	125.61	7.89	0.001	0.070	0.030
NKIRAS1	5.77	12.50	11.16	10.94	1.45	0.042	0.217	0.030
KATNB1	13.40	26.29	21.27	20.28	3.08	0.061	0.761	0.031
LANCL2	24.91	46.42	37.51	42.04	3.55	0.002	0.279	0.031
ENSSSCG00000039500	9.03	19.79	14.58	14.34	2.32	0.040	0.984	0.033
SLA-DMB	6.78	16.02	11.93	11.76	2.01	0.040	0.833	0.033
ENSSSCG00000024163	18.47	33.85	26.50	25.77	3.44	0.051	0.994	0.033
APIG2	10.11	19.66	17.26	16.78	2.24	0.056	0.354	0.036
RAMP2	25.92	52.58	47.48	49.82	5.47	0.016	0.107	0.040
TNFRSF19	3.49	12.42	7.40	11.26	1.17	0.000	0.255	0.042
TFB1M	11.04	21.00	13.65	13.15	2.33	0.064	0.294	0.042
HOGA1	28.88	50.62	50.58	49.22	5.49	0.074	0.075	0.045
RPS19BP1	14.70	27.50	19.27	20.61	2.62	0.015	0.673	0.045
CCDC80	8.04	18.32	16.71	16.49	2.40	0.055	0.184	0.047
KCNJ16	28.68	55.62	55.34	57.79	6.04	0.020	0.023	0.049
mRNAs displaying a choline x DHA antagonistic effect, with DHA having greater impact (162 mRNAs)								
PLAC9	7.66	4.71	2.63	6.44	0.80	0.584	0.043	0.0002
MTDH	97.08	54.71	50.73	57.68	6.22	0.012	0.003	0.0009
ENSSSCG00000036083	11.79	4.06	3.88	5.86	1.28	0.037	0.027	0.0010
WAPL	64.52	35.87	32.99	44.98	5.73	0.160	0.063	0.0016
MAP7	14.56	8.30	7.43	8.09	0.97	0.009	0.001	0.0018

Table III-4.1-1 (continued).

CNBP	281.57	157.10	155.06	190.29	22.31	0.066	0.055	0.0021
PDLIM5	42.05	25.69	22.54	32.11	3.64	0.381	0.097	0.0022
SYDE2	23.23	11.99	11.36	15.17	2.13	0.106	0.062	0.0023
NAA15	34.28	18.22	17.11	20.11	2.83	0.031	0.013	0.0027
ENSSSCG00000016687	25.36	13.74	13.61	14.04	1.77	0.006	0.005	0.0032
DNAJA2	38.91	23.43	20.88	27.05	3.26	0.189	0.047	0.0042
HIST1H2AC	2.08	0.25	0.08	0.43	0.39	0.042	0.014	0.0043
ARL5B	26.89	11.36	7.32	10.48	3.11	0.052	0.002	0.0049
ZNF746	2.89	1.63	0.80	2.68	0.50	0.551	0.325	0.0054
RLIM	31.24	17.32	15.94	17.93	2.57	0.035	0.011	0.0064
AADAC	10.51	0.75	0.67	3.96	2.12	0.153	0.143	0.0064
ALB	15102. 2	5514.5 7	4524.94	6639.8 1	1977. 2	0.071	0.025	0.0067
CEBPZ	48.56	29.38	23.33	30.49	4.29	0.190	0.012	0.0068
PTPRU	9.10	3.60	2.83	4.73	1.28	0.170	0.055	0.0076
KPNA1	60.01	42.74	37.32	44.01	3.94	0.213	0.016	0.0077
NAA50	29.77	17.05	14.59	18.71	2.89	0.153	0.029	0.0080
ENSSSCG00000022634	9.10	5.53	2.91	4.03	0.82	0.147	0.000	0.0082
PLAA	25.55	13.50	11.93	13.04	2.22	0.025	0.005	0.0084
CD53	19.38	10.25	8.13	12.26	2.24	0.290	0.057	0.0084
MARCH5	36.10	15.00	13.57	16.47	3.99	0.041	0.020	0.0088
SLC19A2	17.03	8.75	7.51	9.77	1.77	0.118	0.031	0.0089
PFKFB3	24.10	9.34	7.94	8.74	2.89	0.020	0.006	0.010
DCK	27.23	14.93	11.95	14.76	2.72	0.094	0.009	0.011
OTUD4	25.88	15.01	11.37	13.60	2.38	0.082	0.003	0.011
TRIM26	32.97	16.33	15.94	16.93	3.25	0.023	0.018	0.011
ZNF800	11.91	5.09	5.06	5.48	1.29	0.024	0.023	0.012
HPD	352.24	67.50	52.13	90.80	62.43	0.052	0.031	0.013
EAF1	43.08	23.78	22.00	24.97	4.51	0.061	0.025	0.013
EIF4E	28.22	14.57	12.89	14.76	2.84	0.053	0.015	0.013
DNAJB14	17.58	10.74	7.89	10.23	1.66	0.207	0.007	0.014
SRRM1	61.84	39.14	31.05	42.56	6.29	0.399	0.046	0.015
TAF1D	82.30	39.25	33.69	42.34	9.73	0.094	0.030	0.015
RNF149	58.70	26.64	25.45	26.98	6.14	0.027	0.018	0.016
SPIDR	73.80	41.27	35.69	40.61	7.15	0.069	0.013	0.016
PSMD12	34.87	14.95	14.94	18.46	4.41	0.083	0.083	0.016
ZNF628	11.39	5.25	4.57	5.95	1.45	0.115	0.047	0.016
EIF1AX	76.68	51.05	38.96	46.70	6.58	0.180	0.003	0.016
DDX18	74.03	22.99	22.59	25.98	10.13	0.035	0.032	0.017
DAZAP1	41.91	27.86	24.90	28.50	3.46	0.143	0.026	0.017
ENSSSCG00000032016	1.70	1.02	0.06	2.07	0.52	0.224	0.580	0.018
DPH3	22.91	10.41	7.33	8.69	2.61	0.053	0.004	0.018

Table III-4.1-1 (continued).

RGCC	29.97	9.69	9.66	15.74	5.18	0.194	0.192	0.020
PPTC7	43.84	13.68	12.46	14.34	6.17	0.039	0.026	0.021
PLEC	106.24	69.49	61.83	72.81	9.37	0.195	0.044	0.021
GPCPD1	28.75	7.35	4.52	8.10	4.62	0.073	0.021	0.021
MPHOSPH10	26.17	11.14	8.56	11.80	3.54	0.125	0.031	0.021
HES5	2.16	0.20	0.04	0.12	0.48	0.033	0.013	0.021
ATAD3A	39.82	27.00	21.46	26.69	3.84	0.312	0.018	0.021
DDA1	14.68	7.99	6.50	9.86	2.05	0.424	0.136	0.021
SLC30A1	28.51	13.22	9.27	13.61	4.05	0.184	0.027	0.022
HNRNPAB	105.48	66.29	66.20	73.73	9.15	0.111	0.109	0.022
ZYX	96.44	56.88	52.36	66.44	11.11	0.260	0.131	0.023
SBNO1	29.81	15.40	14.00	15.30	3.10	0.054	0.021	0.023
LETM1	44.89	28.64	24.51	30.03	4.46	0.245	0.045	0.023
PLAT	5.87	0.98	0.56	1.41	1.16	0.051	0.104	0.024
PRRG4	8.60	2.68	1.89	3.77	1.54	0.224	0.095	0.024
POLR1B	32.50	17.04	16.14	20.85	4.35	0.213	0.148	0.024
TCERG1	43.27	22.67	22.48	26.51	5.02	0.124	0.116	0.026
SRGN	27.54	13.97	10.23	14.24	3.56	0.211	0.031	0.026
ETF1	92.81	47.51	41.23	48.43	10.68	0.099	0.032	0.027
IFNGR1	22.63	14.14	11.85	12.92	2.17	0.080	0.007	0.027
GSPT1	106.43	63.96	57.98	62.73	9.57	0.073	0.021	0.027
ZNF555	11.53	3.24	2.58	3.62	2.00	0.080	0.041	0.027
YBX3	104.24	59.21	42.31	53.83	11.47	0.178	0.010	0.027
NDUFAF6	13.76	5.69	4.90	5.78	1.84	0.072	0.031	0.028
C11orf96	7.93	3.43	1.93	4.26	1.45	0.463	0.089	0.028
ENSSSCG00000013155	72.49	42.20	37.12	39.03	6.67	0.050	0.010	0.028
ENSSSCG00000007743	137.67	85.38	80.24	92.54	14.35	0.162	0.082	0.028
ENSSSCG00000004294	85.66	52.74	43.48	55.87	9.34	0.301	0.056	0.028
NIFK	62.41	34.35	28.32	34.13	7.06	0.144	0.028	0.030
GPATCH4	28.38	12.50	10.30	15.67	4.57	0.270	0.121	0.031
ZBTB24	10.80	4.19	3.64	3.74	1.39	0.036	0.016	0.031
B3GNT5	2.71	0.96	0.50	0.79	0.43	0.115	0.013	0.031
MFSD4B	9.13	4.73	2.75	5.28	1.49	0.543	0.067	0.031
STK38L	7.26	3.77	2.32	3.55	0.99	0.287	0.020	0.032
ENSSSCG00000021591	58.62	26.39	20.62	29.94	8.86	0.224	0.073	0.033
ALYREF	23.10	16.54	12.10	15.46	2.55	0.477	0.012	0.035
ZBTB21	2.41	0.82	0.28	0.50	0.39	0.108	0.006	0.036
ENSSSCG00000033700	31.05	18.63	17.27	18.99	3.16	0.107	0.047	0.037
FLVCR1	17.27	10.17	5.94	7.95	1.97	0.230	0.003	0.037
ENSSSCG00000005358	45.24	23.45	20.82	27.24	6.30	0.241	0.119	0.037
TGM3	32.75	1.47	1.10	1.29	7.16	0.039	0.035	0.037
AHR	26.01	11.93	10.98	13.18	3.64	0.121	0.075	0.038

Table III-4.1-1 (continued).

ODC1	100.15	70.63	54.18	67.81	9.72	0.429	0.021	0.039
CEBPB	87.72	29.64	29.21	31.23	13.45	0.053	0.050	0.039
DDIT4	138.82	54.66	47.96	49.79	18.72	0.048	0.023	0.039
SREBF1	171.32	124.76	89.09	126.79	19.11	0.821	0.049	0.039
IGFBP4	262.61	168.74	142.60	169.25	29.70	0.238	0.042	0.040
DDX3X	283.22	103.40	93.75	99.50	40.81	0.054	0.034	0.041
ANKRD33	3.23	0.26	0.11	0.38	0.76	0.085	0.058	0.042
TPM4	148.27	82.59	77.34	87.99	16.96	0.135	0.078	0.042
RRN3	38.27	24.46	20.46	24.19	3.91	0.233	0.038	0.043
PTP4A2	62.62	38.11	29.56	31.81	6.04	0.091	0.005	0.044
WFS1	21.88	10.62	8.73	9.26	3.02	0.066	0.016	0.045
ENSSSCG00000013370	43.98	7.19	5.74	7.21	9.92	0.064	0.046	0.046
CHCHD10	12.18	6.49	5.30	5.73	1.42	0.084	0.015	0.047
GATAD2A	49.37	32.90	29.47	31.38	4.25	0.111	0.023	0.048
SLC30A5	32.11	21.64	16.58	20.60	3.38	0.363	0.025	0.048
SLC3A2	48.29	22.63	22.17	25.14	7.06	0.112	0.099	0.048
EHD4	32.21	15.55	13.91	15.70	4.35	0.107	0.052	0.049
MID1IP1	19.67	10.46	8.43	9.54	2.48	0.116	0.022	0.049
ENSSSCG00000038403	13.75	5.63	0.50	10.65	4.26	0.820	0.362	0.050
DAXX	29.17	43.36	43.44	35.19	2.03	0.151	0.140	0.0001
SLC15A1	80.19	189.82	223.31	158.32	20.07	0.279	0.011	0.0002
FBP2	9.05	29.32	31.04	16.86	3.87	0.457	0.247	0.0002
ENSSSCG00000035706	53.05	148.51	153.33	133.64	14.35	0.011	0.005	0.0003
SGSM2	24.46	54.95	59.11	44.95	5.29	0.154	0.036	0.0005
SEMA4G	66.16	102.83	107.94	90.28	6.69	0.184	0.046	0.0006
ABCA4	13.75	31.31	46.15	21.50	5.69	0.512	0.044	0.0006
TEAD2	8.39	13.65	15.38	10.70	1.37	0.834	0.152	0.0013
ARHGAP1	58.80	98.79	100.27	88.90	7.32	0.058	0.038	0.0015
VPS11	21.03	34.77	34.79	31.33	2.41	0.046	0.045	0.0017
SLC26A11	22.12	42.51	43.41	30.09	4.72	0.469	0.365	0.0017
DGAT2	82.85	177.31	203.71	162.64	19.55	0.180	0.011	0.0018
NOS3	13.04	27.46	28.26	22.44	2.83	0.160	0.099	0.0022
FES	15.77	23.22	27.98	20.45	2.42	0.988	0.049	0.0031
MRPS18B	56.82	89.69	91.54	84.75	6.24	0.042	0.022	0.0033
MMS19	18.93	29.00	31.31	26.42	2.29	0.274	0.045	0.0035
PLCG2	43.81	55.41	69.30	51.04	4.54	0.485	0.034	0.0039
ENSSSCG00000004082	14.43	24.20	25.84	20.84	2.25	0.316	0.097	0.0041
CPN1	83.02	117.86	130.42	110.14	8.66	0.425	0.037	0.0051
SEPT10	32.34	46.76	51.52	45.94	3.44	0.191	0.010	0.0054
ACOX2	136.57	189.21	230.24	195.47	14.29	0.551	0.002	0.0067
SUFU	1.44	3.94	4.86	2.80	0.75	0.780	0.153	0.0068
ZDHHC4	27.95	46.38	57.07	47.47	4.89	0.363	0.004	0.0069

Table III-4.1-1 (continued).

FKBP10	16.65	48.62	52.49	36.25	8.15	0.350	0.168	0.0074
XKR8	2.40	4.16	7.21	3.77	0.92	0.369	0.024	0.0089
SP5	1.33	4.52	5.21	3.77	0.80	0.304	0.072	0.010
BMF	37.00	58.29	68.39	61.58	5.10	0.164	0.002	0.010
SMARCAL1	10.52	16.70	19.34	16.73	1.59	0.275	0.011	0.011
PSP-II	2.94	17.49	20.03	7.01	5.18	0.880	0.518	0.011
TSPAN15	47.88	69.47	79.74	65.57	6.49	0.582	0.045	0.013
MYO7A	11.52	22.27	25.34	25.30	2.16	0.017	0.001	0.016
SIRT3	12.95	24.56	26.34	22.03	3.04	0.248	0.091	0.016
RASL11A	10.48	27.19	32.24	24.86	4.79	0.335	0.051	0.018
ENSSSCG00000002746	18.02	32.05	37.21	34.40	3.37	0.106	0.004	0.019
HIF3A	11.28	22.02	25.40	21.67	2.76	0.234	0.024	0.019
BANP	3.59	6.82	11.21	4.80	1.94	0.419	0.160	0.020
STN1	2.62	5.00	7.69	3.41	1.31	0.487	0.207	0.020
STAB1	146.34	244.81	261.32	242.17	24.50	0.115	0.029	0.023
WNT2	4.31	7.18	12.56	8.08	1.59	0.606	0.007	0.026
TRMT1	21.58	32.47	38.85	34.29	3.56	0.344	0.008	0.027
ZFP64	4.92	10.70	11.21	10.62	1.33	0.073	0.035	0.031
CRY2	36.36	57.15	61.43	55.01	5.70	0.239	0.066	0.031
PATZ1	12.04	22.26	23.94	22.44	2.48	0.104	0.028	0.032
ENSSSCG00000002761	1.85	1.55	6.09	2.86	0.64	0.013	0.000	0.035
TSPAN7	51.81	84.10	84.26	84.99	6.84	0.029	0.028	0.036
CBX8	1.09	3.39	4.24	3.07	0.77	0.477	0.085	0.037
ENSSSCG00000005257	5.33	9.58	15.60	10.09	2.17	0.778	0.023	0.037
PRPS2	42.41	59.97	69.79	63.70	5.44	0.297	0.008	0.037
YPEL3	11.24	19.92	25.11	20.12	3.20	0.568	0.037	0.042
LSR	66.80	112.28	122.98	108.74	13.28	0.276	0.072	0.043
CCDC149	29.78	46.49	61.59	53.89	5.55	0.443	0.002	0.045
ACCS	5.99	13.69	18.42	11.39	3.41	0.924	0.159	0.045
PSMB10	12.48	20.71	24.29	22.48	2.40	0.191	0.009	0.046
MGRN1	50.05	81.61	89.61	87.95	7.86	0.071	0.008	0.046
NSDHL	70.68	117.23	126.92	109.83	15.58	0.343	0.122	0.047

Note: The expression level of each mRNA was measured in counts per million reads (CPM).

Data are presented as a least square means \pm standard error of the mean (SEM). Choline x DHA = maternal supplemental choline and DHA interaction effect.

Table III-4.1-2 Statistical result of miRNAs in 2 x 2 Factory Design.

Gene	Treatment				SEM	<i>p</i> -values		
	Choline+ DHA-	Choline +DHA+	Choline- DHA-	Choline- DHA+		Cholin e	DHA	Choline x DHA
miRNAs display choline effect, without choline x DHA interaction (1 miRNA)								
miR-503	2553.00	5208.17	4177.67	7018.00	959.00	0.010	0.093	0.930
miRNAs display DHA effect, without choline x DHA interaction (6 miRNAs)								
miR-221	1012.63	1178.38	1457.13	2302.63	342.17	0.151	0.030	0.329
miR-4677	0.75	1.13	0.13	0.25	0.33	0.458	0.032	0.710
miR-219a-2	10.25	6.13	12.75	19.25	3.53	0.739	0.035	0.143
miR-31	0.75	0.63	1.50	2.00	0.49	0.704	0.038	0.527
miR-26a-1	31.75	23.88	37.25	56.63	8.84	0.521	0.039	0.134
miR-450a	628.25	585.50	768.88	1258.75	193.44	0.258	0.045	0.180
miRNAs displaying a choline x DHA antagonistic effect, with choline having greater impact (19 miRNAs)								
miR-101-1	29.50	18.38	26.00	49.75	6.26	0.322	0.034	0.010
miR-182	28.75	11.63	19.13	35.13	5.98	0.256	0.926	0.010
let-7a-1	3813.63	2011.25	2395.25	4442.75	701.97	0.863	0.477	0.011
let-7a-2	3796.88	2001.75	2377.63	4422.38	699.49	0.860	0.480	0.011
let-7f-2	1832.38	958.00	1107.75	2065.88	351.11	0.906	0.590	0.014
let-7f-1	1916.50	1005.88	1164.38	2159.63	366.26	0.909	0.588	0.015
miR-218b	104.25	52.63	70.75	123.75	21.62	0.975	0.392	0.022
let-7i	199.13	106.50	123.75	241.75	43.70	0.774	0.499	0.023
miR-101-2	4.00	1.00	3.13	6.25	1.28	0.961	0.098	0.024
miR-29a	3850.25	2149.50	2654.00	4449.63	745.85	0.950	0.466	0.026
let-7c	1157.88	694.00	839.38	1459.88	241.81	0.749	0.363	0.033
miR-218-1	181.63	90.88	128.88	222.00	41.20	0.977	0.350	0.034
miR-26b	1321.88	856.50	1215.38	1997.38	283.19	0.581	0.079	0.036
miR-21	7971.63	4871.38	5209.50	9206.50	1650.41	0.788	0.637	0.040
let-7d	489.25	294.25	319.13	548.13	98.71	0.865	0.675	0.041
miR-205	2.00	4.88	1.13	0.88	0.73	0.003	0.084	0.042
miR-30b	14217.00	8727.75	11471.63	19565.63	3201.41	0.687	0.217	0.043
miR-190a	60.63	43.50	53.88	108.13	16.95	0.283	0.099	0.044
let-7e	1822.75	1282.50	1352.00	2456.50	397.15	0.483	0.384	0.048
miRNAs displaying a choline x DHA antagonistic effect, with DHA having greater impact (6 miRNAs)								
miR-92a-1	6.25	2.50	1.75	7.88	1.50	0.436	0.773	0.003
miR-10b	110.13	51.38	23.88	132.25	29.05	0.400	0.927	0.008
miR-144	2086.38	1468.00	1208.38	2825.88	474.51	0.301	0.617	0.026
miR-582	72.25	42.50	34.75	63.38	12.48	0.964	0.511	0.027

Table III-4.1-2 (continued).

miR-1260a	575.13	415.63	343.25	608.75	93.70	0.838	0.576	0.031
miR-183	5.13	2.50	2.38	5.00	1.32	1.000	0.925	0.041

Note: The expression level of each miRNA was measured in expression value. Data are presented as a least square means \pm standard error of the mean (SEM). Choline x DHA = maternal supplemental choline and DHA interaction effect.

Table III-4.2 The effect of maternal supplemental choline on the metabolic pathways identified by IPA analysis.

Ingenuity Canonical Pathways	-log(p-value)	Ratio	z-score	Genes Modified in the Pathway
Cardiac Hypertrophy Signaling (Enhanced)	1.75	0.0202	-2.53	CSF2RB,GNA13,IL1R2,ITPR3,MAPKAPK2, NAPEPLD,PDE4B,PPP3CC,SMPDL3B,STAT3
IL-6 Signaling	2.19	0.0397	-2.236	IL1R2,IL1RAP,MAPKAPK2,MCL1,STAT3
IL-3 Signaling	2.2	.0506	-2	CSF2RB,JAK1,PPP3CC,STAT3
Th1 Pathway	1.58	0.0331	-2	CD86,JAK1,PSEN2,STAT3
Acute Phase Response Signaling	1.58	0.0278	-2	CRABP1,HAMP,IL1RAP,NOLC1,STAT3

Note: Ingenuity canonical pathways according to core analysis of mRNAs display the choline effect without choline x DHA interaction. The “Ratio” represents the percentage of altered genes within the total number of genes in each pathway. The “z-score” is a statistical measure of the match between expected relationship direction and observed gene expression. A positive z-score indicates activation, while a negative score indicates inhibition.

Table III-4.3 The effect of maternal supplemental DHA on the metabolic pathways identified by IPA analysis.

Ingenuity Canonical Pathways	-log(p-value)	Ratio	z-score	Genes Modified in the Pathway
Cardiac Hypertrophy Signaling (Enhanced)	2.72	0.0242	-2.714	CSF2RB,EDA,GNA13,HDAC4,IL1R1,IL1R2, IL4R,ITGA3,MKNK2,PDE10A,PIK3R1,SMPDL3B
Tec Kinase Signaling	3	0.0405	-2.449	GNA13,ITGA3,PIK3R1,RHOD,RHOU,RND3,TNFRSF21
Phospholipase C Signaling	3.14	0.0338	-2.333	ATF4,CREB3L3,GNA13,HDAC4,ITGA3, RHOD,RHOU,RND3,RPS6KA3
Sphingosine-1-phosphate Signaling	2.38	0.0427	-2.236	GNA13,PIK3R1,RHOD,RHOU,RND3
IL-6 Signaling	2.24	0.0397	-2.236	IL1R1,IL1R2,IL1RAP,MCL1,PIK3R1
3-phosphoinositide Biosynthesis	1.76	0.0301	-2.236	DUSP1,MTMR9,PIK3R1,PPP2R3A,PTPN1
CXCR4 Signaling	1.75	0.0299	-2.236	GNA13,PIK3R1,RHOD,RHOU,RND3
Signaling by Rho Family GTPases	1.56	0.0237	-2.236	GNA13,ITGA3,PIK3R1,RHOD,RHOU,RND3
Superpathway of Inositol Phosphate Compounds	1.46	0.0251	-2.236	DUSP1,MTMR9,PIK3R1,PPP2R3A,PTPN1
Thrombin Signaling	1.39	0.024	-2.236	GNA13,PIK3R1,RHOD,RHOU,RND3

Table III-4.3 (continued).

Systemic Lupus Erythematosus in T Cell Signaling Pathway	1.95	0.024	-2.121	ATF4,CREB3L3,GNA13,PIK3R1,PPP2R3A, RHOD,RHOU,RND3
Hepatic Fibrosis Signaling Pathway	3.19	0.0293	-2.111	ATF4,CREB3L3,FLT4,IL1R1,IL1R2,IL1RAP, ITGA3,PIK3R1,RHOD,RHOU,RND3
Actin Nucleation by ARP-WASP Complex	2.21	0.0494	-2	ITGA3,RHOD,RHOU,RND3
Regulation of Actin-based Motility by Rho	1.85	0.0388	-2	ITGA3,RHOD,RHOU,RND3
Cholecystokinin/Gastrin-mediated Signaling	1.64	0.0336	-2	GNA13,RHOD,RHOU,RND3
D-myo-inositol (1,4,5,6)- Tetrakisphosphate Biosynthesis	1.4	0.0282	-2	DUSP1,MTMR9,PPP2R3A,PTPN1
D-myo-inositol (3,4,5,6)- tetrakisphosphate Biosynthesis	1.4	0.0282	-2	DUSP1,MTMR9,PPP2R3A,PTPN1
PPAR Signaling	1.82	0.0381	2	IL1R1,IL1R2,IL1RAP,PPARD

Table III-4.3 (continued).

RhoGDI Signaling	1.54	0.0265	2	GNA13,ITGA3,RHOD,RHOU,RND3
------------------	------	--------	---	----------------------------

Note: Ingenuity canonical pathways according to core analysis of mRNAs display the DHA effect without choline x DHA interaction. The “Ratio” represents the percentage of altered genes within the total number of genes in each pathway. The “z-score” is a statistical measure of the match between expected relationship direction and observed gene expression. A positive z-score indicates activation, while a negative score indicates inhibition.

Table III-4.4 The interaction effect of maternal supplemental choline and DHA on the metabolic pathways identified by IPA analysis.

Ingenuity Canonical Pathways	-log(p-value)	Ratio	z-score	Genes Modified in the Pathway
Pathways involving genes displaying a choline x DHA synergistic effect				
Acute Phase Response Signaling	5.25	0.0216	-2	APCS,CP,CRP,OSMR
Pathways involving genes displaying a choline x DHA antagonistic effect, with choline having greater impact				
Sirtuin Signaling Pathway	3.83	0.0344	-2.121	ABCA1,CPS1,MAPK3,NQO1,PPARGC1A,PPIF,PRKA A2,RELB,SOD2,TIMM8A
tRNA Splicing	3.27	0.087	-2	FICD,PDE12,PDE4D,SMPDL3A
PPAR α /RXR α Activation	1.67	0.0258	-2	ABCA1,MAPK3,PPARGC1A,PRKAA2,RELB
NAD Signaling Pathway	1.45	0.0265	-2	PPARGC1A,PRKAA2,SLC36A4,SOD2
Pathways involving genes displaying a choline x DHA antagonistic effect, with DHA having greater impact				
RNA Polymerase I Transcription	3.55	0.08	-2	GATAD2A,POLR1B,RRN3,TAF1D
Sirtuin Signaling Pathway	1.42	0.0172	2	NOS3,PFKFB3,POLR1B,SIRT3,SREBF1

Note: Ingenuity canonical pathways according to core analysis of mRNAs display the choline x DHA interaction effect. The “Ratio” represents the percentage of altered genes within the total number of genes in each pathway. The “z-score” is a statistical measure of the match between expected relationship direction and observed gene expression. A positive z-score indicates activation, while a negative score indicates inhibition.

Table III-4.5 The list of miRNAs and their target mRNAs with same statistical category.

Gene	Treatment				SEM	P values		
	Choline- DHA-	Choline+ DHA-	Choline- DHA+	Choline +DHA+		Cholin e	DHA	Choline x DHA
miRNAs and their target mRNAs displaying a choline effect, without choline x DHA interaction								
miR-503	2553.00	5208.17	4177.67	7018.00	959.00	0.01	0.093	0.93
LIPG	26.94	0.89	1.53	0.71	6.57	0.049	0.063	0.066
LURAP1L	12.47	4.10	5.92	5.40	1.88	0.027	0.18	0.054
GADD45G	26.87	6.96	10.29	5.06	5.46	0.046	0.16	0.076
SPOUT1	9.51	17.63	12.57	15.47	1.94	0.0090	0.82	0.19
miRNAs and their target mRNAs displaying a DHA effect, without choline x DHA interaction								
miR-221	1012.63	1178.38	1457.13	2302.63	342.17	0.151	0.030	0.329
PIK3R1	51.25	30.03	23.90	27.40	6.58	0.19	0.031	0.071
TIMP3	209.23	48.60	38.32	45.33	41.66	0.076	0.046	0.054
TM4SF1	105.50	36.30	31.15	29.13	19.38	0.077	0.045	0.094
miR-31	0.75	0.63	1.50	2.00	0.96	0.72	0.049	0.55
CASR	1.04	7.12	13.98	7.89	3.01	0.99	0.030	0.053
DDX21	88.59	45.83	42.08	43.47	11.08	0.074	0.037	0.058
FLOT1	22.44	32.56	37.80	37.51	2.91	0.10	0.0019	0.086
miRNAs displaying a choline x DHA antagonistic effect, with choline having the greater impact								
Let-7f	1832.38	958.00	1107.75	2065.88	366.80	0.91	0.61	0.020
DUSP16	43.65	21.03	24.09	27.60	5.06	0.071	0.21	0.016
CDKN1A	5.47	1.57	2.76	3.50	0.95	0.11	0.68	0.023
PIGA	39.71	15.86	17.36	19.36	5.97	0.080	0.13	0.041
miR-182	28.75	11.63	19.13	35.12	6.10	0.27	0.93	0.012
SLC35G1	31.74	11.44	12.05	14.14	4.63	0.061	0.079	0.024
TMEM42	6.04	12.16	12.71	10.43	1.44	0.10	0.20	0.0077
miR-218	181.63	90.88	128.88	222.00	43.70	0.98	0.38	0.046
SLC6A1	1.08	6.39	2.97	1.65	1.08	0.076	0.20	0.0052
miR-26b	1321.88	856.50	1215.38	1997.38	298.28	0.60	0.096	0.047
FAM98A	23.54	10.87	13.00	16.06	2.61	0.078	0.32	0.0060
miR-29a	3850.25	2149.50	2654.00	4449.63	793.16	0.95	0.49	0.037
PPIC	10.13	17.79	16.74	15.23	1.60	0.066	0.22	0.0084
miRNAs displaying a choline x DHA antagonistic effect, with DHA having the greater impact								
miR-1260a	575.13	415.63	343.25	608.75	93.92	0.84	0.58	0.033
DAXX	29.17	43.36	43.44	35.19	1.87	0.13	0.12	0.0001
miR-144	2086.38	1208.38	1468.00	2825.88	491.61	0.32	0.63	0.032
PLAT	5.87	0.98	0.56	1.41	1.22	0.056	0.11	0.026

Note: Choline x DHA = Choline and DHA interaction effect. Data are presented as a least square means \pm standard error of the mean (SEM).

Table III-4.6 RT-qPCR validation for miRNAs and their target mRNAs.

Gene	Treatment				SEM	P values		
	Choline- DHA-	Choline+ DHA-	Choline- DHA+	Choline+ DHA+		Cholin e	DHA	Choline x DHA
miRNAs and their target mRNAs displaying a choline effect, without choline x DHA interaction								
miR-503	1.00	1.98	1.49	2.50	0.39	0.020	0.21	0.97
LIPG	1.00	0.039	0.32	0.036	0.16	0.0007	0.067	0.070
LURAP1L	1.00	0.31	0.57	0.59	0.11	0.0055	0.48	0.0031
GADD45G	1.00	0.074	0.32	0.31	0.065	0.0001	0.0032	0.0001
SPOUT1	1.00	0.53	1.01	0.49	0.12	0.0006	0.89	0.86
miRNAs and their target mRNAs displaying a DHA effect, without choline x DHA interaction								
miR-221	1.00	1.29	4.25	3.19	0.77	0.62	0.0033	0.40
PIK3R1	1.00	0.71	0.54	0.83	0.070	0.98	0.024	0.0006
TIMP3	1.00	0.76	0.060	0.072	0.082	0.18	0.0001	0.14
TM4SF1	1.00	0.75	0.15	0.13	0.088	0.13	0.0001	0.17
miR-31	1.00	1.27	17.85	11.98	3.20	0.39	0.0003	0.35
CASR	1.00	1.22	3.32	4.07	0.67	0.48	0.0009	0.69
DDX21	1.00	0.36	0.21	0.28	0.044	0.0001	0.0001	0.0001
FLOT1	1.00	1.87	2.48	2.62	0.47	0.30	0.029	0.45
miRNAs displaying a choline x DHA antagonistic effect, with choline having greater impact								
Let-7f	1.00	0.45	0.56	1.35	0.14	0.39	0.12	0.0001
DUSP16	1.00	0.51	0.55	0.88	0.12	0.54	0.76	0.0036
CDKN1A	1.00	0.77	1.13	1.93	0.14	0.053	0.0001	0.0014
PIGA	1.00	0.83	0.58	1.32	0.15	0.079	0.86	0.0063
miR-182	1.00	0.71	0.55	0.75	0.11	0.70	0.078	0.038
SLC35G1	1.00	0.38	0.44	0.97	0.095	0.62	0.87	0.0001
TMEM42	1.00	3.27	2.63	1.11	0.39	0.35	0.50	0.0001
miR-218	1.00	0.37	0.57	0.83	0.20	0.35	0.95	0.037
SLC6A1	1.00	4.61	3.68	1.68	0.53	0.15	0.82	0.0001
miR-26b	1.00	0.28	0.85	1.68	0.15	0.73	0.0006	0.0001
FAM98A	1.00	0.27	0.78	0.94	0.12	0.025	0.068	0.0012
miR-29a	1.00	0.52	0.46	2.37	0.15	0.0001	0.0002	0.0001
PPIC	1.00	1.81	1.42	0.86	0.16	0.46	0.12	0.0004
miRNAs displaying a choline x DHA antagonistic effect, with DHA having greater impact								
miR-1260a	1.00	0.95	1.80	3.47	0.62	0.20	0.013	0.17
DAXX	1.00	1.61	1.62	0.99	0.15	0.93	0.97	0.0001
miR-144	1.00	0.68	0.58	1.22	0.15	0.23	0.65	0.0014
PLAT	1.00	0.73	0.52	1.17	0.16	0.34	0.91	0.027

Note: Choline x DHA = Choline and DHA interaction effect. Data are presented as a least square means \pm standard error of the mean (SEM).

CHAPTER III FIGURES

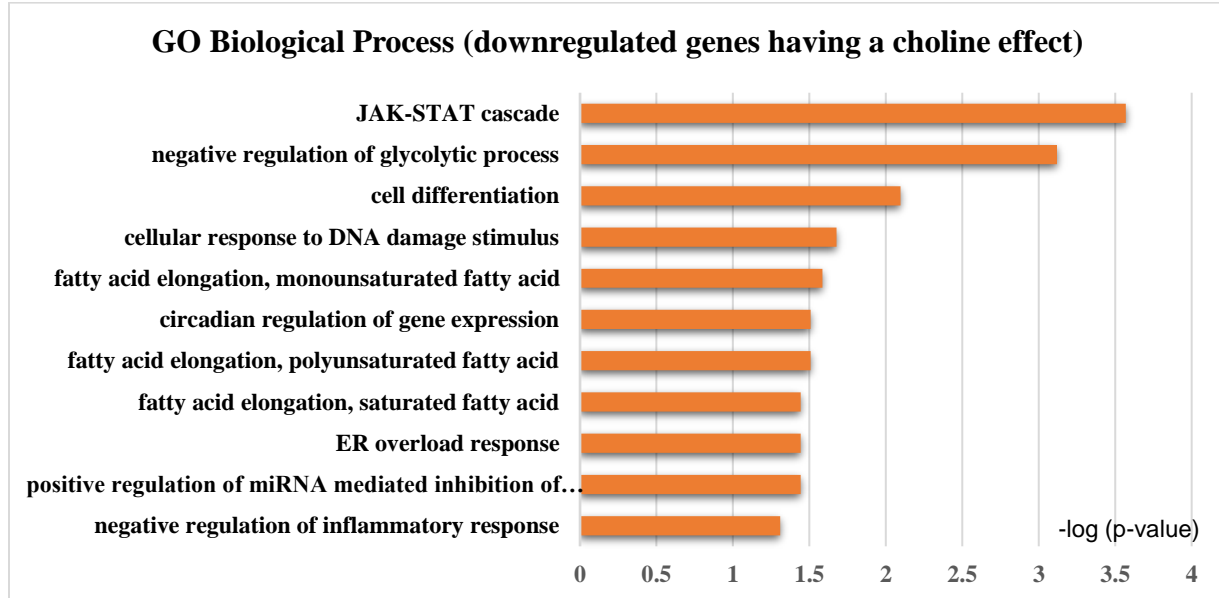


Figure III-4.2 Gene ontology (GO) biological process annotations for fetal hepatic mRNAs displaying a maternal supplemental choline effect, without Choline x DHA interaction.

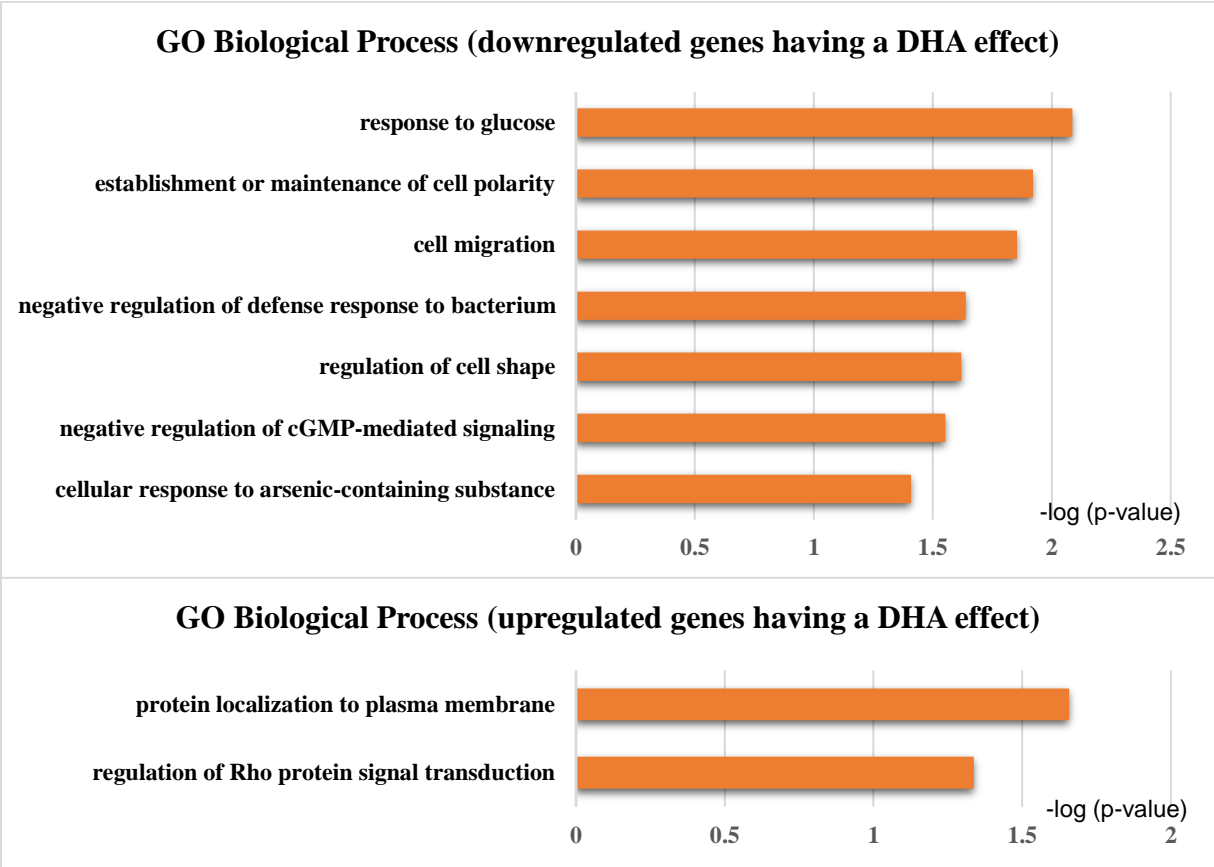


Figure III-4.3 Gene ontology (GO) biological process annotations for fetal hepatic mRNAs displaying a maternal supplemental DHA effect, without Choline x DHA interaction.

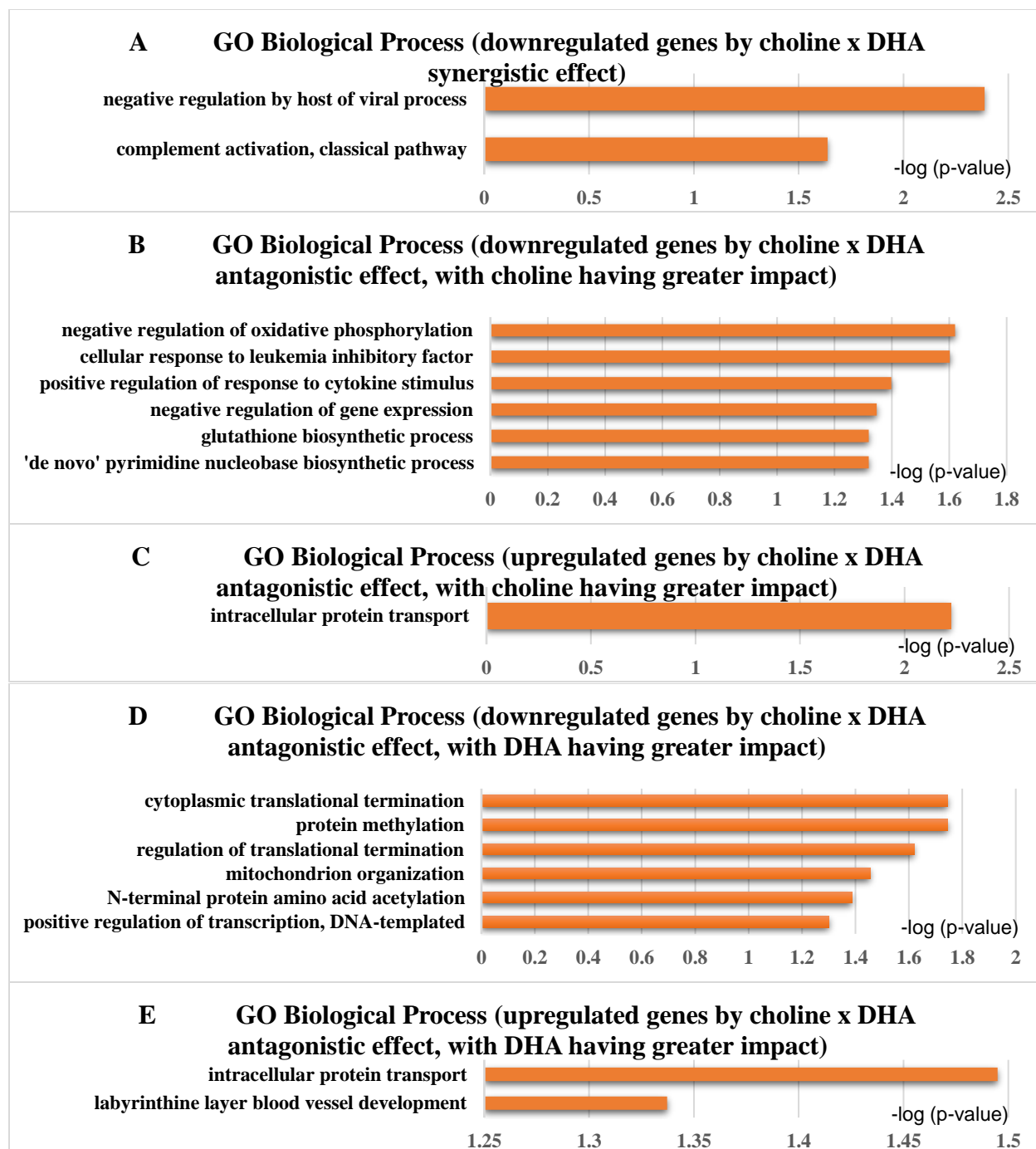


Figure III-4.4 Gene ontology (GO) biological process annotations for fetal hepatic mRNAs displaying a maternal supplemental choline x DHA interaction effect.

A. Genes downregulated by choline x DHA synergistic effect. B. Genes downregulated by choline x DHA antagonistic effect, with choline having a greater impact. C. Genes upregulated by choline x DHA antagonistic effect, with choline having a greater impact. D. Genes downregulated by choline x DHA antagonistic effect, with DHA having a greater impact. E. Genes upregulated by choline x DHA antagonistic effect, with DHA having a greater impact.

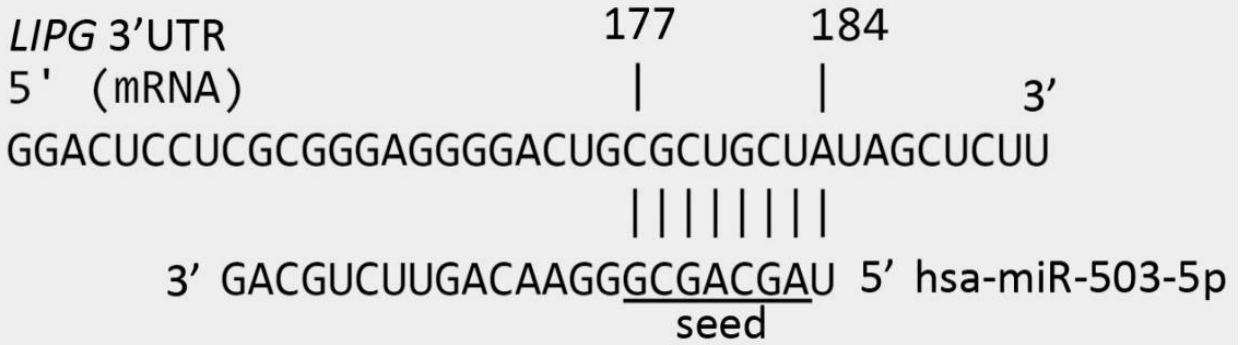


Figure III-4.7-1 Schema showing potential binding sites of miR-503 with *LIPG* mRNA. The seed region of miR-503 has an 8-nucleotide match with *LIPG* 3'UTR region from 177 to 184 bp.

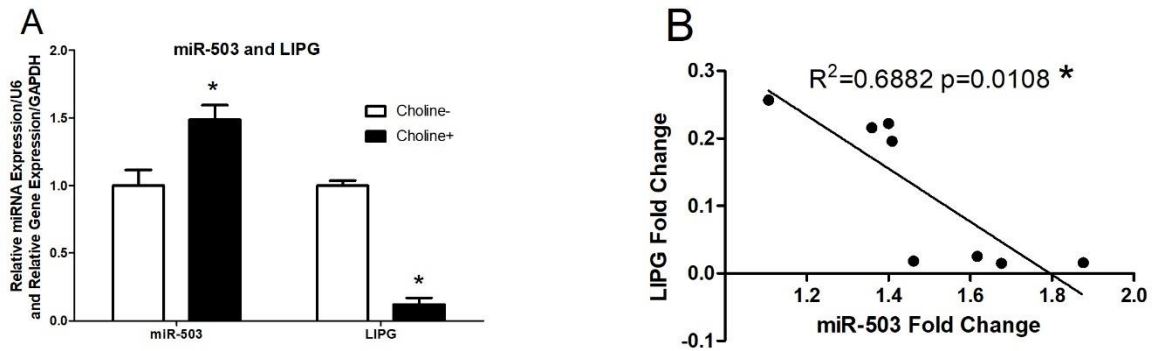


Figure III-4.7-2 Relative expression of hepatic miR-503 and LIPG gene and their correlational analysis in fetal pigs from dams with or without choline supplementation ($n = 8$). The data are expressed as fold-change (mean \pm SEM). *The significance level was set at $p < 0.05$. A. The effect of choline on miR-503 and LIPG and B. The correlation between miR-503 and LIPG.

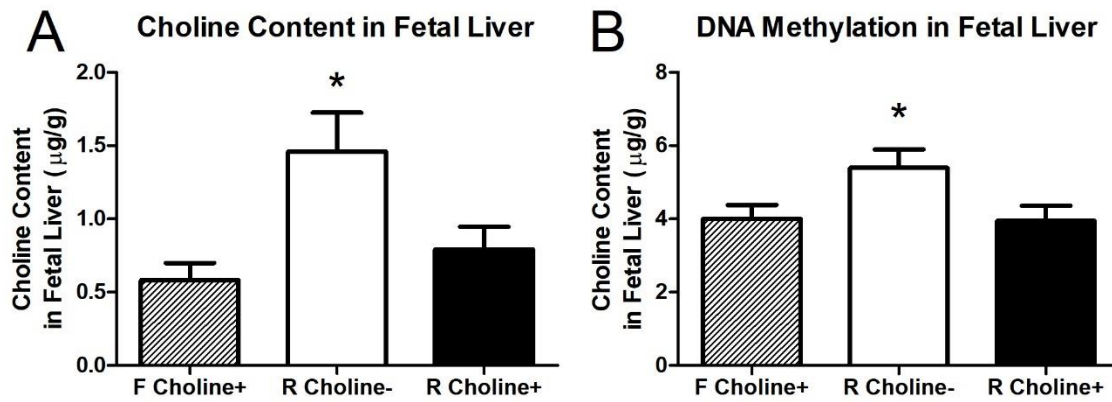


Figure III-4.7-3 Hepatic choline content and global DNA methylation status in fetal pigs from dams in full-nutrition (F) group and restricted-nutrition (R) group with or without maternal choline supplementation ($n = 8$). The data are expressed as fold-change (mean \pm SEM). *The significance level was set at $p < 0.05$. A. Hepatic choline content and B. Global DNA methylation in fetal liver (data was adopted from a previous study (Lima, et al., 2017)).

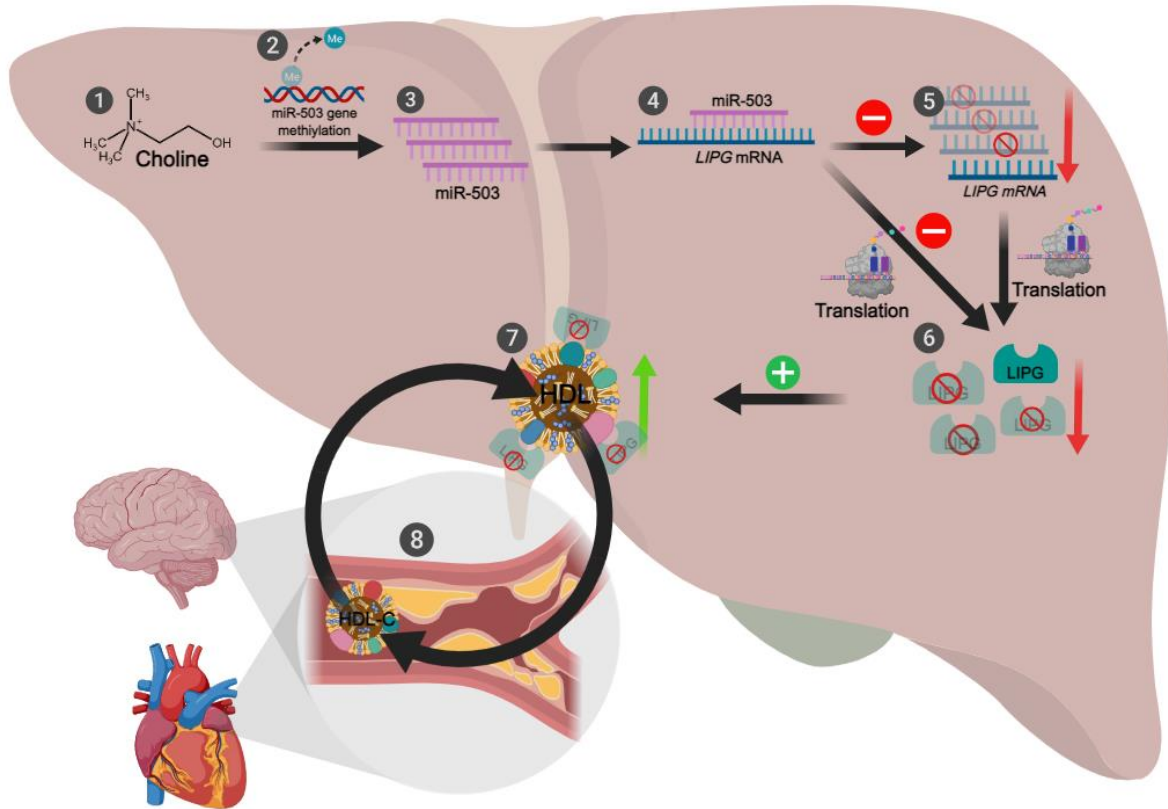


Figure III-4.7-4 Schema showing our hypothesized pathway. (1) Choline chemical structure. (2) DNA methylation process. (3) MiR-503 molecules. (4) MiR-503 destabilizes *LIPG* mRNA transcripts. (5) Decreased *LIPG* mRNA expression. (6) Reduced *LIPG* enzyme production. (7) Boosted HDL content, due to less hydrolysis by *LIPG*. (8) The process of HDL-C removing excess cholesterol from the blood vessel of brain and heart to liver for elimination. The red down-arrows indicate down-regulation, and green up-arrows indicate up-regulation. Minus signs indicate inhibition and plus signs indicate promotion.

Chapter IV: Modulation of MicroRNA-503 Alters Endothelial Lipase Expression and High-Density Lipoprotein Level in Porcine Liver Organoids

IV-1. Abstract

High-density lipoprotein cholesterol (HDL-C) helps clear excess cholesterol in circulation, reducing the risk of atherosclerotic cardiovascular disease (ASCVD), and its metabolism is regulated in part by endothelial lipase (LIPG). Evidence from our recent findings in fetal pig liver suggested that the expression of miR-503 and *LIPG* were correlated with hepatic choline level and global DNA methylation status. Maternal choline supplementation in pregnant pigs was found to determine both the hepatic choline level and global DNA methylation status in the fetal liver. To investigate possible mechanisms, we explored how choline modified miR-503 expression, subsequently increasing HDL by regulating *LIPG* gene expression and protein content. Liver organoids were isolated from neonatal pigs within the first 24 h of birth. Isolated liver organoids were developed in the OIM medium in three-dimensional (3D) culture, following a 2D culture in the OGM medium. During 2D culture, liver organoids were transfected with various concentrations (1, 10, 100 nM) of miR-503 mimics with or without co-transfected with same concentration of miR-503 inhibitor. Results showed that the cytotoxicity (0.64%) and viability (95.50%) of the organoids remained unaffected across all the tested miR-503 mimic concentrations. MiR-503 mimic at concentrations of 1, 10, and 100 nM significantly suppressed *LIPG* gene expression ($p < 0.05$), with corresponding suppression of LIPG protein production observed only at 10 nM ($p < 0.05$). No significant difference was observed between all miR-503 mimic co-transfected with miR-503 inhibitor groups and the control group ($p > 0.05$). Notably, the HDL content in liver organoids exhibited a notable increase upon transfection with miR-503 mimic at all concentrations ($p < 0.05$). However, co-transfection of miR-503 mimic with its

inhibitor did not show any observable impact on the increase ($p > 0.05$). In conclusion, our study underscores the regulatory impact of miR-503 on both *LIPG* gene expression and protein production, thereby influencing HDL levels. Despite efforts to modulate choline concentrations in liver organoids, no discernible differences in miR-503 and *LIPG* gene expression were observed ($p > 0.05$).

IV-2. Introduction

Cardiovascular disease (CVD) is the number one cause of death worldwide. It was reported that about 17.9 million people died from CVDs in 2019, representing 32% of all global deaths (World Health Organization, 2021). Of these deaths, 85% were a result of heart attacks and strokes that occurred due to the buildup of cholesterol plaque on the inner walls of the blood vessels, leading to the obstruction of blood flow in the arteries (Levinson & Wagner, 2015). This process is called atherosclerosis and related disease called atherosclerotic cardiovascular disease (ASCVD). In most cases, ASCVD is a multifactorial disease, and the risk factors include low-density lipoprotein cholesterol (LDL-C), triglycerides, high-density lipoprotein cholesterol (HDL-C), blood pressure, obesity, diabetes, unhealthy diet, smoking, and physical inactivity (Cole, et al., 2021; Johns Hopkins Medicine, 2024). However, more and more evidence from case studies show that epigenetic modification plays an important role in the occurrence and development of ASCVD (Shi, et al., 2022).

Epigenetics refers to changes in gene expressions that are not caused by changes in the underlying DNA sequence but rather by modifications to the DNA molecule. The modifications usually are influenced by nutrients, physiological status, and environmental factors, such as diet, exercise, and exposure to toxins, as well as by genetic factors (Feinberg, 2018). By current definition, epigenetic regulations include DNA methylation, histone modification, and noncoding RNA such as miRNA regulation. Through these mechanisms, ASCVD-related genes and protein expression levels can be modified during fetal development, further affecting the progression of ASCVD in adults (Shi, et al., 2022).

The critical role of epigenetic modifications in the development and progression of ASCVD has been established in many studies. For example, microRNAs (miRNAs), which are

small RNA molecules that regulate gene expression, are involved in the regulation of processes related to ASCVD. Rayner *et al.* (2011) reported that pharmacological inhibition of miR-33a and miR-33b could improve dyslipidemia associated with cardiovascular disease risk via raising the HDL and lowering the very-low-density lipoprotein (VLDL). MiRNA-106a-3p and miRNA-342-5p have an effect of reducing atherosclerosis on endothelial cells (Liu, *et al.*, 2020; Xing, *et al.*, 2020), whereas miRNA-92a raises the occurrences of atherosclerosis (Chang, *et al.*, 2019). In addition, changes in DNA methylation patterns have been associated with an increased risk of ASCVD. DNA methylation is a process in which a methyl group is added to a cytosine nucleotide in DNA, and this can affect gene expression by modifying its transcription. For example, Zhu, *et al.* found that suppressing monocarboxylate transporter 3 (MCT3) by DNA methylation impacted atherosclerosis development (Zhu, *et al.*, 2005). Westerman, *et al.* found that DNA methylation status in three regions (associated with genes of Solute Carrier Family 9 Member A1 (SLC9A1), A5 (SLC1A5), and trinucleotide Repeat Containing Adaptor 6C (TNRC6C) genes) were associated with cardiovascular disease risk (Westerman, *et al.*, 2019). These studies indicate that the relationship between ASCVD and epigenetics is complex and multifactorial. Therefore, further research is needed and important for fully understanding the mechanisms underlying this relationship and developing new strategies for the prevention and treatment of ASCVD.

HDL-C is known as “good cholesterol”, due to its beneficial effect against ASCVD (Madsen, *et al.*, 2017). One of the important functions of HDL is to transport cholesterol from the extrahepatic cells and tissues back to the liver for elimination. It also removes cholesterol deposited in the walls of blood vessels (Tora, *et al.*, 2020; Annema & Tietge, 2011). Moreover, HDL-C may reduce blood vessel injury via its anti-inflammatory and antioxidant functions

(Madsen, et al., 2017). The biogenesis of HDL happens in the liver (70%) and intestine (30%), and it consists of a central core of esterified cholesterol, a monolayer of phospholipids, free cholesterol, and apolipoprotein (apo) A-I and A-II (Levinson & Wagner, 2015). The catabolism (biodegrading) of HDL particles is mainly via hydrolysis catalyzed by endothelial lipases (lipases G, LIPG) (Annema & Tietge, 2011).

LIPG is of particular interest, as it can be upregulated in inflammatory conditions such as atherosclerosis and is a primary determinant of HDL levels (Yu, et al., 2018). As a member of the triglyceride lipase family, LIPG plays a central role in dietary fat absorption and lipoprotein metabolism (Tora, et al., 2020). However, unlike other triglyceride lipase family members, LIPG primarily functions as a phospholipase with minor triglyceride lipase activity (Yu, et al., 2018). Thus, involvement in lipoprotein metabolism is the predominate task of LIPG. This enzyme is secreted from vascular endothelial cells and hepatocytes (Choi, et al., 2002) in which HDL is synthesized. Thus, it has drawn great interest, not only because it changes in inflammatory conditions, but also as a critical determinant of HDL levels. The hydrolysis of HDL by LIPG occurs when the enzyme interacts with the HDL particle and catalyzes the cleavage of ester bonds in the phospholipids and triglycerides that make up the particle. The resulting smaller HDL particles can then be taken up by the liver, in which their cholesterol can be metabolized into bile acids, and then excreted from the body through feces (Vitali, et al., 2017). The effect of LIPG on HDL was observed in manipulation of gene in rodent animal models. Overexpression of *LIPG* in transgenic mice caused serum level of HDL-C to be reduced dramatically (Jaye, et al., 1999), while in *LIPG* knockout mice HDL-C levels were significantly increased (Ishida, et al., 2003). Additionally, LIPG hydrolyzes the SN-1 ester bond of phosphatidylcholine present in HDL-C particles, resulting in a release in lysophosphatidylcholine and subsequently reducing

HDL-C and HDL (Hirata, et al., 1999). These findings demonstrated that HDL is the primary substrate of LIPG. Because of the critical role of LIPG in reducing HDL-C level, it has become the target for treating ASCVD. Interestingly, RNA-sequencing data from our previous study (reference previous chapter here) indicated that the *LIPG* gene was modified in fetal pigs' liver from dams fed with supplemental choline via an epigenetic mechanism, in which miR-503 expression also was altered and might impact *LIPG* gene regulation because *LIPG* was predicted to a target of miR-503.

The miRNAs are short, noncoding endogenous RNAs with 20–27 nucleotides in length and are processed from stem-loop regions of longer RNA transcripts into primary miRNA, precursor miRNAs and mature miRNAs (Bartel, 2018). The biological function of miRNA is as post-transcriptional regulators of gene expression via interacting with the 3 prime untranslated region (3' UTR) of its target mRNAs then repressing translation and accelerating target mRNA degradation (Ameres & Zamore, 2013; Lee, et al., 2004). MiR-503 belongs to the extended miR-16 family, and evidence showed that miR-503 is involved in a variety of cellular processes, including apoptosis, cell proliferation, migration, and angiogenesis (He, et al., 2021). Evidence also showed that miR-503 is implicated in human diseases, such as cancer (Wu, et al., 2018; Yang, et al., 2014; Zhou, et al., 2013), pulmonary arterial hypertension (Kim, et al., 2013), and diabetes mellitus (Kaur, et al., 2022).

In addition, dysregulation of miR-503 might contribute to CVD due to its role in various pathologies, such as angiogenesis (He, et al., 2021; Wen, et al., 2018), cardiac fibrosis (Zhou, et al., 2016), and oxidative stress (Rubattu, et al., 2017). In mouse endothelial progenitor cells, miR-503 suppressed angiogenesis by targeting Apelin (Wen, et al., 2018). In diabetic mice with limb ischemia, antagonizing miR-503 improved angiogenesis and blood flow recovery by

upregulating cell division cycle 25 A (*cdc25A*) and cyclin E1 (*CCNE1*) (Caporali, et al., 2011). Another group reported that miR-503 exacerbated ischemia/reperfusion injury via inactivation of PI3K/Akt and STAT3 pathways (He, et al., 2022). Overall, miR-503 exhibits anti-angiogenic properties. Moreover, increased miR-503 could promote cardiac fibrosis through its target gene Apelin-13 in mice (Zhou, et al., 2016). Together, miR-503 is critical for cardiovascular system health. However, the effect of miR-503 enrichment on *LIPG* expression has not been reported in literature.

Notably, in recent years miRNA Target-Prediction Strategies has been applied to predict its target mRNA, more and more miRNA-mRNA interaction and mechanism have been revealed. Through our preliminary data, both *LIPG* gene and miR-503 were modified in fetal pigs from dams with supplementation of choline via epigenetic mechanisms. In addition, from these data we predicted for the first time that *LIPG* is a target gene of miR-503 with negative correlation. Again, considering the roles of miR-503, *LIPG* and HDL-C in CVD, we hypothesize that miR-503 regulates its target *LIPG*, thereby affecting HDL-C metabolism. To investigate and confirm the regulatory role of miR-503, herein, we focus on studying the effects of modifying miR-503 level on *LIPG* gene expression, *LIPG* protein production and downstream HDL-C concentration *in vitro* using liver organoids as a model. We expect that our explorations will provide necessary scientific foundation for miR-503 as a candidate to treat ASCVD in this project.

DNA methylation generally is referred to as the addition of methyl groups to the DNA molecule by DNA methyltransferases (DNMT). It happens primarily on the 5-carbon of the cytosine residues of Cytidine-Guanine dinucleotides (CpG, p indicates a phosphate group between the two nucleotides). Around 75% of CpG dinucleotides are methylated in mammals (Tost, 2010), and it proposed as a “silencing” epigenetic mark (Jones, 2012). DNA methylation

affects genes transcription through the methylation of DNA itself because it may physically interfere with the recruitment and binding of transcriptional proteins to the gene (Choy, et al., 2010). Additionally, methylated DNA may be bound by other proteins and then alter chromatin structure, subsequently impacting gene transcription (Vymetalkova, et al., 2019). DNA methylation plays a crucial role in fetal development by regulating gene expression, cellular differentiation, imprinting, and response to environmental cues. A paradigmatic example is Agouti mouse model; the maternal methyl dietary content affects the coat color of the offspring (Wolff, et al., 1998). In the last decades, more and more evidence has showed that genome-wide epigenetic status is established starting from early life, while different cell types have different epigenetic patterns carried through later life (Zeisel, 2017). Thus, epigenetic patterns in early life have impacts on organ's function and metabolism in later life.

DNA methylation regulates gene expression through repressing gene transcription. Likewise, DNA methylation can also inhibit the expression of miRNA by suppressing the transcription of genes that code for miRNA. It is estimated that 10% of miRNA expression is controlled through DNA methylation from a previous report (Macfarlane & Murphy, 2010). Result from a recent study showed that miR-503 expression is downregulated by DNA hypermethylation in human endometriotic cyst stromal cells compared to normal endometriotic stromal cells. In addition, this methylation on miR-503 contributes to disrupting the cell function through its target genes (Hirakawa, et al., 2016). In our previous study, we also noticed that maternal supplementation of choline decreased DNA methylation and increased miR-503 expression. Therefore, it is highly possible that DNA methylation is the mechanism that modifies the level of miR-503 during fetal development and this epigenetic modification will last to entire life.

Choline is an essential substrate for various molecules such as phosphatidylcholine (PC) and sphingomyelin, which are required for the structural and functional integrity of cell membranes (Morita & Ikeda, 2022). Most importantly, choline is a key nutrient that plays a critical role in DNA methylation, particularly in fetal programming of development (Niculescu, et al., 2006). Choline is involved in the synthesis of S-adenosylmethionine (SAM), which is a methyl donor that is required for DNA methylation (Kok, et al., 2015). SAM donates a methyl group to the DNA molecule, resulting in the addition of a methyl group to the cytosine residue (Kovacheva, et al., 2007). Methylation modified DNA is less accessible to the cellular machinery responsible for transcribing genes into proteins, which results in various diseases.

To illustrate the involvement of choline in regulation of noncoding RNA transcript by DNA methylation, there is an example of choline-deficient diet modification of epigenetics in mice. Insulin-like growth factor II (IGF2) is a critical growth factor, which is repressed by a long noncoding RNA transcript from the H19 gene (Bell & Felsenfeld, 2000; Claycombe, et al., 2013). In turn, H19 expression is controlled by the methylation of a fragment within both genes called Igf2-DMR2. Feeding pregnant rats with choline-deficient diets caused Igf2-DMR2 hypermethylation in fetal liver. Thus, H19 was downregulated and IGF2 expression increased (Kovacheva, et al., 2007). Other studies on maternal choline-deficient diets also indicate that choline is an essential nutrient for epigenetic modulation of gene expression (Cooney, et al., 2002; Niculescu, et al., 2006; Craciunescu, et al., 2003). Data from our previous study showed that the maternal choline supplementation in pregnant pigs decrease/restore high hepatic choline level and global DNA methylation status (observed in offspring from dams without choline supplementation) to normal (compared to offspring from full-nutrition dams) in their offspring (**Figure III-4.7-3**). With the decrease in DNA methylation, the miR-503 expression increased

and *LIPG* expression reduced, suggesting that the changes in miR-503 and its predicted gene *LIPG* may be associated with the DNA methylation induced by choline supplementation.

Therefore, we hypothesize that the expression of miR-503 was upregulated via methylation of noncoding RNA transcription after choline was added into feed-intake limited pregnant pigs.

Together, we hypothesis that choline content affects DNA methylation in liver, which may occur in miR-503 promoter region and regulate miR-503 expression. Released miR-503 will repress *LIPG* gene expression and protein translation, further increase HDL level by decreasing the hydrolysis effect carried by LIPG. With the elevated level of HDL-C, eventually decreases the risk of ASCVD (**Figure III-4.7-4**).

Recently, organoid technology has been established and attracted more attention as a cell culture tool for studying biology in health and disease. Organoids are defined as three-dimensional (3D) *in-vitro*-grown multi-cell clusters with near-native microanatomy that arise from self-organizing mammalian pluripotent or adult stem cells and exhibiting similar organ functionality as the tissue of origin (Kretzschmar & Clevers, 2016). In classical two-dimensional (2D) cell culture, primary cells gradually undergo morphological changes and specific function loss within a short period, and eventually die (Xiang, et al., 2019). However, organoids have the property of stem cells that can be expanded stably over long periods (Zhu, et al., 2021). Unlike cell lines which are genetically modified and thus have transformed genotypes and phenotypes compared with primary cells (Grabinger, et al., 2014), the organoid culture maintains *in vivo* features of original donor even after many passages (Sato, et al., 2009). Furthermore, organoids contain all cells within an organ (Zhao, et al., 2022), and exhibit cell–cell and cell–extracellular matrix interactions that are essential for maintaining biological functions, and tissue specific cellular processes (Prior, et al., 2019; Harrison, et al., 2021). Thus, organoids can more closely

reflect normal physiology or disease pathogenesis in specific organs (Yoo & Donowitz, 2019). In this project, we will explore the hypothesized regulatory pathway (choline – miR-503 – LIPG – HDL-C) using a pig liver organoid system.

IV-3. Materials and Methods

IV-3.1. Liver Organoids Isolation and Culture

Culture medium and solution preparation:

Organoid Initiation Medium (OIM): 5 mL Organoid Growth Supplement (STEMCELL 100-0389, Vancouver, BC, Canada), 50 mL Organoid Supplement (STEMCELL 100-0389, Vancouver, BC, Canada), 44.8 mL Organoid Basal Medium (STEMCELL 100-0389, Vancouver, BC, Canada), 200 µL 5mM Y-27632 in water (STEMCELL 100-0389, Vancouver, BC, Canada), 100 µL Gentamicin antibiotics (Sigma-Aldrich G1397, St. Louis, MO, USA).

Organoid Growth Medium (OGM): 5 mL Organoid Growth Supplement, 95 mL Organoid Basal Medium, 100 µL Gentamicin antibiotics.

Solution A (Wash Solution): 700 µL fetal bovine serum (FBS) (Thermo Fisher A3160501, Waltham, MA, USA), 69.3 mL DMEM/F-12 with 15 mM HEPES (STEMCELL 36254, Vancouver, BC, Canada).

Solution B (Tissue Dissociation Cocktail): 62.5 mg Collagenase type IV (STEMCELL 07427, Vancouver, BC, Canada), 24.75 mL DMEM/F-12 with 15 mM HEPES, 250 µL DNase I (1 mg/mL) solution (STEMCELL 07900, Vancouver, BC, Canada).

Solution C (TrypLE + BSA): 10 mL TrypLE™ Express Enzyme, no phenol red (Thermo Fisher 12604039, Waltham, MA, USA), 400 µL of 25% BSA.

Solution D (AdvDMEM + DNase I): 25 mL Advanced DMEM/F-12 (Thermo Fisher 12634028, Waltham, MA, USA), 1 mL of 25% Bovine Serum Albumin (BSA) (Sigma-Aldrich

A8022, St. Louis, MO, USA), 150 μ L DNase I solution (1 mg/mL); 50 μ L of 5 mM Y-27632 (STEMCELL 72302, Vancouver, BC, Canada).

Solution E (DMEM/F-12 + BSA): 2 mL of 25% BSA, 100 μ L of 5 mM Y-27632, 47.9 mL DMEM/F-12 + 15mM HEPES.

Liver Organoids isolation protocol:

The neonatal pig was euthanized following American Veterinary Medical Association-approved exsanguination procedures under anesthesia. Liver tissue was harvested from the left lateral lobe for hepatic organoid isolation. Then, approximately 1 g of liver tissue was sectioned into 3-5 mm pieces within a petri dish using ice-cold PBS. The tissue pieces were transferred to a 50 mL falcon tube on ice via a 25 mL serological pipette, gently mixed by pipetting 5 times. After allowing the tissue pieces to settle, the supernatant was discarded, and a 10 mL of cold Solution A was added. The sample was vigorously pipetted 10 times using a 10 mL pipette, and after settling, the supernatant was removed.

Next, 5 mL of warm Solution B was added to the tissue, and the sample was pipetted vigorously 10 times before being incubated in a 37°C water bath for 15 minutes. Following incubation, the sample was removed from the water bath, vigorously pipetted to resuspend the tissue pieces, and allowed to settle. The supernatant was collected and transferred to a 50 mL tube on ice. This process of adding Solution B, incubating, pipetting, and collecting the supernatant was repeated 4 - 5 times until no tissue pieces remained.

Once the tissue digestion was completed, the supernatant was pooled and centrifuged at 290 x g for 5 minutes, and the supernatant was discarded. Subsequently, 10 mL of Solution C was added to the pellet, vigorously pipette the entire volume up and down 10 times and incubated in a 37°C water bath for 10 minutes. After further resuspension using a 10 mL pipette,

the sample was incubated for an additional 10 minutes. Following vigorously pipette the entire volume up and down 10 times, 10 mL of Solution D and 25-30 mL of cold Solution A were added to the tube to reach a total volume of 50 mL. Then the tube was centrifuged at 290 x g for 10 minutes, the supernatant was discarded, and 2 mL of cold Solution D was added to the pellet and resuspended. Subsequently, 8 mL of ammonium chloride (STEMCELL 07800, Vancouver, BC, Canada) was added to the tube, mixed by pipetting, and kept on ice for 5 minutes to lyse red blood cells. The tube was centrifuged at 290 x g for 10 minutes, the supernatant was discarded, and the pellet was resuspended in 15 mL of cold Solution A and transferred to a 15 mL tube. After centrifugation at 290 x g for 10 minutes and discarding the supernatant, 10 mL of Solution D was added to the pellet, and the tube was centrifuged again at 290 x g for 5 minutes. Finally, as much supernatant as possible was removed from the tube.

Three-dimensional (3D) organoids culture:

We prepared a gel-OIM mixture in a 1:1 ratio and thoroughly resuspended it with the organoids pellet. Subsequently, 50 μ L of the resulting organoid solution—comprising organoid, gel, and OIM—was dispensed into the center of each well within a 48-well plate to form gel domes. After a 10-minute incubation to solidify the gel domes, we cautiously added 280 μ L of OIM to each well, carefully directing it along the well's edges to avoid disturbing the gel domes. The plate underwent incubation at 37°C for 1-2 weeks, with regular OIM replacement every 3 days throughout the incubation period.

Passing for two-dimensional (2D) subculture:

A new 48-well plate was coated with a 2% gel solution before passing started, by adding 150 μ L to each well and allowing it to incubate for 1 hour. From the 3D organoid cultures, OIM medium was aspirated and discarded from all wells without disturbing the gel dome. Then 280

μL of Solution C was added to the center of each dome and forcefully mixed the content by pipetting 45 times, ensuring to avoid bubble formation. We then added 280 μL of Solution E to the wells and collected the contents into a 15 mL tube. Following this, we rinsed the wells with Solution E and transferred the rinse to the same 15 mL tube. The tube was then centrifuged at 290 x g for 5 minutes, and the resulting pellet was re-suspended in OGM, and kept it on ice. After the 48-well plates were coated with a 2% gel solution, we removed the 2% gel solution from the wells and added approximately 200 μL of organoid solution, containing roughly 50 organoids, to the sides of the wells, avoiding disturbance to the gel coating. Then the plate was incubated at 37°C, and the OGM was changed every 2-3 days.

IV-3.2. Urea Assay (Functional Validation of Liver Organoids)

Urea, a specific metabolic substance of hepatocytes, was utilized to validate the normal functionality of the isolated and cultured liver organoids. After completing the 2D culture of liver organoids (total 96 h), the culture media from control group was collected for urea assay. The assay was performed using QuantiChrom™ Urea Assay Kit (BioAssay Systems DIUR-100, Hayward, CA, USA). Following the kit instructions, 50 μL of fresh OGM medium (blank), 50 μL of 5 mg urea/dL diluted solution (standard), and 50 μL of OGM from 2D organoids culture were placed into separate wells. Then, to all of wells were added 200 μL of working reagent (provided in the kit) that was mixed equivalent amounts of the Reagent A and Reagent B (provided in the kit) right before conducting the assay. After 50 minutes of incubation at room temperature, the plate was read OD at 430 nm. Results were calculated based on user's manual.

IV-3.3. MiR-503 Mimic Transfection and Co-transfection with miR-503 Inhibitor

The miRNA mimics are chemically synthesized double-strand RNAs, which mimic the function of endogenous mature miRNAs. The miRNA inhibitors are the counterpart of their

paired miRNA mimics (Saliminejad, et al., 2019). They are chemically modified single-stranded RNA molecules designed to specifically bind to and inhibit their paired miRNA mimics and endogenous miRNA molecules. MiR-503 mimic (Thermofisher 4464066-ssc-miR-503, Waltham, MA, USA) and miR-503 inhibitor (Thermofisher 4464084-ssc-miR-503, Waltham, MA, USA) were mixed with transfection kit Lipofectamine 3000 (Thermofisher L3000015, Waltham, MA, USA) following manufacturer's instruction. At 48 h after 2D culture, different concentrations of miR-503 mimic and its inhibitor with Lipofectamine 3000 were added into culture medium for 7 treatment groups: 0 nM (control), 1 nM, 10 nM, and 100 nM of miR-503 mimic, 1 nM of miR-503 mimic + 1 nM of miR-503 inhibitor, 10 nM of miR-503 mimic + 10 nM of miR-503 inhibitor, and 100 nM of miR-503 mimic + 100 nM of miR-503 inhibitor. After 48 h of transfection (at time of 96 h after 2D culture), liver organoids or medium were collected for subsequent assays.

IV-3.4. MiR-503 Mimic Transfection Efficiency Assay - RT-qPCR

After 48 h of miR-503 mimic transfection, two wells of liver organoids were used for total RNA extraction. TRI Reagent (Sigma-Aldrich T9424, St. Louis, MO, USA) was used to lyse organoids, chloroform was used to separate RNA from other cellular components, isopropanol was used to precipitate RNA, and 70% ethanol was used to purify and clean RNA molecules. The miScript II RT Kit (Qiagen 218161, Hilden, Germany) was used for miRNA cDNA synthesis. Forward primer miR-503 (**TableIII-3.2**) was synthesized by Sigma-Aldrich (St. Louis, MO, USA), reverse primer was miScript Universal Primer from miScript II RT Kit. RT-qPCR was conducted using iQ™ SYBR® Green Supermix (Bio-Rad 1708886, Hercules, CA, USA) and CFX Connect Real-Time PCR Detection System (Bio-Rad 1855201, Hercules, CA, USA). U6 snRNA (**TableIII-3.2**) was used as the housekeeping gene to normalize miRNA

expression and relative gene expression was calculated using the $2^{-\Delta\Delta CT}$ method (Wang, et al., 2023).

IV-3.5. Organoids Viability and Cytotoxicity Assay

After 48 h of miR-503 transfection or miR-503 mimic co-transfection with miR-503 inhibitor, one well of liver organoids were collected for cytotoxicity and viability assay. Viability assay used the Trypan Blue (Thermofisher 15250061, Waltham, MA, USA) method to count live cells (unstained) and dead cells (blue) using a hemocytometer. Cytotoxicity assay was performed using Cytotoxicity Detection Kit^{PLUS} (LDH) (Sigma-Aldrich 4744926001, St. Louis, MO, USA). Briefly, medium and organoids were collected and centrifuged at 300g for 5 min. We transferred 50 μ L x 2 (to make duplicates) of supernatant to each well as sample blank. Adding 5 μ L lysis to all of rest sample to lysis cell and release lactate dehydrogenase (LDH) from live cell, vortex to mix and let sit for 5 min. Lysed samples were centrifuged at 300 x g for 5 min and transferred 50 μ L x2 (to make duplicates) of supernatant to each well as sample lysed. Prepare the reaction mixture by combining the catalyst and dye accordingly, and then add 50 μ L to all wells. Plate was incubated in 37°C water bath for 10 – 30 min until turned red. Adding 25 μ L stop solution to each well after reaction occurs and read plate under 490 nm spectrometer. The result was expressed as relative cytotoxicity to control group.

IV-3.6. LIPG mRNA Expression Level Analysis – RT-qPCR

After 48 h of miR-503 transfection or miR-503 mimic co-transfection with miR-503 inhibitor, two wells of liver organoids were collected for RT-qPCR assay. Total RNA extracted from organoids was used to synthesize cDNA by QuantiTect Reverse Transcription Kit (Qiagen 205313, Hilden, Germany). *LIPG* primers (**TableIII-3.2**) was created using Primer Designing Tool (<https://www.ncbi.nlm.nih.gov/tools/primer-blast/>), and synthesized by Sigma-Aldrich (St.

Louis, MO, USA). RT-qPCR was conducted using iQ™ SYBR® Green Supermix (Bio-Rad 1708886, Hercules, CA, USA) and CFX Connect Real-Time PCR Detection System (Bio-Rad 1855201, Hercules, CA, USA). *GAPDH* gene (TableII3.2) was used as the housekeeping gene to normalize mRNA expression and relative gene expression was calculated using the $2^{-\Delta\Delta CT}$ method.

IV-3.7. LIPG Protein Expression Analysis – Western Blot

After 48 h of miR-503 transfection or miR-503 mimic co-transfection with miR-503 inhibitor, two wells of liver organoids were used for western blot assay. Organoids were lysed by RIPA Lysis and the extraction buffer (Thermofisher 89901, Waltham, MA, USA), then the concentration of total protein of supernatant was measured using Pierce™ BCA Protein Assay Kits (Thermofisher 23225, Waltham, MA, USA). Calculated amount of sample containing 10 µg of total protein was mixed with 4x Laemmli Sample Buffer (Bio-Rad 1610747, Hercules, CA, USA) plus 50 mM DTT, and heated at 70°C for 10 min. Then samples were loaded into 10% Criterion™ TGX Stain-Free™ Protein Gel (Bio-Rad 5678033, Hercules, CA, USA) and electrophoresed using a Criterion Cell Electrophoresis tank (Bio-Rad 135BR, Hercules, CA, USA) and PowerPac™ HC Power Supply (Bio-Rad 043BR, Hercules, CA, USA) at 150 volts. The running buffer was Tris/Glycine/SDS premixed electrophoresis buffer (Bio-Rad 1610732, Hercules, CA, USA). After gel running, proteins were transferred to nitrocellulose membranes (Bio-Rad 1620112, Hercules, CA, USA) by making a transfer “sandwich” consisting of sponge + filter paper + membrane + gel + filter paper + sponge. The transferring process used Tris/Glycine Buffer (Bio-Rad 1610734, Hercules, CA, USA) and was conducted in a Criterion™ Blotter tank (Bio-Rad 560BR, Hercules, CA, USA) under 400 mA for 1 h.

The membrane was first blocked with 5% non-fat milk in Tris-Buffered Saline (TBS)

buffer (14 mM NaCl, 20 mM Tris, pH 7.6) for 1 h at room temperature. Then it was incubated in 1 $\mu\text{g}/\text{mL}$ of LIPG primary antibody (Fisher Scientific NB018567, Waltham, MA, USA) and 1 $\mu\text{g}/\text{mL}$ of housekeeping protein β -Actin (BMP-2) antibody (Fisher Scientific NB600503SS, Waltham, MA, USA) overnight under 4°C. After washing 4 times for 10 min each with TBST (TBS + 0.1% Tween 20), the membrane was incubated in 0.15 $\mu\text{g}/\text{mL}$ of Anti-rabbit biotinylated antibody (Fisher Scientific NC1590886, Waltham, MA, USA) for 1 h in room temperature. Then the membrane was washed 4 times for 10 min each with TBST and incubated in VECTASTAIN ABC-HRP Reagent (Fisher Scientific NC9206402, Waltham, MA, USA): 5 μL of A + 5 μL of B + 500 μL of TBST for 30 min. After 10 min x 4 times washing, the membrane was incubated in ECL substrate (Bio-Rad 1705062, Hercules, CA, USA) for 5 min and the chemiluminescence was detected using a ChemiDoc Imaging System (Bio-Rad 12003153, Hercules, CA, USA). The LIPG and β -Actin bands intensities were measured using ImageJ 1.48V software (NIH, Bethesda, Maryland, USA). Relative LIPG protein expression was normalized using β -Actin.

IV-3.8. HDL Measurement

After 48 h of miR-503 mimic and its inhibitor transfection, organoids culture medium was collected for HDL measurement using EnzyChrom™ AF HDL and LDL/VLDL Assay Kit (BioAssay Systems E2HL-100 Hayward, CA, USA). We vortex-mixed 20 μL sample and 20 μL Precipitation Reagent (provided in the kit) in tube and centrifuged them for 5 minutes at 9500 x g. Then 24 μL supernatant was transferred into new tube/PCR strip and added 96 μL Assay Buffer to tube. Prepare Cholesterol Standard by adding 5 μL 300 mg/mL cholesterol to 145 μL Assay Buffer. Prepare 10x dilution by adding 10 μL of Cholesterol Standard just prepared to 90 μL Assay Buffer. Next, we transferred 50 μL of medium samples to black 96-well plate, 50 μL of diluted Cholesterol Standard and 50 μL of Assay buffer as “blank”. For each well, we

prepared Working Reagent: 55 μ L Assay Buffer + 1 μ L Enzyme + 1 μ L Dye and 50 μ L of Working Reagent was added to wells. After 30 minutes incubation at room temperature, fluorescence was read at 530nm and 585nm. The HDL content was calculated based on user's manual and normalized according to protein concentration.

IV-3.9. Choline Treatment

When transitioning to 2D culture, the culture medium was supplemented with various concentrations of choline across 6 treatment groups: 0 nM (control), 0.001 mM, 0.01 mM, 0.1 mM, 1 mM, and 10 mM of choline chloride (Sigma-Aldrich C7527, St. Louis, MO, USA). After 48 h of choline exposure (at time of 96 h after 2D culture), liver organoids were collected for choline assay, *LIPG* qPCR analysis, and miR-503 qPCR analysis.

IV-3.9. Choline Measurement in Liver Organoids

Choline content in liver organoids after a 96-h treatment was measured using Amplitude[®] Choline Quantitation Kit (AAT Bioquest 40007, Sunnyvale, CA, USA). Liver organoids were collected by gently scraping them using a cell scraper following a rinse with PBS. After collection, the organoids underwent three freeze-thaw cycles to facilitate the release of choline from within the cells. Subsequently, we quantified the choline content according to the instructions provided in the kit manual, and the calculations were based on the protein concentration of the samples.

IV-3.10. Statistical Analysis

All data were analyzed using General Linear Models (GLM) model in SAS software 9.4 (Cary, NC USA). The analyses were conducted following a randomized block design and *p*-values < 0.05 were considered statistically significant.

IV-4. Results

IV-4.1. Liver Organoid Urea Assay

Urea assay was conducted to validate the metabolic function of liver organoids. At 48 h after transfection, urea was detected in culture medium with the concentration of 107 $\mu\text{g/g}$ total protein, which equal to 26.7 $\mu\text{g/g}$ total protein per 24 h, indicating the isolated and cultured liver organoid had expected metabolic activity and function of hepatocytes due to their unique role in urea production.

IV-4.2. MiR-503 Transfection Efficiency Assay

Transfection efficiency assay was conducted after 48 h of miR-503 mimic transfection ($n = 5$). As the results from RT-qPCR assay showed in **Figure IV-4.2**, the transfection efficiency of liver organoids at 1 nM of miR-503 mimic was numerally 1.43-folds of the control, but no significant difference was detected ($p = 0.7612$). When increasing the miR-503 mimic concentration to 10 nM, the miR-503 expression increased 5.78 -fold in the transfected organoids as compared to the control ($p < 0.05$). Further increased to 100 nM elevated miR-503 expression to 11.85-fold ($p < 0.05$). The kinetic assay showed that miR-503 level inside the cell is positively related to transfected concentration of miR-503 mimic in the culture media ($p < .0001$, $R^2 = 0.5632$).

IV-4.3. Cytotoxicity and Cell Viability Assay

Cytotoxicity assay of liver organoids was performed after 48 h of transfection ($n = 5$). No significant differences were obtained across all groups ($p > 0.05$). The relative cytotoxicity (compared to control group) ranged from 0.039% for 1 nM of miR-503 mimic group to 1.64% for the 10 nM of miR-503 mimic + its inhibitor group (**Figure IV-4.3-1**).

Cell viability assay was also conducted after 48 h of transfection ($n = 5$). No significant difference was detected for the cell viability among all groups ($p > 0.05$). The average cell

viability was 95.50% (**Figure IV-4.3-2**).

IV-4.4. LIPG mRNA Expression Level Analysis – RT-qPCR

After 48 h of transfection, *LIPG* gene expression was determined for all groups ($n = 5$). In 1, 10, and 100 nM miR-503 mimic transfection groups, the relative *LIPG* expression was decreased to 76% ($p < 0.05$), 46% ($p < 0.05$), and 68% ($p < 0.05$), respectively, compared to control group (**Figure IV-4.4**). The kinetic assay showed that relative *LIPG* expression and transfected concentration of miR-503 mimic fit a quadratic regression ($p < 0.001$, $R^2 = 0.63$). No significant difference was observed between all miR-503 mimic co-transfected with miR-503 inhibitor groups and the control group ($p > 0.05$).

IV-4.5. LIPG Protein Expression Analysis – Western Blot

After 48 h of transfection, LIPG protein expression was determined for all groups ($n = 5$). In 1 nM of miR-503 mimic transfection group, the relative LIPG protein expression was 84% of control group ($p = 0.066$). In 10 nM group, the relative LIPG expression was decreased to 24% ($p < 0.001$) compared to control group. However, in 100 nM group, the relative LIPG expression level was 89% of control group ($p > 0.05$) (**Figure-IV-4.5**). The kinetic assay showed that relative LIPG protein level and transfected concentration of miR-503 mimic fit a quadratic regression ($p < 0.001$, $R^2 = 0.93$). No significant difference was detected between all miR-503 mimic co-transfected with miR-503 inhibitor groups and control group ($p > 0.05$).

IV-4.6. HDL Measurement

After 48 h of transfection, HDL content in culture medium was analyzed for all groups ($n = 5$). In the control group, the detected HDL content was 7.61 $\mu\text{g}/\text{mg}$ total protein (**Figure IV-4.6**). In 1, 10, and 100 nM miR-503 mimic transfection groups, HDL content increased to 9.24 ($p < 0.05$), 9.46 ($p < 0.05$), and 9.26 $\mu\text{g}/\text{mg}$ total protein ($p < 0.05$), respectively. The kinetic assay

showed that HDL content tends to fit a quadratic regression with transfected concentration of miR-503 mimic ($p = 0.056$, $R^2 = 0.29$), but also fit a linear regression with relative *LIPG* gene expression ($p < 0.05$, $R^2 = 0.55$). No significant difference was obtained between all miR-503 mimic co-transfected with miR-503 inhibitor groups and control group ($p > 0.05$).

IV-4.7. Choline Measurement in Liver Organoids

After 96 h of choline treatment, the choline content in control of liver organoids was 1.48 $\mu\text{mol/g}$ total protein. In 0.001, 0.01, and 0.1 mM of choline treatment group, the choline content was 1.56, 1.57, and 1.92 $\mu\text{mol/g}$ total protein, respectively, and no significant difference was observed between these groups and control group ($p > 0.05$). In 1 nM, and 10 nM of choline treatment groups, the choline content was increased to 3.59 ($p < 0.05$) and 9.66 ($p < 0.05$) $\mu\text{mol/g}$ total protein, respectively (**Figure II-4.7**). The kinetic assay showed that choline content inside the cell is positive related to the concentration of choline in culture media ($p < 0.001$, $R^2 = 0.99$).

IV-4.8. LIPG and miR-503 Expression Level Analysis

No significant differences were detected in the gene expressions of *LIPG* and miR-503 in liver organoids treated with varying concentrations of choline after 96 h ($p > 0.05$), as listed in **Figure IV-4.8-1** and **-2**.

IV-5. Discussion

Organoid cultures have emerged as an alternative *in vitro* model for reproducing tissue structures within a controlled environment (Prior, et al., 2019). Although liver organoid models have been successfully established for mice, rats, and humans (Iqbal, et al., 2023), there is currently no documentation of well-established pig liver organoids in the literatures. In our investigation, we successfully isolated and cultivated liver organoids from the livers of newborn

pigs in a three-dimensional (3D) culture (**Figure IV-5-1**). These organoids progressed to form spheroid structures, consistent with the observations reported by Broutier *et al.* (2016). By day 4-6 of post-seeding, the organoids reached a state of maturation. Despite their inability to be propagated through generations, they were prepared for transition to a 2D culture. We confirmed the normal functionality of pig liver organoids by assessing the specific metabolic product of hepatocytes - urea. The measured urea production in culture medium with our isolated organoid was 26.7 $\mu\text{g/g}$ total protein per 24 h, falling within the range of 9 to 90 $\mu\text{g/g}$ total protein per 24 h, as reported in sheep liver organoids by Saheli *et al.* (2018). Although 2D organoid culture sacrifices spatial structure, it preserves essential cell-cell interactions. Given the limitations in passage to the next generation, 2D continues to be a favorable option, while the 3D structure may hinder the access of drugs or infections to the inner regions of the organoids (Wilson, et al., 2017). In the future, we will make further efforts to enhance and optimize the pig liver organoid model and methodology.

In this investigation, we conducted a series of transfections in the liver organoids isolated from neonatal piglets with various concentrations of miR-503 mimic and its inhibitor. The results from these studies demonstrated that miR-503, indeed, has a regulatory role in modulating *LIPG* gene and protein expression. Furthermore, the results from kinetic assay revealed quadratic regression relationships between both relative *LIPG* gene and protein expression and the transfected concentration of miR-503 mimic. From this observed pattern, we suggest that the potential feedback regulatory mechanisms could be dominant in the miR-503 – *LIPG* regulation. Moreover, miR-503 was reported to have a key role in various cellular processes for over 10 years, in which miR-503 involved in many critical functions including apoptosis, cell proliferation, migration, angiogenesis (Zhou, et al., 2013; He, et al., 2021), and several human

diseases such as lung cancer, pulmonary hypertension (Yang, et al., 2014; Kim, et al., 2013; Kaur, et al., 2022). However, the role of miR-503 in regulating LIPG expression has not been reported. This finding provides further evidence of the critical role of miR-503 as a regulator in the liver.

LIPG is of particular interest recently, as it is a primary determinant of HDL levels through hydrolysis and breakdown processes (Yu, et al., 2018). In our study, HDL content exhibited a negative correlation with relative *LIPG* gene expression ($p < 0.05$, $R^2 = 0.55$). This finding is consistent with observations from other studies (Ishida, et al., 2003; Tora, et al., 2020). At 1 nM of miR-503 mimic transfection, LIPG protein levels decreased to 84% of control group, while HDL increased to 121.4% of control group. In contrast, at 10 nM of miR-503 mimic, LIPG decreased to 24% of control group, while HDL increased to 124.4% of control group. Comparing the reduction in LIPG protein from 84% to 24% (60% difference), the increase in HDL from 121.4% to 124.4% (3% difference) is relatively small. These findings not only confirm the role of LIPG in HDL regulation but also suggest the potential involvement of other regulatory mechanisms. For instance, hepatic lipases may play a role in HDL regulation (Annema & Tietge, 2011).

Next, we conducted an experiment to manipulate choline concentrations in the culture medium, aiming to observe potential alterations in miR-503 expression and its target gene, *LIPG*. Initially, to validate the modifications in choline content within the organoids, we performed a choline measurement assay, which indeed confirmed an increased choline content within the cells. However, despite this observed increase, our subsequent qPCR analysis did not show any significant changes in miR-503 or *LIPG* levels. This lack of regulatory effect of choline on miR-503 expression could potentially be attributed to the presence of other one-carbon sources in the

culture medium, offering alternative methyl groups for gene methylation. The culture medium used in our experiments encompasses various one-carbon sources, including folate, choline, methionine, serine, and glycine (Huch, et al., 2015). It's conceivable that when the DNA methylation process becomes saturated with these one-carbon sources, artificially increasing choline concentration might not elicit further changes in DNA methylation, explaining our observed lack of alteration in miR-503 expression levels.

Returning to the goal of our thesis, the development of ASCVD is attributed to the accumulation of cholesterol plaque on the inner lining of blood vessels (Madsen, et al., 2017). However, HDL can transport excess cholesterol build-up in arterial walls and reduce the risk of ASCVD (Ouimet, et al., 2019). By modulating HDL levels through the downregulation of LIPG using miR-503 mimic, there is a potential to reduce the risk of atherosclerotic cardiovascular diseases. Due to their regulatory role on mRNA with high degrees of specificity, efficacy, and accuracy, miRNAs are being considered as practical therapeutic options (Naghizadeh, et al., 2020). To achieve effective therapeutic goals, miRNA mimics (synthesized double stranded RNAs) or anti-miRNAs have been developed in recent years (Petrovic & Ergun, 2018).

Currently, therapeutic approaches to cancer to replenish tumor suppressive miRNAs (by miRNA mimics) or to suppress oncomiRs (by anti-miRs) are in the preclinical progress (Shah, et al., 2016). For example, miR-34 mimics are currently being tested in a phase I clinical trial (NCT01829971) in several types of cancer. MiR-34 mimics, encapsulated in lipid nanoparticles, showed significant inhibition of tumor growth in mouse models of liver, prostate, and lung cancer without severe adverse effects (Rupaimoole & Slack, 2017). Another example is anti-miRs targeted at miR-122, which underwent phase II trials for treating hepatitis C virus (HCV). In contrast to the widely accepted mechanism of mRNA silencing due to miRNA binding,

miR-122 plays an important role in the replication and stability of HCV (Jopling, et al., 2005). Inhibition of miR-122 using antimiR-122 resulted in a significant reduction in infection load and reduced liver damage in mouse models of HCV infection (Elmén, et al., 2008). Clinical results indicated the beneficial effect of antimiR-122 toward HCV, moreover the clinically manageable severity suggesting that the treatment is safe. Despite the considerable number of preclinical studies conducted over the years in the field of miRNA therapeutics, only a limited number of them have progressed to clinical development. One of the biggest challenges in developing miRNA-based therapeutics is to identify the best miRNA candidates or miRNA targets for each disease type. Based on our findings, we suggest that miR-503 could be a candidate for further investigation in comprehending HDL regulation.

IV-6. References

- Ameres, S. L. & Zamore, P. D., 2013. Diversifying microRNA sequence and function. *Nature reviews. Molecular cell biology*, 14(8), p. 475–488.
- Annema, W. & Tietge, U., 2011. Role of hepatic lipase and endothelial lipase in high-density lipoprotein-mediated reverse cholesterol transport. *Curr. Atheroscler. Rep*, Volume 13, p. 257–265.
- Bartel, D. P., 2018. Metazoan MicroRNAs. *Cell*, pp. 173(1), 20–51.
- Bell, A. & Felsenfeld, G., 2000. Methylation of a CTCF-dependent boundary controls imprinted expression of the *Igf2* gene. *Nature*, Volume 405, p. 482–485.
- Broutier, L. et al., 2016. Culture and establishment of self-renewing human and mouse adult liver and pancreas 3D organoids and their genetic manipulation. *Nature protocols*, 11(9), p. 1724–1743.
- Caporali, A. et al., 2011. Deregulation of microRNA-503 contributes to diabetes mellitus–induced impairment of endothelial function and reparative angiogenesis after limb ischemia. *Circulation*, 123(3), p. 282–291.
- Chang, Y. et al

., 2019. Extracellular microRNA-92a mediates endothelial cell-macrophage communication. *Arterio. Thromb. Vasc. Biol*, Volume 39, p. 2492–2504.
- Choi, S. et al., 2002. Endothelial lipase: a new lipase on the block. *J. Lipid Res*, Volume 43, p. 1763–1769.
- Choy, M. et al., 2010. Genome-wide conserved consensus transcription factor binding motifs are hyper-methylated. *BMC genomics*, Volume 11, p. 519.

Claycombe, K. et al., 2013. Prenatal low-protein and postnatal high-fat diets induce rapid adipose tissue growth by inducing Igf2 expression in Sprague Dawley rat offspring. *J. Nutr*, Volume 143, p. 1533–1539.

Cole, J. et al., 2021. Atherosclerotic cardiovascular disease in hyperalphalipoproteinemia due to LIPG variants. *J Clin Lipidol*, 15(1), pp. 142-150.e2.

Cooney, C., Dave, A. & Wolff, G., 2002. Maternal methyl supplements in mice affect epigenetic variation and DNA methylation of offspring. *The Journal of nutrition*, 132(8 Suppl), p. 2393S–2400S.

Craciunescu, C. et al., 2003. Choline availability during embryonic development alters progenitor cell mitosis in developing mouse hippocampus. *The Journal of nutrition*, 133(11), p. 3614–3618.

Elmén, J. et al., 2008. LNA-mediated microRNA silencing in non-human primat. *Nature*, 452(7189), p. 896–899.

Feinberg, A., 2018. The key role of epigenetics in human disease prevention and mitigation. *N. Engl. J. Med*, Volume 378, p. 1323–1334.

Grabinger, T. et al., 2014. Ex vivo culture of intestinal crypt organoids as a model system for assessing cell death induction in intestinal epithelial cells and enteropathy. *Cell death & disease*, 5(5), p. e1228.

Harrison, S. et al., 2021. Liver Organoids: Recent Developments, Limitations and Potential. *Frontiers in medicine*, Volume 8, p. 574047.

He, Y. et al., 2021. The Causes and Consequences of miR-503 Dysregulation and Its Impact on Cardiovascular Disease and Cancer. *Front Pharmacol.*, Volume 12, p. 629611.

He, Y. et al., 2022. MicroRNA-503 Exacerbates Myocardial Ischemia/Reperfusion Injury via

Inhibiting PI3K/Akt- and STAT3-Dependent Prosurvival Signaling Pathways. *Oxid Med Cell Longev*, Volume 2022, p. 3449739.

Hirakawa, T. et al., 2016. miR-503, a microRNA epigenetically repressed in endometriosis, induces apoptosis and cell-cycle arrest and inhibits cell proliferation, angiogenesis and contractility of human ovarian endometriotic stromal cells. *Human reproduction (Oxford, England)*, 31(11), p. 2587–2597.

Hirata, K. et al., 1999. Cloning of a unique lipase from endothelial cells extends the lipase gene family. *J Biol Chem*, Volume 274, p. 14170–14175.

Huch, M. et al., 2015. Long-term culture of genome-stable bipotent stem cells from adult human liver. *Cell*, 160(1-2), p. 299–312.

Iqbal, W., Wang, Y., Sun, P. & Zhou, X., 2023. Modeling Liver Development and Disease in a Dish. *Int J Mol Sci*, 24(21), p. 15921.

Ishida, T. et al., 2003. Endothelial lipase is a major determinant of HDL level. *The Journal of clinical investigation*, 111(3), p. 347–355.

Jaye, M. et al., 1999. A novel endothelial-derived lipase that modulates HDL metabolism. *Nat Genet*, Volume 21, p. 424–428.

Johns Hopkins Medicine, 2024. *Coronary Heart Disease* (<https://www.hopkinsmedicine.org/health/conditions-and-diseases/coronary-heart-disease>), Baltimore: The Johns Hopkins University.

Jones, P., 2012. Functions of DNA methylation: islands, start sites, gene bodies and beyond. *Nature reviews. Genetics*, 13(7), p. 484–492..

Jopling, C. et al., 2005. Modulation of hepatitis C virus RNA abundance by a liver-specific microRNA. *Science*, Volume 309, p. 1577–1581.

Kaur, P., Kotru, S., Singh, S. & Munshi, A., 2022. Role of miRNAs in diabetic neuropathy: mechanisms and possible interventions. *Mol Neurobiol.* , 59(3), pp. 1836-1849.

Kim, J. et al., 2013. An endothelial apelin-FGF link mediated by miR-424 and miR-503 is disrupted in pulmonary arterial hypertension. *Nature Medicine*, 19(1), p. 74–82.

Kok, D. et al., 2015. The effects of long-term daily folic acid and vitamin b12 supplementation on genome-wide DNA methylation in elderly subjects. *Clin. Epigenetics*, Volume 7, p. 121.

Kovacheva, V. et al., 2007. Gestational choline deficiency causes global and Igf2 gene DNA hypermethylation by up-regulation of Dnmt1 expression. *J. Biol. Chem*, Volume 282, p. 31777–31788.

Kretzschmar, K. & Clevers, H., 2016. Organoids: Modeling Development and the Stem Cell Niche in a Dish. *Dev Cell*, 38(6), pp. 590-600.

Lee, Y. et al., 2004. MicroRNA genes are transcribed by RNA polymerase II. *The EMBO journal*, pp. 23(20), 4051–4060.

Levinson, S. & Wagner, S., 2015. Implications of reverse cholesterol transport: recent studies. *Clin Chim Acta*, Volume 439, pp. 154-61.

Liu, Y. et al., 2020. Exosome-mediated miR-106a-3p derived from ox-LDL exposed macrophages accelerated cell proliferation and repressed cell apoptosis of human vascular smooth muscle cells. *Eur. Rev. Med Pharm. Sci*, Volume 24, p. 7039–7050.

Macfarlane, L. & Murphy, P., 2010. MicroRNA: Biogenesis, Function and Role in Cancer. *Current genomics*, 11(7), p. 537–561.

Madsen, C., Varbo, A. & Nordestgaard, B., 2017. Extreme high high-density lipoprotein cholesterol is paradoxically associated with high mortality in men and women: two prospective cohort studies. *Eur Heart J*, Volume 38, p. 2478–2486.

Morita, S. & Ikeda, Y., 2022. Regulation of membrane phospholipid biosynthesis in mammalian cells. *Biochem Pharmacol*, Volume 206, p. 115296.

Naghizadeh, S. et al., 2020. The role of miR-34 in cancer drug resistance. *Journal of cellular physiology*, 235(10), p. 6424–6440.

Niculescu, M., Craciunescu, C. & Zeisel, S., 2006. Dietary choline deficiency alters global and gene-specific DNA methylation in the developing hippocampus of mouse fetal brains. *FASEB J*, 20(1), pp. 43-9.

Ouimet, M., Barrett, T. & Fisher, E., 2019. HDL and Reverse Cholesterol Transport: Basic Mechanisms and their Roles in Vascular Health and Disease. *Circ Res*, p. 124(10): 1505–1518.

Petrovic, N. & Ergun, S., 2018. MiRNAs as potential treatment targets and treatment options in cancer. *Molecular Diagnosis & Therapy*, 22(2), p. 157–168.

Prior, N., Inacio, P. & Huch, M., 2019. Liver organoids: from basic research to therapeutic applications. *Gut*, Volume 68, p. 2228–37.

Prior, N., Inacio, P. & Huch, M., 2019. Liver organoids: from basic research to therapeutic applications. *Gut*, 68(12), pp. 2228-2237.

Rubattu, S. et al., 2017. Reduced brain UCP2 expression mediated by microRNA-503 contributes to increased stroke susceptibility in the high-salt fed stroke-prone spontaneously hypertensive rat. *Cell Death Dis*, 8(6), p. e2891.

Rupaimoole, R. & Slack, F., 2017. MicroRNA therapeutics: towards a new era for the management of cancer and other diseases. *Nat Rev Drug Discov*, 16(3), pp. 203-222.

Saheli, M. et al., 2018. Three-dimensional liver-derived extracellular matrix hydrogel promotes liver organoids function. *Journal of cellular biochemistry*, 119(6), p. 4320–4333.

Saliminejad, K., Khorram Khorshid, H., Soleymani Fard, S. & Ghaffari, S., 2019. An overview

of microRNAs: Biology, functions, therapeutics, and analysis methods. *Journal of cellular physiology*, 234(5), p. 5451–5465.

Sato, T. et al., 2009. Single Lgr5 stem cells build crypt-villus structures in vitro without a mesenchymal niche. *Nature*, 459(7244), p. 262–265.

Shah, M. et al., 2016. microRNA Therapeutics in Cancer - An Emerging Concept. *EBioMedicine*, Volume 12, p. 34–42.

Shi, Y. et al., 2022. Epigenetic regulation in cardiovascular disease: mechanisms and advances in clinical trials. *Signal Transduct Target Ther*, 7(1), p. 200.

Tora, G. et al., 2020. Identification of Reversible Small Molecule Inhibitors of Endothelial Lipase (EL) That Demonstrate HDL-C Increase In Vivo. *Journal of medicinal chemistry*, 63(4), p. 1660–1670.

Tost, J., 2010. DNA methylation: an introduction to the biology and the disease-associated changes of a promising biomarker. *Molecular biotechnology*, 44(1), p. 71–81.

Vitali, C., Khetarpal, S. & Rader, D., 2017. HDL Cholesterol Metabolism and the Risk of CHD: New Insights from Human Genetics. *Curr Cardiol Rep*, Volume 19, p. 132.

Vymetalkova, V. et al., 2019. DNA methylation and chromatin modifiers in colorectal cancer. *Molecular aspects of medicine*, Volume 69, p. 73–92.

Wen, Y. et al., 2018. MiR-503 suppresses hypoxia-induced proliferation, migration and angiogenesis of endothelial progenitor cells by targeting Apelin. *Peptides*, Volume 105, p. 58–65.

Westerman, K. et al., 2019. DNA methylation modules associate with incident cardiovascular disease and cumulative risk factor exposure. *Clinical epigenetics*, 11(1), p. 142.

Wilson, S. et al., 2017. Alpha-defensin-dependent enhancement of enteric viral infection. *PLoS*

Pathog, Volume 13, p. e1006446.

Wolff, G., Kodell, R., Moore, S. & Cooney, C., 1998. Maternal epigenetics and methyl supplements affect agouti gene expression in A(vy)/a mice. *FASEB J*, Volume 12, p. 949–57.

World Health Organization, 2021. *Cardiovascular diseases (CVDs): Fact sheet*, s.l.:

[https://www.who.int/news-room/fact-sheets/detail/cardiovascular-diseases-\(cvds\)](https://www.who.int/news-room/fact-sheets/detail/cardiovascular-diseases-(cvds)).

Wu, J. et al., 2018. miR-503 suppresses the proliferation and metastasis of esophageal squamous cell carcinoma by triggering autophagy via PKA/mTOR signaling. *Int J Oncol.*, 52(5), pp. 1427-1442.

Xiang, C. et al., 2019. Long-term functional maintenance of primary human hepatocytes in vitro. *Science (New York, N.Y.)*, 364(6438), p. 399–402.

Xing, X. et al., 2020. Adipose-derived mesenchymal stem cells-derived exosome-mediated microRNA-342-5p protects endothelial cells against atherosclerosis. *Aging*, 12(4), p. 3880–3898.

Yang, Y. et al., 2014. MiR-503 targets PI3K p85 and IKK- β and suppresses progression of non-small cell lung cancer. *Int. J. Cancer*, Volume 135, pp. 1531-1542.

Yoo, J. & Donowitz, M., 2019. Intestinal enteroids/organoids: A novel platform for drug discovery in inflammatory bowel diseases. *World J Gastroenterol*, 25(30), pp. 4125-4147.

Yu, J., Han, S., Wolfson, B. & Zhou, Q., 2018. The role of endothelial lipase in lipid metabolism, inflammation, and cancer. *Histol Histopathol*, 33(1), pp. 1-10.

Zeisel, S., 2017. Choline, Other Methyl-Donors and Epigenetics. *Nutrients*, 9(5), p. 445.

Zhao, Z. et al., 2022. Organoids. *Nature reviews. Methods primers*, Volume 2, p. 94.

Zhou, B. et al., 2013. MicroRNA-503 targets FGF2 and VEGFA and inhibits tumor angiogenesis and growth. *Cancer Letters*, 333(2), p. 159–169.

Zhou, Y. et al., 2016. MicroRNA-503 promotes angiotensin II-induced cardiac fibrosis by

targeting Apelin-13. *Journal of cellular and molecular medicine*, 20(3), pp. 495-505.

Zhu, S., Goldschmidt-Clermont, P. & Dong, C., 2005. Inactivation of monocarboxylate transporter MCT3 by DNA methylation in atherosclerosis. *Circulation*, Volume 112, p. 1353–1361.

Zhu, X., Zhang, B., He, Y. & Bao, J., 2021. Liver Organoids: Formation Strategies and Biomedical Applications. *Tissue engineering and regenerative medicine*, 18(4), p. 573–585.

CHAPTER III FIGURES

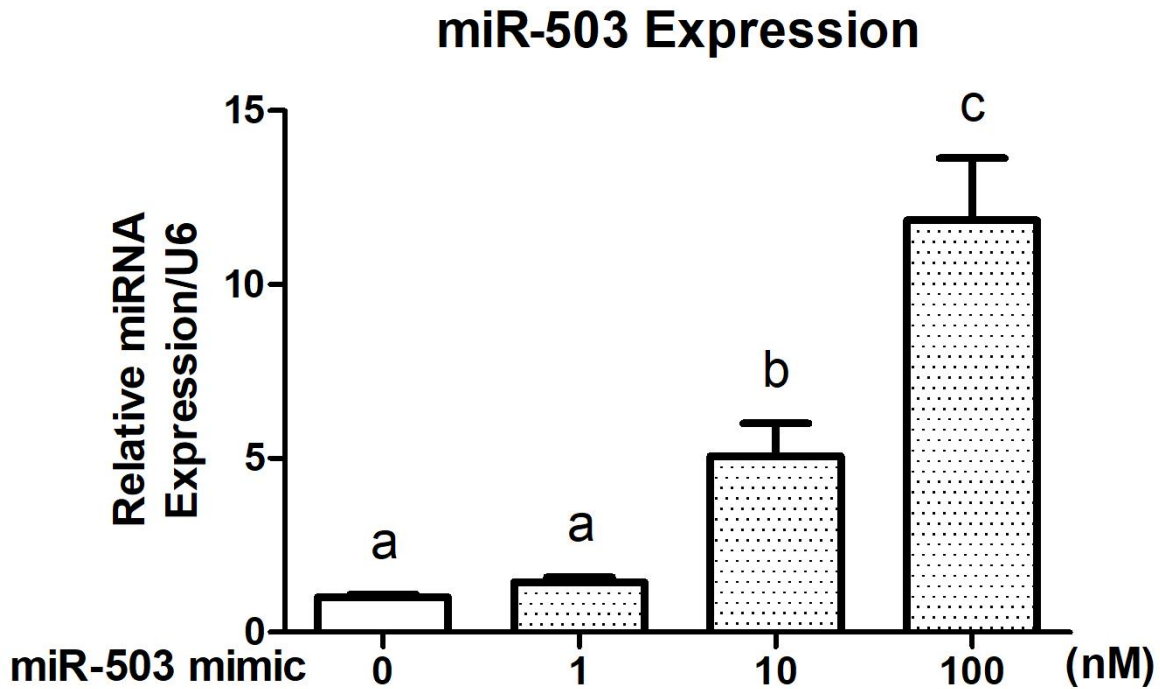


Figure IV-4.2 Transfection efficiency of liver organoids after 48 h of transfection ($n = 5$). RT-qPCR results showed the miR-503 expression level of liver organoids after 48 h of miR-503 mimic transfection at different concentrations. Different letters indicate significant differences (lsmeans \pm SEM; $p < 0.05$).

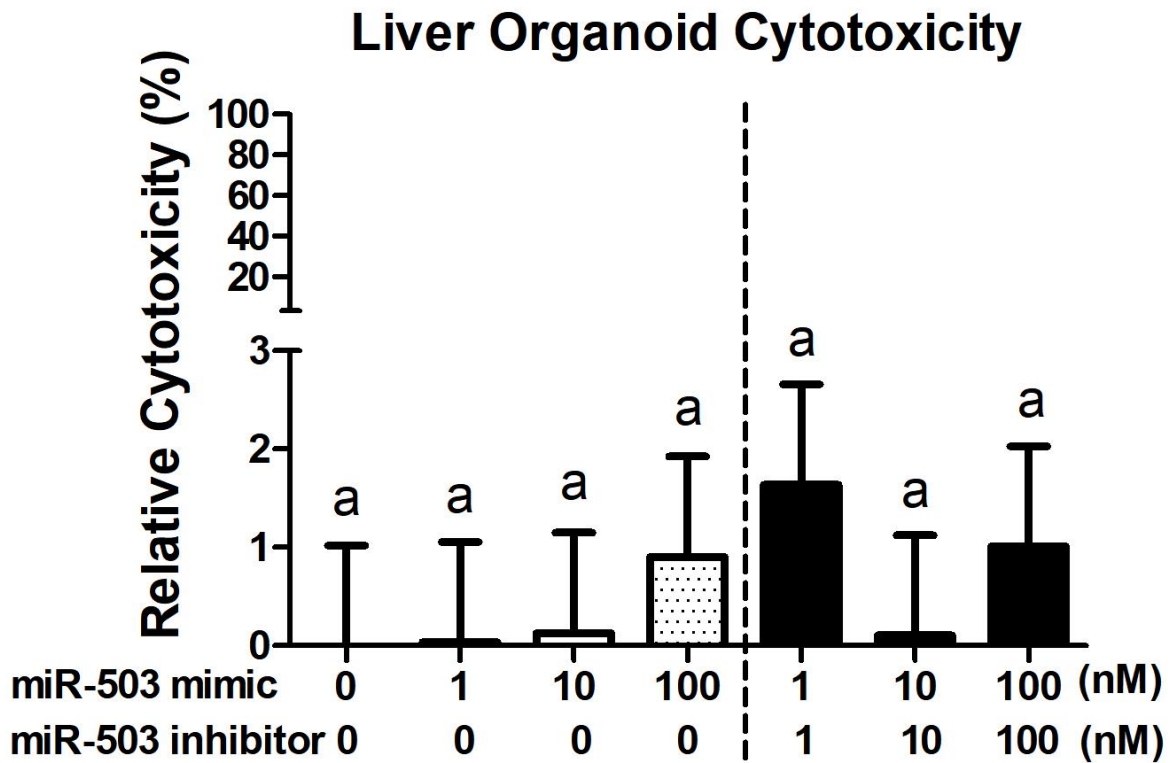


Figure IV-4.3-1 Cytotoxicity assay of liver organoids after 48 h of transfection ($n = 5$). This figure showed the cytotoxicity of liver organoids after 48 h of miR-503 transfection or miR-503 mimic co-transfection with miR-503 inhibitor. Same letters indicate no significant differences (lsmeans \pm SEM; $p < 0.05$).

Liver Organoids Viability

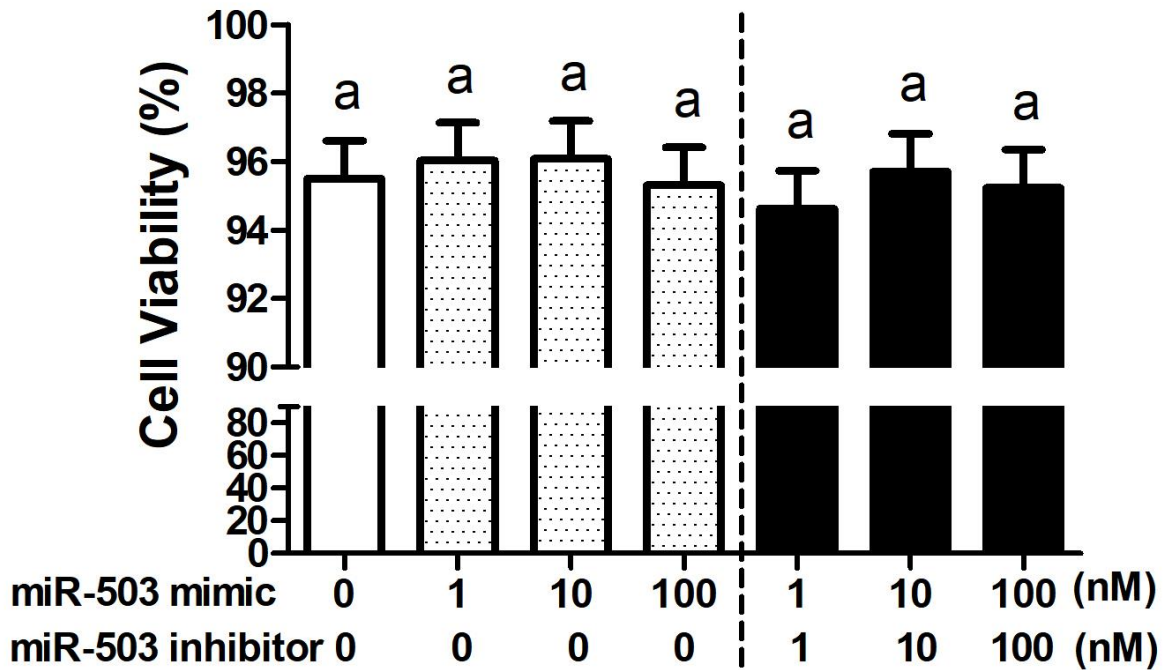


Figure IV-4.3-2 Cell viability assay of liver organoids after 48 h of transfection ($n = 5$). This figure showed the viability of liver organoids after 48 h of miR-503 transfection or miR-503 mimic co-transfection with miR-503 inhibitor. Same letters indicate no significant differences (lsmeans \pm SEM; $p < 0.05$).

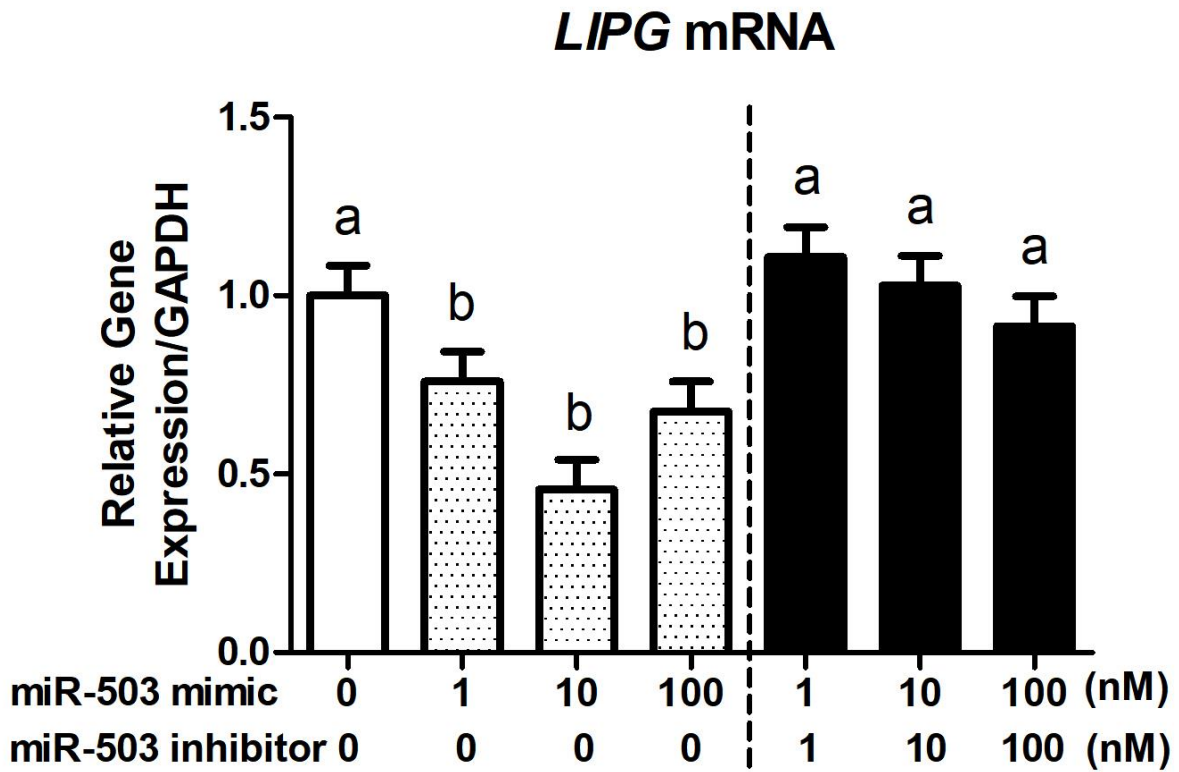


Figure IV-4.4 LIPG gene expression assay of liver organoids after 48 h of transfection ($n = 5$). RT-qPCR results showed the relative *LIPG* gene expression after 48 h of miR-503 transfection or miR-503 mimic co-transfection with miR-503 inhibitor. Different letters indicate significant differences (lsmeans \pm SEM; $p < 0.05$)

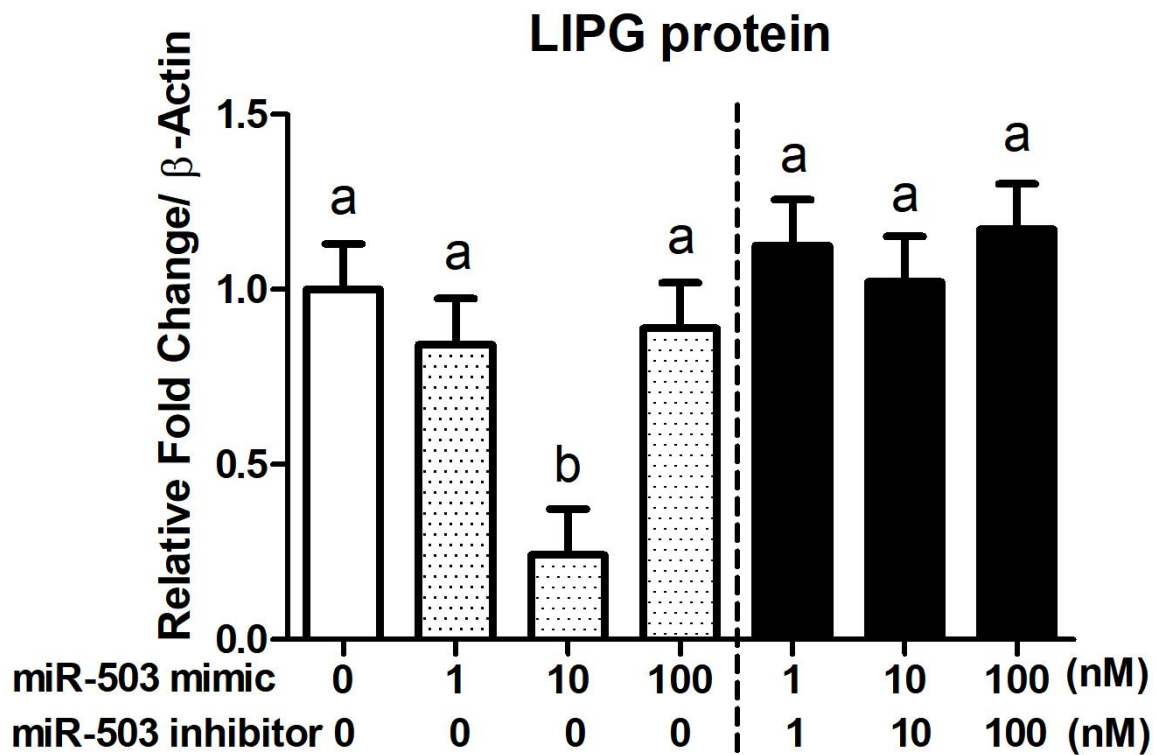
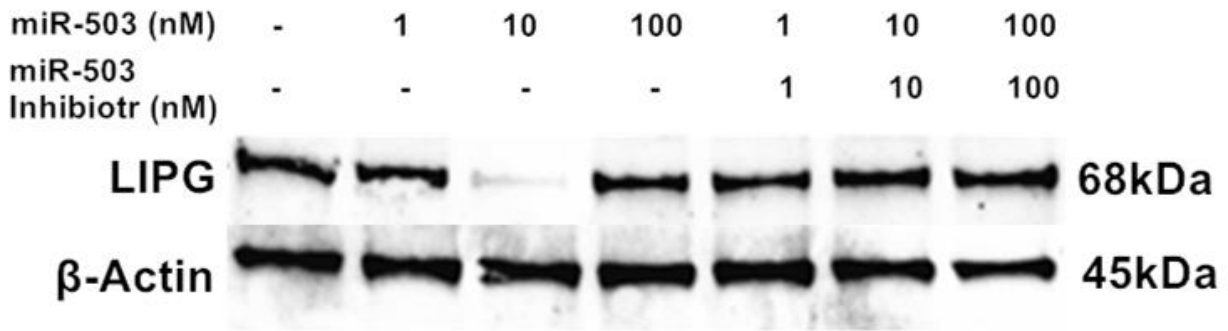


Figure IV-4.5 LIPG western blot assay of liver organoids after 48 h of transfection ($n = 5$). The upper section displays the western blot images of LIPG and β -Actin with varied treatments. The lower section presents the analysis results for the relative LIPG protein expression after 48 h of miR-503 transfection or miR-503 mimic co-transfection with miR-503 inhibitor. Different letters indicate significant differences (lsmeans \pm SEM; $p < 0.05$)

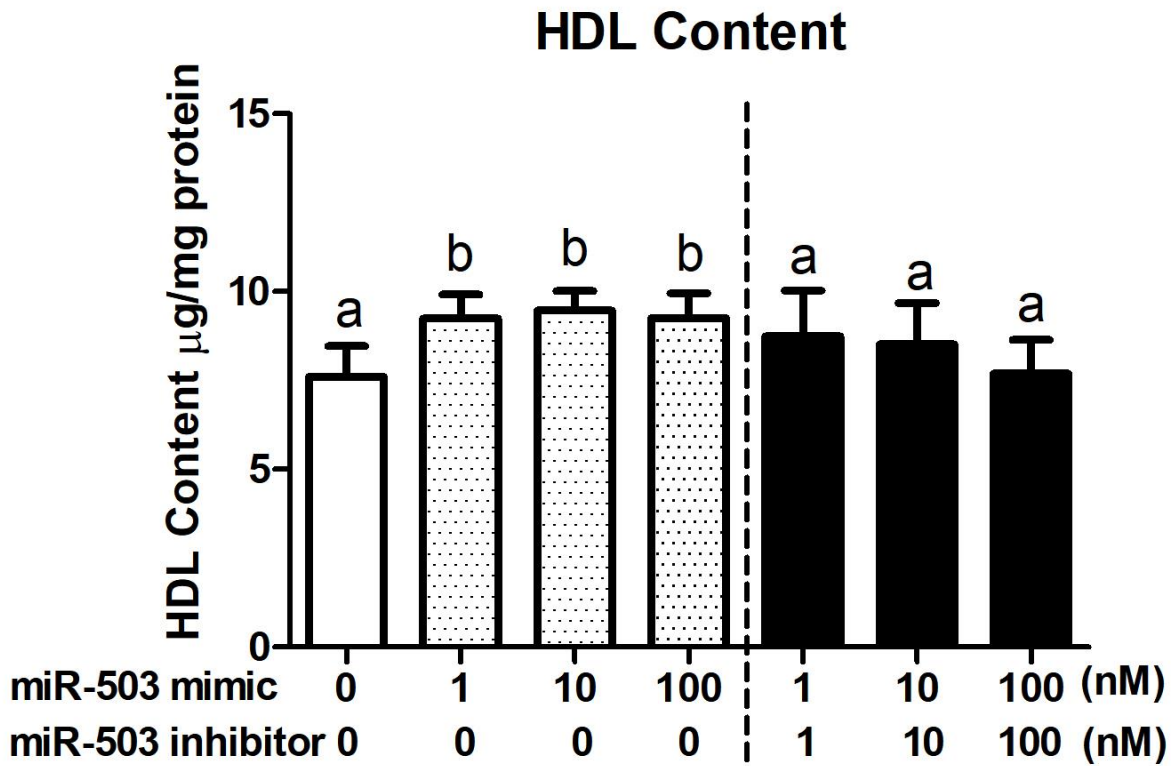


Figure IV-4.6 HDL measurement in culture medium after 48 h of transfection ($n = 5$). This figure showed the HDL content in culture medium after 48 h of miR-503 transfection or miR-503 mimic co-transfection with miR-503 inhibitor. Different letters indicate significant differences (lsmeans \pm SEM; $p < 0.05$)

Choline Content

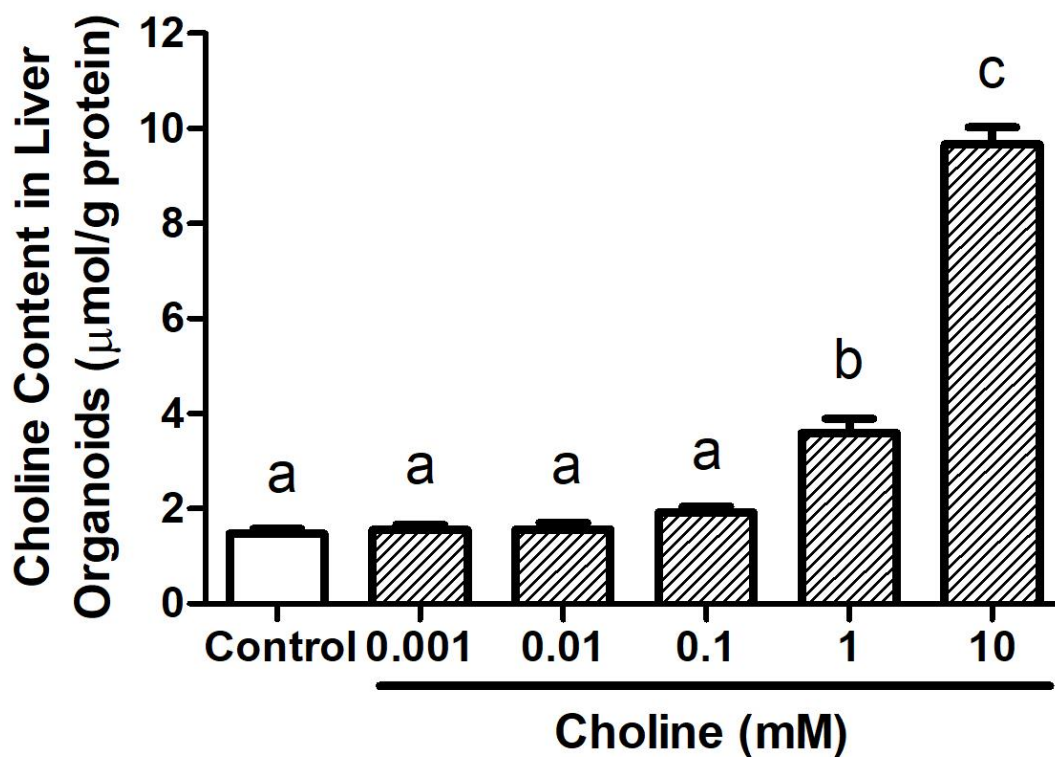


Figure IV-4.7. Measurement of choline content in liver organoids treated with varying concentrations of choline after 96 h. This figure showed the choline content in different group of liver organoids treated with varying concentrations of choline after 48 h. Different letters indicate significant differences (lsmeans \pm SEM; $p < 0.05$)

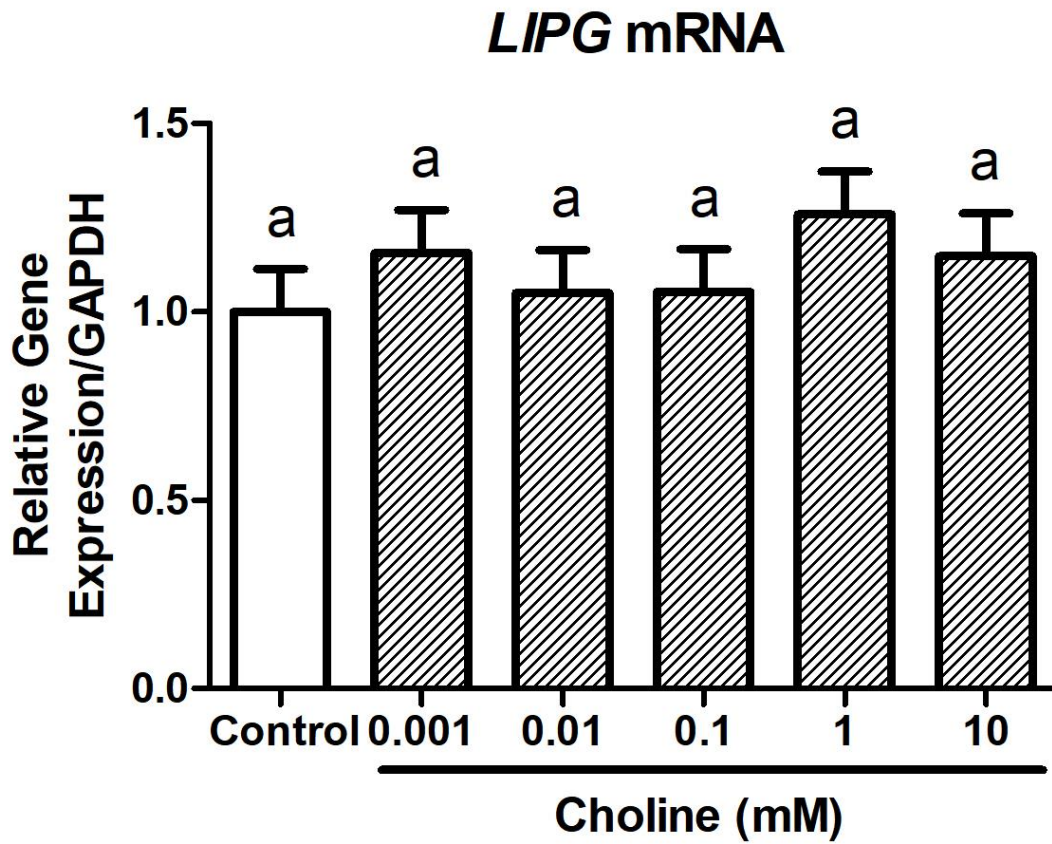


Figure IV-4.8-1 LIPG mRNA expression level assay in liver organoids treated with varying concentrations of choline after 96 h. This figure showed the relative LIPG gene expression in different groups of liver organoids treated with varying concentrations of choline after 48 h. Same letter indicate no significant differences (1smeans \pm SEM; $p > 0.05$)

miR-503 Expression

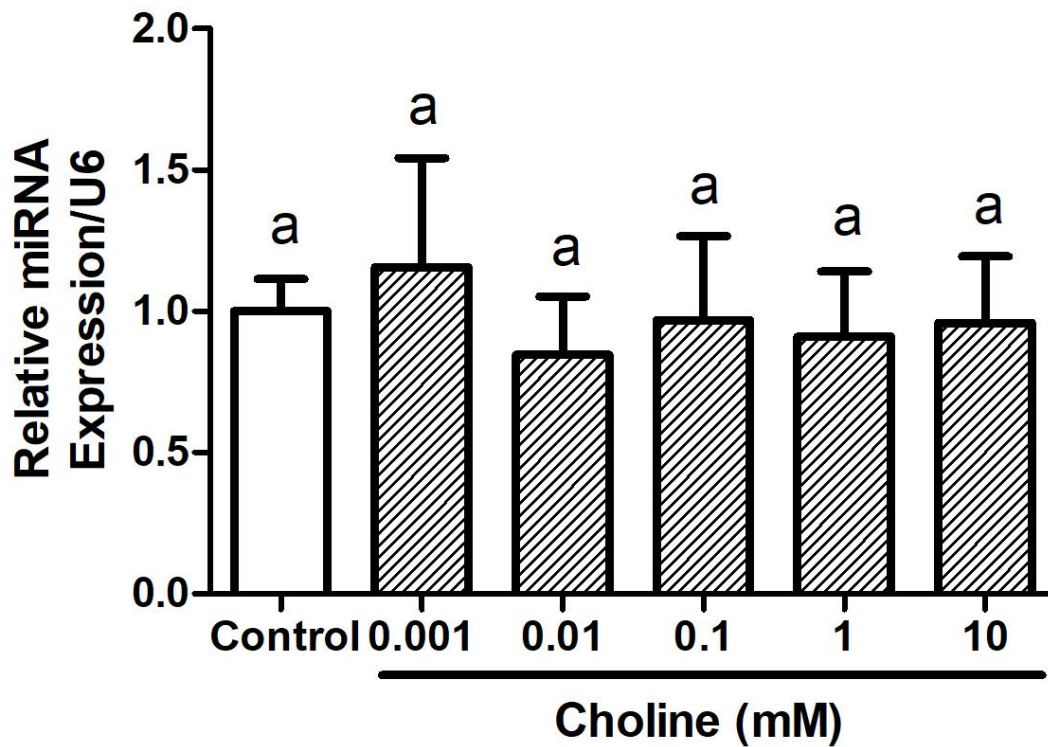


Figure IV-4.8-2 MiRNA-503 expression level assay in liver organoids treated with varying concentrations of choline after 96 h. This figure showed the relative miRNA-503 expression in different groups of liver organoids treated with varying concentrations of choline after 48 h. Same letter indicate no significant differences (lsmeans \pm SEM; $p > 0.05$)

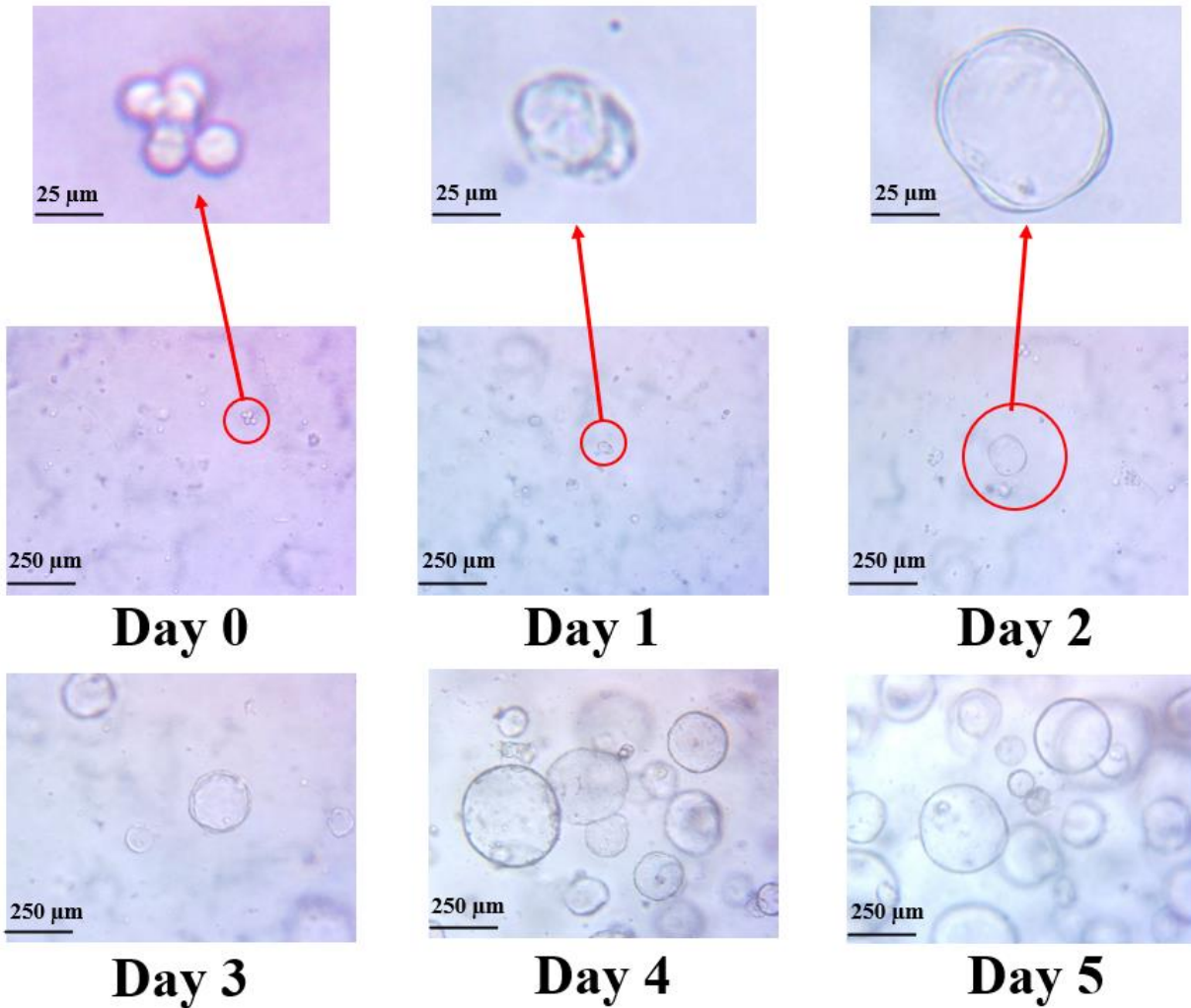


Figure IV-5-1 Examples of isolated and growing three-dimensional (3D) pig liver organoids. Newly isolated organoids increase their lumen volume after 2 d in culture and it will form full organoids (mature) after 4-5 d in culture. Red circle and arrow indicate magnified organoids. Scale bars of 250 or 25 μm are displayed in the lower-left corner of each picture.

Chapter V: General Conclusions and Future Directions

V-1. General Conclusions

Undernutrition during pregnancy remains a critical global public health problem that causes neonatal mortality and overall disease burden within impoverished populations in developing countries. Even though prevalence has decreased in recent decades, nearly 10% of women are undernourished (assessed by height and body mass index below 18.5 kg/m²), especially in South Asia with the highest prevalence of undernutrition estimated at 24.0% in 2014. Maintaining good nutritional status during pregnancy is important for a healthy pregnancy outcome. Maternal undernutrition during pregnancy will not only cause short-term consequences, such as mortality, morbidity, disability but also impact intellectual ability, adult size, reproductive performance, metabolic and cardiovascular disease. However, the potential impairments of maternal undernutrition to metabolic pathways in offspring are not defined completely.

Firstly, employing both mRNA sequencing and miRNA sequencing on identical liver samples first revealed differential expression in hundreds of genes in the fetal liver due to maternal feed restriction during pregnancy. These genes play roles in diverse biological processes such as gene expression regulation, protein translation, wound healing, cell spreading, DNA repair, and oxidative stress response. By utilizing IPA analysis, the pathways regulated by these mRNA expressions were categorized into energy production, immune response, and cell growth and proliferation. Additionally, we identified dozens of miRNAs showing distinct expression patterns in the same liver samples. Most importantly, the findings obtained from correlation analysis between miRNA and mRNA in our study illustrated that maternal undernutrition increased the activities of oxidative phosphorylation, death receptor signaling,

neuroinflammation signaling, and estrogen receptor signaling pathways in the fetal liver, where miRNAs were evidenced as potential regulators for mRNAs in these pathways. The stimulation of oxidative phosphorylation pathway was validated using RT-qPCR. The correlational analysis indicated that miR-221, 103, 107, 184, and 4497 correlate with their target genes *NDUFA1*, *NDUFA11*, *NDUFB10* and *NDUFS7* in this pathway. These results provide the framework for further understanding the negative impacts of maternal undernutrition on hepatic metabolic pathways via miRNA-mRNA interactions in full-term fetus.

Secondly, by conducting 2 (choline) x 2 (DHA) factorial analysis and IPA analysis, we revealed the impact of maternal supplementing choline and DHA during gestational feed restriction on the gene and pathway level in their offspring. Results showed that cardiac hypertrophy signaling, IL-6 signaling, IL-3 signaling, Th1 pathway, and acute phase response signaling were inhibited by maternal supplemental choline. 17 pathways (5 inositol-related pathways and 5 immune-related pathways and other 7 pathways) were inhibited by maternal supplementation of DHA, while PPAR signaling and RhoGDI signaling were stimulated. Furthermore, acute phase response signaling was modified by the choline x DHA synergistic effect. While sirtuin signaling pathway, tRNA splicing, PPAR α /RXR α activation, and NAD signaling pathway, RNA polymerase I transcription pathway were modified by the choline x DHA antagonistic effect. Through miRNA target prediction, we identified 20 miRNA-mRNA pairings and validated 10 of them using RT-qPCR. They are miR-503 targeting *LIPG* and *SPOUT1*, miR-221 targeting *TIMP3* and *TM4SF1*, miR-31 targeting *CASR* and *FLOT1*, *Let-7f* targeting *DUSP16* and *CDKN1A*, miR-26b targeting *FAM98A*, and miR-144 targeting *PLAT*.

Thirdly, we proposed a regulatory pathway based on the above result. Choline regulates miR-503 expression, subsequently affecting miR-503's target mRNA *LIPG* and repress *LIPG*

translation. The decrease in LIPG protein content boosts HDL-C levels by reducing HDL-C hydrolysis. Maintaining sufficient HDL-C in circulation helps reduce the risk of ASCVDs. Next, we utilized pig liver organoids to validate the proposed pathways. The results from urea assay, cytotoxicity assay, and viability assay showed that liver organoids consistently maintained normal functionality across all the tested miR-503 mimic concentrations during the experiment. Analysis of *LIPG* gene expression indicated that miR-503 indeed plays a regulatory role, leading to downregulation and fitting a quadratic regression. Western blot assay for LIPG also demonstrated miR-503's ability to downregulate LIPG protein expression with quadratic regression regulation. Consequently, liver organoids exhibited a significant increase in HDL content upon transfection with miR-503 mimic at all concentrations. Together, these results support our hypothesis: miR-503 destabilizes its target mRNA *LIPG*, repressing *LIPG* translation and reducing the production of LIPG protein, consequently boosting HDL content. However, the results from choline treatment did not reflect its regulation on miR-503 expression. The reasons for this discrepancy may be complex and warrant further investigation.

V-2. Future Directions

From the first study, we acquired a wealth of information that merits further exploration. For instance, we identified several genes in fetal liver that were reported to be affected by maternal undernutrition for the first time, including *ACTC1*, *GLI1*, *FGF21*, *CPM*, *TSPO*, *TSPOAP1*, *ITGA3*, *HSD11B1*, *FMO5*, *RND1*, *MRPS15*, *CHMP2A*, *PLK3*, *ELMOD1*, and *CRABP1*. These genes offer potential avenues for in-depth investigation into their biological functions, the discovery of new pathways, or their utilization as biomarkers and therapy targets. On the other hand, this research will contribute to unraveling the mechanisms behind the adverse effects induced by maternal undernutrition in offspring. By offering additional insights and

detailed information, it endeavors to provide solutions to address and mitigate the impact of this problem.

Secondly, maternal supplemental choline was found to impact 144 genes, including some reported for the first time to be associated with maternal choline, such as *PAK4*, *CYP4A24*, *MAOA*, *ELOVL2*, *GLS2*, *LPIN2*, and *AGO2*. Similarly, 151 genes were modified by maternal supplemental DHA, with some genes newly reported to be associated with maternal DHA, including *FLOT1*, *PBX2*, *SLC16A1*, *SLC7A4*, *RND3*, *PPARD*, and *UFMI*. Furthermore, we examined the interaction effect of maternal supplementation with choline and DHA on fetal hepatic gene expression. Currently, there is very limited research dedicated to this aspect. As a result, most of the genes, regardless of whether they exhibit synergistic or antagonistic effects, are being documented for the first time in our study. Delving into the functions of these genes contributes to a better understanding of the role of maternal choline and DHA supplementation and their interaction effect during gestational nutrition restriction on fetal development. It further contributes to addressing and mitigating the impact of maternal undernutrition by providing detailed information and possible solutions. Additionally, many mRNA and miRNA correlations were reported for the first time in this study. For example, miR-31 targeting *CASR*, Let-7f targeting *PIGA*, miR-1260a targeting *DAXX*, and miR-182 targeting *SLC35G1* and *TMEM42* are all not reported. Their upstream regulator and downstream target gene, pathway, or organ needs to be explored.

Furthermore, in our third study, we demonstrated the regulatory role of miR-503 on HDL content by regulating LIPG. In the future, we can evaluate the value of miR-503 in the development and progression of ASCVD and the possibility of becoming a candidate of miRNA-based therapies.

Lastly, given that our study employed swine as a model, our findings can contribute to broadening our understanding and applying the results to address issues in the swine industry, such as IUGR and high piglet mortality.